ABSTRACT

ASSESSMENT OF MODERN SEDIMENT STORAGE IN THE FLOODPLAIN OF THE LOWER TAR RIVER, NORTH CAROLINA

By

Dimitri Quafisi

November, 2010

Chair: Dr. Stephen J. Culver

Major Department: Geological Sciences

Rivers transport water, sediment, and other constituents from the continent to the sea, but in route material can often become stored temporarily or permanently. Along the Atlantic Coast of the United States, coastal plain rivers such as the Tar River are characterized as low-gradient meandering systems that develop wide floodplains which are subjected to frequent and prolonged flooding. As a result, these rivers are believed to experience storage of sediment, particularly near their estuarine mouths. The lower portion of rivers and their attached estuaries are also environmentally and economically important serving as critical habitat (e.g., nurseries for fish), recreational areas, and transportation pathways. Excess sediment is often considered a significant pollutant and can have adverse effects on biota. Suspended sediment also can supply excess nutrients and trace metals from anthropogenic activity.

Previous work in North Carolina suggests that alluvial storage can make up the majority (>50%) of the total sediment delivered to rivers. This study more closely examines the nature of lower floodplain sediment storage and more specifically focuses on calculating sediment accumulation along the Tar River. Cores were collected from three sites along seven different transects perpendicular to the main channel. Analysis of ^{210}Pb and ^{137}Cs were employed to calculate sediment accumulation rates, and grain-size data were made to inform radionuclide and

sedimentation interpretations. Sedimentation rates within the study area range from 0.09 to 1.08 cm/yr. However, several sites appear to have non-steady-state deposition possibly due to major overbank flood events. Grain-size data indicate a mixture of sand and mud at all sites with some variability in the nature of sediment accumulating. Using core observations and LiDAR topographic data, storage across the system is estimated to be approximately 1.26×10^5 t/yr or roughly 66% of the total incoming sediment measured at Tarboro, NC (1.89×10^5t/yr) in previous works.

ASSESSMENT OF MODERN SEDIMENT STORAGE IN THE FLOODPLAIN OF THE LOWER TAR RIVER, NORTH CAROLINA

A Thesis

Presented To

The Faculty of the Department of Geological Sciences

East Carolina University

In Partial Fulfillment

of the requirements for the Degree

Masters of Science in Geology

by

Dimitri Quafisi

November, 2010

ASSESSMENT OF MODERN SEDIMENT STORAGE IN THE FLOODPLAIN OF THE LOWER TAR RIVER, NORTH CAROLINA

By

Dimitri Quafisi

APPROVED BY:

DIRECTOR OF THESIS _____
Dr. J.P. Walsh

CO-DIRECTOR _____
Dr. D. Reide Corbett

COMMITTEE MEMBER _____
Dr. Michael O'Driscoll

COMMITTEE MEMBER _____
Dr. Tom Allen

CHAIR OF GEOLOGICAL SCIENCES _____
Dr. Stephen J. Culver

DEAN OF GRADUATE SCHOOL _____
Dr. Paul Gemperline

ACKNOWLEDGMENTS

I would like to thank the organizations that contributed to the funding of this research and its investigators; RENCI, the Department of Geological Sciences, and East Carolina University. Special thanks go out to my advisors Dr. Walsh and Dr. Corbett and committee members Dr. O'Driscoll and Dr. Allen for all of their help and guidance throughout this project. I would also like to thank Jim Watson and John Woods for their tireless efforts to make research possible for staff and students in this department. I also appreciate the help of Joey Kiker, Steve Anstine, Andrew Dietsche, Scott Elkins, and Brian Burgess for their help in the field and in the lab. Finally and most importantly I would like to thank my wife Mary Quafisi and my family for their loving and understanding support throughout my life, without their involvement all of this would have not been possible.

DEDICATION

This thesis is dedicated to my Grandfather Bill W. Swindell, his influence in my life drove me to strive for excellence in everything I do. From an early age he taught me to work hard, treat others with compassion, and above all other thing put family first. Some of my favorite memories are those of spending summers helping in his workshop, milling and machining parts to repair various things around their house. From these experiences I learned valuable math and problem solving skills as well as gaining the confidence that any problem can be overcome with hard work and perseverance. This is why I dedicate this work to him, to let him know he will always be missed and never forgotten.

TABLE OF CONTENTS

TABLE CAPTIONS

FIGURE CAPTIONS

48. Long profile of river and estimated sediment load for the Tar River. Above, the long profile shows the volume of calculated sequestration within each representative reach. All rates are reported in ($x10^4$ t/yr). Below, estimated sediment load below each represented river reach, sediment loads are reported in thousands of tonnes per year._____ 84

LIST OF SYMBOLS AND ABBREVIATIONS

A_Z	Excess ^{210}Pb at depth Z
A_0	Excess ^{210}Pb at surface
APES	Albemarle-Pamlico Estuarine System
Be	Beryllium
Bi	Bismuth
Cs	Cesium
DEM	Digital Elevation Model
Dpm/g	Decays per Minute per Gram
LiDAR	Light Detection and Ranging
λ	^{210}Pb decay constant
Pb	Lead
Po	Polonium
Ra	Radium
s	Accumulation Rate
SDR	Sediment Delivery Ratio
$t_{1/2}$	Half-Life

1. Introduction

Rivers are the main mechanism for the transportation of water, sediment, and other constituents from land to the sea. Along the Atlantic Coast of the United States, the coastal plain is characterized by low-gradient meandering rivers that develop wide floodplains subject to frequent and prolonged flooding (Simmons, 1993; Hupp, 2000; Johnson, 2007; O'Driscoll et al., 2010). In North Carolina, rivers such as the Tar typically have low stream power with available accommodation space in coastal plain river reaches allowing for storage of sediment upstream of estuaries, resulting in low sediment yields and loads at river mouths (Simmons, 1993; Phillips, 2006).

The lower portion of rivers and their attached estuaries are environmentally and economically important, acting as vital habitat (e.g., nurseries for fish), recreational areas (e.g., fishing grounds), and transportation pathways (e.g., personal and commercial vessels) (Giese et al., 1979). Pollutants are stressors on these environments and can have adverse effects on the associated ecosystem. Excess sediment is often considered a significant pollutant in rivers (Servizi and Martens, 1992; Watts et al, 2003, Walling, 2004; Walling, 2005) and estuaries (EPA, 1992; 1994; Daskalakis and O'Conner, 1995; Hupp, 2000) and can have adverse effects on biota (Clark et al., 1985; Sear, 1993; Soulsby et al., 2001; Walling, 2004). Suspended sediment also can contribute to pollution in the form of excess nutrients (Allan, 1986; Walling, 2004; Walling, 2005; Horowitz, 2008) and trace metals from anthropogenic activity (Allan, 1986; Cooper, 2004). To better protect these important natural resources, knowledge of the sediment dynamics

within the lower river system needs to be better understood. Floodplains in particular are expected to play an important role in most rivers with respect to sediment sequestration.

Floodplains have been reported to be a significant sink for sediment within river systems (Wolman and Leopold, 1957; He and Walling, 1996; Walling and He, 1997; Allison, 1998; Goodbred and Kuehl, 1998; Walling et al., 1998; Hupp, 2000; Walling, 2004; Knox, 2006; Mizugaki et al., 2006). Previous studies have reported deposition rates of 2-3 mm/yr in the Roanoke River of North Carolina (Hupp, 1999) and 0-10 mm/yr on British floodplains (Nicholas and Walling, 1997). Table 1 shows a collection of floodplain sediment accumulation rates from around the world. Although the accumulation rates appear relatively small, floodplain sedimentation when extrapolated over areas of several square kilometers can remove a large fraction of the total sediment delivered to streams, as seen in Phillips (1991).

Floodplains are characterized as very dynamic systems with large variability between locations and even within sites (Wolman and Leopold, 1957; He and Walling, 1996; Walling and He, 1997; Allison, 1998; Goodbred and Kuehl, 1998; Walling et al., 1998; Hupp, 2000; Walling, 2004; Knox, 2006; Mizugaki et al., 2006). Table 1 presents the considerable variation in sedimentation of rivers. This can be attributed to the large variability in the nature of floodplains due to their complex behavior, topography, and morphology. Phillips (2007) investigated the flow regime in the coastal plain of the Trinity River in Texas. Phillips found that during high flow events coastal backwater effects and tributaries becoming distributaries complicated the overall flow patterns which would ultimately complicate the sediment dynamics. As a result, it is necessary to

gain a system-specific understanding of sediment dynamics, and this is the main focus of this study, to characterize floodplain sedimentation within the Tar River system.

Table 1: Sediment accumulation rates in select floodplains around the world.

Location	Sediment accumulation Rate	Citation
Lower Mississippi Alluvial Valley, TN	0.09 to 6.20 cm/yr	Pierce and King, 2008
Ganges-Brahmaputra, Bangladesh	0.0 to 1.47 cm/yr	Goodbred and Kuehl, 1998
River Ouse, Yorkshire, UK	0.11 to 1.04 cm/yr	Owens et al., 1999
Quebec, Canada	0.21 to 10.75 cm/yr	Saint-Laurent et al., 2008
Brahmaputra-Jamuna River	0.67 to 1.15 cm/yr	Allison et al., 1998
Tar River, NC, USA	Average 2 mm in one event	Leece et al., 2004
Black Swamp, AR	0.01 to 0.6 cm/yr	Hupp and Morris, 1990
Western TN	0.0 to 0.6 cm/yr	Hupp and Bazemore, 1993
Missouri River	0.03 to 0.64 cm/yr	Heimann and Roell, 2000
Kushiro Mire, Northern Japan	1.9 to 8.9 cm/yr	Mizugaki et al., 2006
Roanoke River, North Carolina	0.23 cm/yr	Hupp et al., 1999

This study has three main objectives: 1) characterize the morphology of the active floodplain in the lower Tar River system, 2) evaluate the variability of sediment accumulation rates within the floodplain, and 3) use these sediment accumulation rates to estimate the amount of sediment storage within the system.

2. Importance and Background

The Tar River is an important source of freshwater and material to the Albemarle-Pamlico Estuarine System (APES), the second largest estuarine system in the United States (Giese et al., 1979; Simmons, 1993; O'Driscoll et al., 2010). Ranking third in overall flow into the APES, the Tar River (153 m^3/s) discharges less water than the

Roanoke (252 m^3/s) and Neuse rivers (173 m^3/s), but more than the Chowan River (130 m^3/s) (Giese et al., 1979). As previously stated, excess sediment can have adverse effects on biota within river and estuarine systems (Servizi and Martens, 1992; EPA, 1992; 1994; Daskalakis and O'Conner, 1995; Hupp, 2000; Watts et al., 2003; Walling, 2005). The APES is an important resource with regards to the commercial fishing industry which accounts for a large portion of the revenue and jobs in North Carolina. North Carolina accounted for approximately 70% and 51%, respectively, of the total weight landed and total value of commercial fish in the southeast region of the United States in 2001 (NMFS 2002). State-managed fish species generated a commercial landings revenue of over $103 million in 2002 (Burgess and Bianchi, 2004). Commercial fishing provides many jobs and important income for North Carolina families in several coastal counties (Diaby, 1997; Diaby, 1999; Bianchi, 2003; Burgess and Bianchi, 2004). In 2001, there where over 4800 commercial fishermen registered in North Carolina (Bianchi, 2003). To protect this industry and the associated jobs a better understanding of stressors on the fishing industry is imperative.

Sediment is a key pollutant to coastal areas, and much of it is generated from erosion far upstream, however, the volume of sediment eroded within a drainage basin is not equal to the amount of sediment transported out of a system, rather it is typically a much smaller amount. The fraction of sediment that escapes a system is known as the Sediment Delivery Ratio (SDR), and this value typically ranges from 7 % to 16 % for North Carolina Rivers (Phillips, 2006; Brown et al., 2009) (Fig. 1).

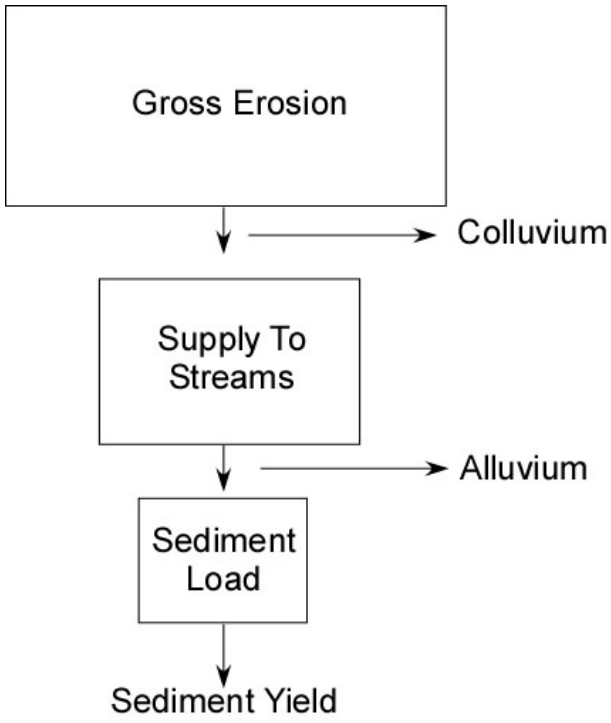

Figure 1: Box diagram modeled after Phillips (1991). Diagram shows gross erosion, subdivided into the main sinks such as colluvium and alluvium and the main transport pathways from gross erosion to sediment yield from the system.

During flood events, water overflows the river banks onto the floodplain and begins to decrease in velocity. Suspended sediment in this standing water begins to settle out and deposits on the floodplain. Sediment accumulated during these events has been shown to represent a significant fraction in annual floodplain sediment budgets (Wolman and Leopold, 1957; He and Walling, 1996; Walling and He, 1997; Allison, 1998; Goodbred and Kuehl, 1998; Walling et al., 1998; Hupp, 2000; Walling, 2004; Knox, 2006; Mizugaki et al., 2006). Sediment accumulation rates are commonly highest in areas adjacent to a channel and diminish with increasing distance from the channel perimeter (Allen, 1964; Kesel et al., 1974; James, 1985; Pizzuto, 1987; Allison et al., 1998; Walling and He, 1998; Walling et al., 1998; Hupp, 2000; Mizugaki et al., 2006). Accumulation rates have also been show to be affected by floodplain topography (Allison et al., 1998;

Walling and He, 1998; Walling et al., 1998) and the magnitude and frequency of flooding (Lambert and Walling, 1987; Asselman and Middelkoop, 1995; Allison et al., 1998; Asselman and Middelkoop, 1998; Walling et al., 1998). Distance from the channel also can affect the quality of material reaching a floodplain. For example, particle diameter has been reported to fine with increasing distance from channel (Allen, 1964; Kesel et al., 1974; Lambert and Walling, 1987; Pizzuto, 1987; Asselman and Middelkoop, 1995; Asselman and Middelkoop, 1998; Walling and He, 1998; Walling et al., 1998).

Radionuclides ^{210}Pb and ^{137}Cs have been shown to be useful tools in measuring sediment accumulation rates in floodplains (He and Walling, 1996; Walling and He, 1997; Allison, 1998; Goodbred and Kuehl, 1998; Mizugaki et al., 2006). These method allow for rates to be measured as far back as 100 years or ~5 half lives of ^{210}Pb. Goodbred and Kuehl, 1998 showed how ^{210}Pb and ^{137}Cs geochronology could be used to measure accretion in the Ganges-Brahmaputra River, rates of greater than 1.47 cm/yr to no accumulation were measured within the floodplain. Similarly Mizugaki et al., 2006 used ^{210}Pb and ^{137}Cs radionuclides coupled with dendrochronology to evaluate the impacts of anthropogenic influences on sedimentation within the Kushiro Mire in Northern Japan, this study revealed that sedimentation rates have increased since channelization occurred within the area.

To estimate sedimentation rates, steady-state accumulation is commonly assumed; however, during flood events massive deposition can occur (Aalto et al., 2003; Saint-Laurent et al., 2007). For example, 15 to 35 mm of sediment accumulated on floodplains within basins in southern Quebec during spring flooding (Saint-Laurent et al., 2007). However, these values are much higher than those reported for the Tar-Pamlico River

during an extreme flood event following Hurricane Floyd in 1999, where sediment deposition averaged 2 mm (Lecce et al., 2004). The fact is a range in sedimentation behavior is evident, and radionuclides can help decipher individual systems.

The Piedmont of North Carolina has long been seen as a region of severe erosion (Meade and Trimble, 1974). Precipitation within the watershed causes raindrop impact erosion, sheet erosion, and rill erosion to occur (Simmons, 1993). This eroded sediment has two different fates. A fraction of sediment remains on hill slopes as colluvium, while the remaining sediment is transported to the adjacent river, stream, or other water body. Once supplied to a river, sediment can either be stored in the river channel or floodplain as alluvium or be transported out of the system to an estuary (e.g., the APES), lake, or the ocean (Figure 1) (Phillips, 1991). Alluvial storage both in channel and floodplain can account for as much as approximately 75% of the total sediment delivered to the main channel of the river or stream, however, the fraction of this sediment that is stored in the floodplain is more likely to be sequestered over a decadal timescale (Phillips, 1991). By quantifying the total amount of sediment sequestered annually on a floodplain, a more accurate sediment budget for a river can be developed and better management strategies can be devised to protect the associated resources.

3. Study Area

North Carolina can be divided into three main physiographic provinces: Mountains (e.g., the Blue Ridge), Piedmont, and Coastal Plain (Figure 2; Simmons, 1993; Harman et al., 1999; Hupp, 2000). A large fraction (approximately 45%) of the State is comprised of the Coastal Plain province, which is characterized by low relief and gentle topography.

Erosion of the Mountains and Piedmont provinces from the Mesozoic to present provides the sediment that has formed the modern Coastal Plain. Geomorphologic and hydrologic processes, predominately driven by climate and sea level fluctuations, have molded this landscape since the Cretaceous (Horton and Zullo, 1991; Hupp 2000). Close to the coast, within ~80 kilometers, the average altitude is approximately 6 meters above sea level (Simmons, 1993). Rivers flowing from the Piedmont to the Coastal Plain are relatively well incised until the Fall Line some, however, are still incised in the Coastal Plain (Figure 3). Past this position the downstream river gradient lessens, and rivers are thought to deposit more sediment both temporarily (e.g., within the channel) and permanently within floodplains (Simmons, 1993; Hupp 2000).

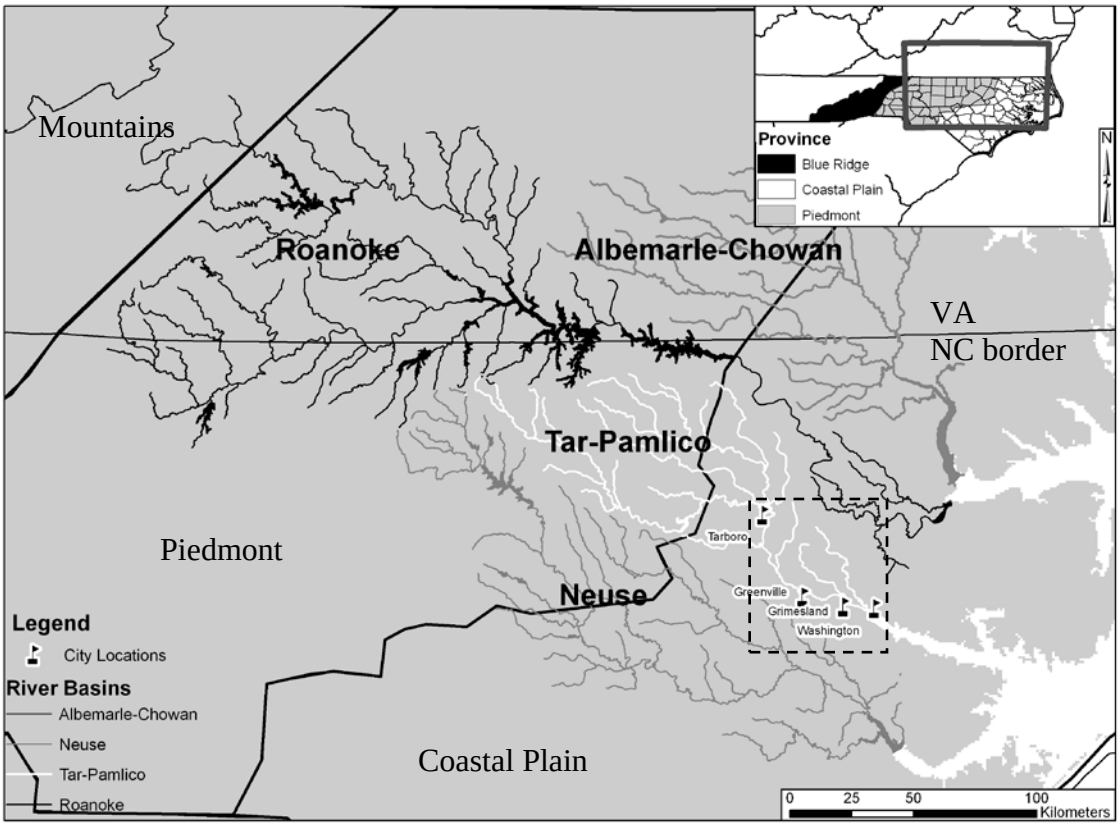

Figure 2: Map of the four major drainage basins supplying water and sediment to the APES. The inset base map depicts the three provinces of North Carolina: the Mountains, Piedmont, and Coastal Plain (Simmons, 1993). The black dashed box shows the study area, shown in greater detail in Figure 5. Thick black lines show the boundaries between the three provinces shown.

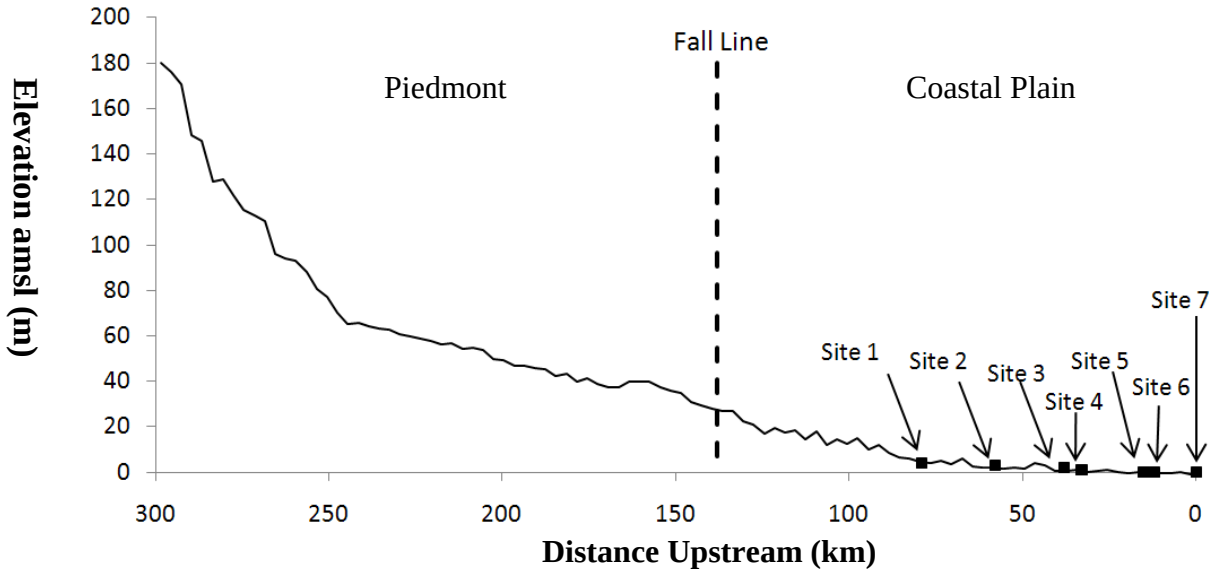

Figure 3: Long profile for the Tar River with distance upstream from the 17 bridge in Washington, NC, the Fall Line is indicated by vertical black dashed line representing transition between the Piedmont and the Coastal Plain Provinces.

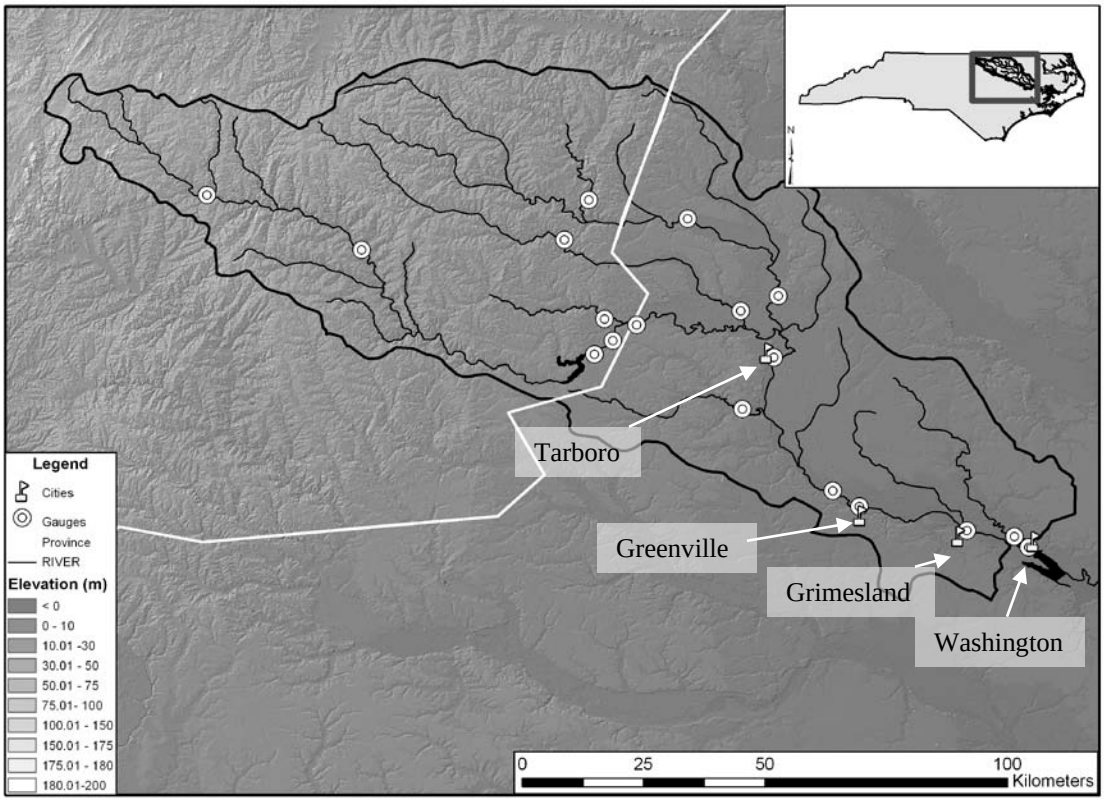

Figure 4: Basin map of the Tar River Basin. Black polygon shows the perimeter of the basin whose elevation reaches 200 meters above sea level. Note, solid white line dividing the drainage basin represents the approximate location of the Fall Line, whereas, the black polygon represents the drainage basin area. Circles represent gauging stations within the drainage basin.

The Tar River Valley is topographically asymmetric with the river incised into the southwestern side of the valley (Figure 5, O'Driscoll et al., 2010). Over the Quaternary, the Tar River channel has migrated southward on the Coastal Plain leaving behind a series of floodplain terraces to the north (O'Driscoll et al., 2010). Like other rivers in the southeastern United States, braided river deposits just north of the present river channel were deposited during cold glacial periods between 17-70 ka (Maddry, 1979; Leigh and Feeney, 1995; Leigh et al., 2004; Leigh, 2006; Leigh, 2008; Moore, 2009). The current Tar-Pamlico River watershed originates in the Piedmont and traverses the Coastal Plain province, encompassing an area of approximately 11,500 km^2 (Giese et al., 1979) (Figure 4 and 5). The study area encompasses a 69 km long reach of river that extends across the Coastal Plain province, from Tarboro to Washington. The elevation ranges from ~36 meters to sea level along this extent (Figure 5). Seven study sites were selected along this river reach (Figure 5); sites were chosen on three criteria: 1) how well the site represents the reach of river within the system, 2) ease of accessibility, and 3) proximity to established gauging stations within the river. Study sites are labeled with Site 1 near Tarboro with numbers increasing downstream to Site 7 near Washington. USGS river gauges are found within or are immediately adjacent to several of the sites: Tarboro gauge (Site 1), 264 Bypass Northwest gauge (Site 3), Greenville gauge (Site 4), Grimesland gauge (Sites 5 and 6), and the Tranters Creek gauge near Washington (Site 7). Land use within the Lower Tar River basin is estimated to be comprised of 40% forest, 43% cropland, 11% wetland, and 6% other (Developed and Water) (McMahon and Lloyd, 1995) (Figure 6), and these land uses are known to influence the solute and sediment load to the river (Simmons, 1993; McMahon and Lloyd, 1995).

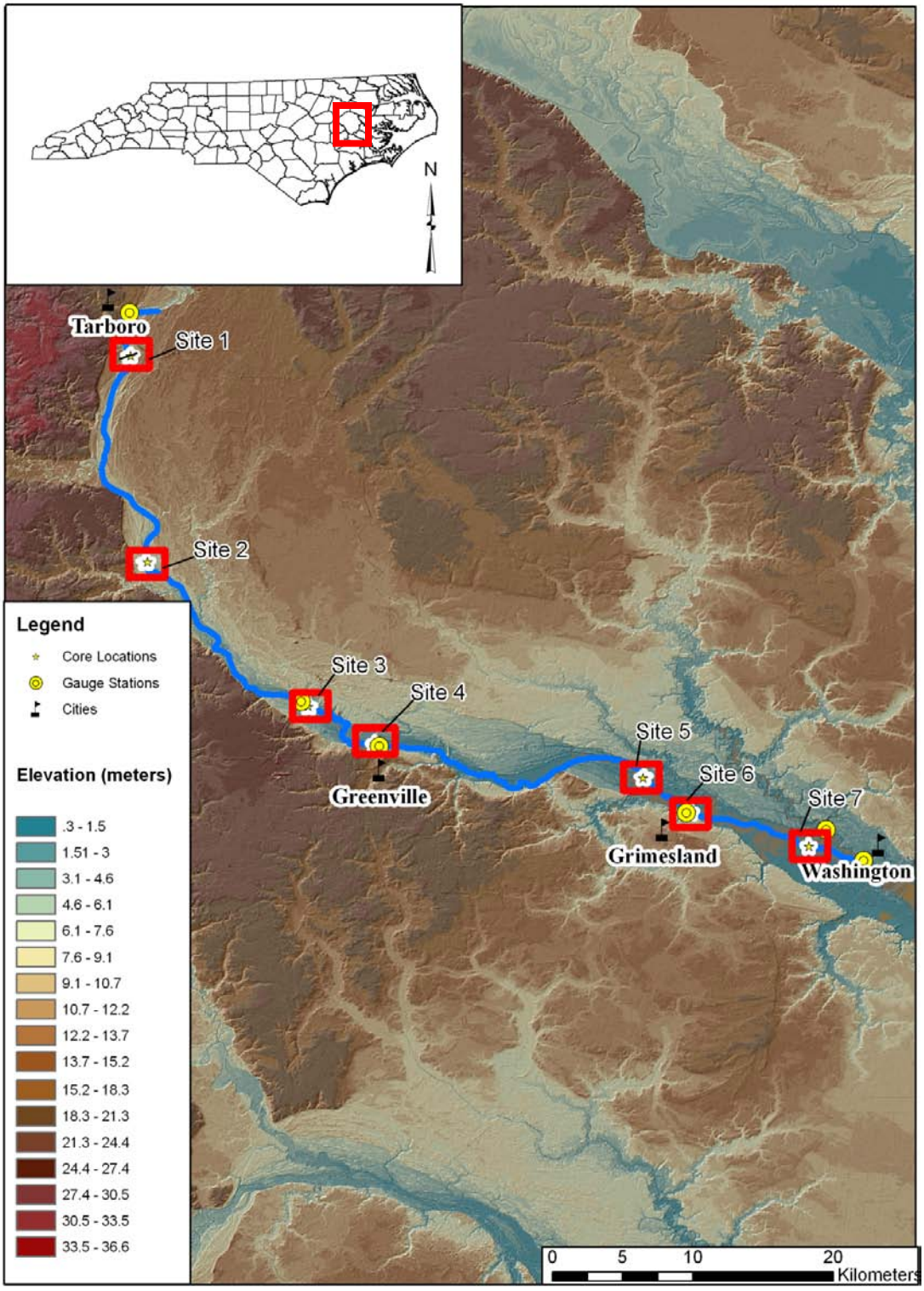

Figure 5: Base map of study area showing the seven individual study sites in red boxes. Note, site numbers increase downstream from Site 1 near Tarboro to Site 7 near Washington.

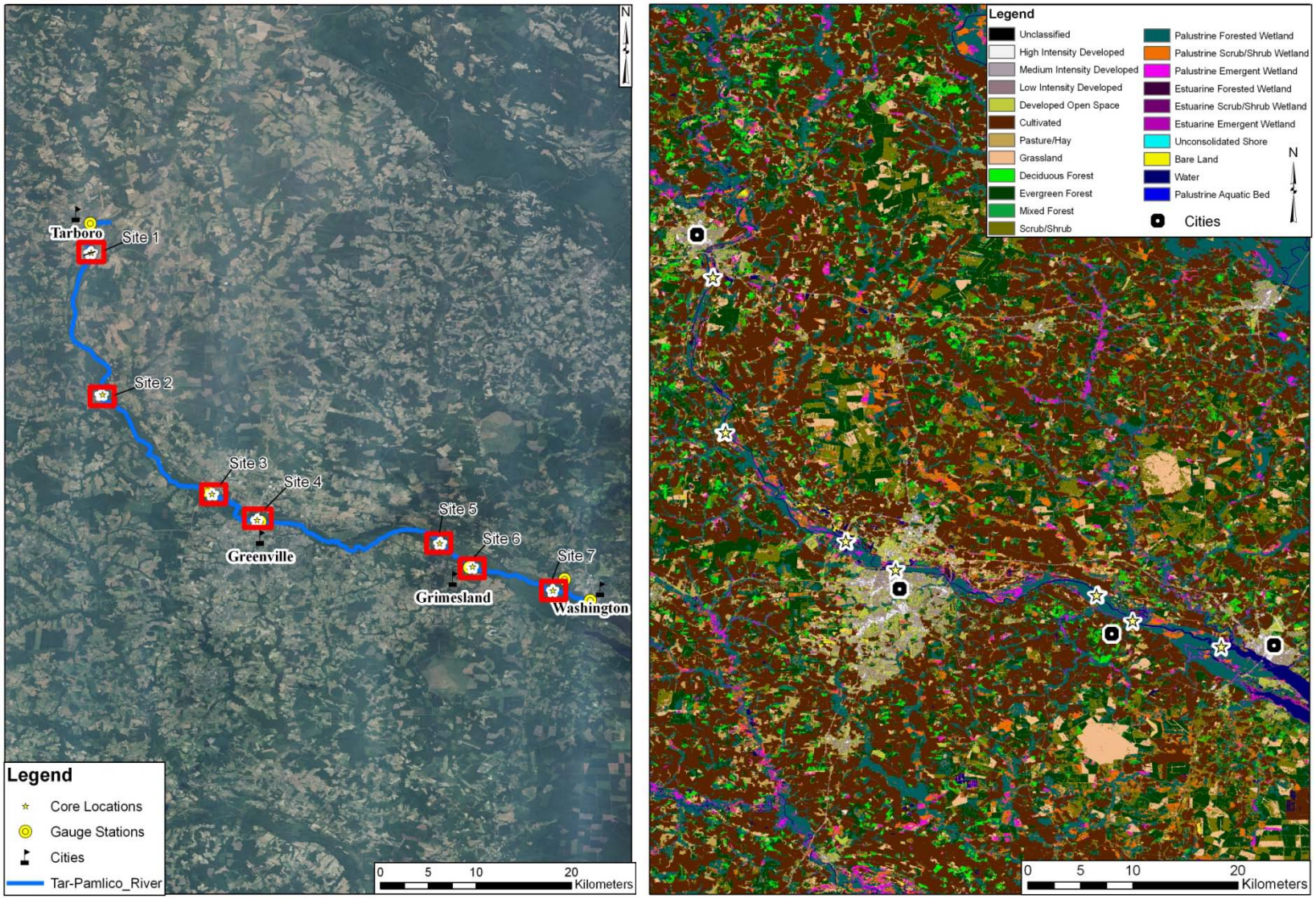

Figure 6: Satellite image (left) and land-cover (right) of the Tar River study area. Aerial photo of study area showing the land cover by cities, agriculture, and undeveloped. Note the roughly even mixture of agriculture and forest across the study area.

Geomorphological and hydrological processes driven by climate and sea level change, play a key role in the sedimentation processes within the present floodplain. For example, the frequency and magnitude of flooding may be expected to vary with base level. Floodplain sedimentation usually results in net sequestration during periods of sea level rise (Hupp, 2000). Landforms created by geomorphological processes such as flooding and river migration range from small channels to vast floodplains. Hydrological conditions and associated sedimentation are responsible for creating and shaping landforms such as scroll topography, point bars, and crevasse splays. These landforms affect floodplain topography which in turn influences future sedimentation within the floodplain by changing flood water behavior (e.g., percent time flooded) (Allison et al., 1998; Walling and He, 1998; Walling et al., 1998).

The average rainfall for North Carolina is 125 cm annually; however, it can vary significantly within the state, ranging from 96 cm in Asheville to 210 cm at Highlands (Simmons, 1993). The Coastal Plain receives a more consistent range of precipitation between 112 and 140 cm per year (Simmons, 1993). The upper Tar-Pamlico watershed has an annual rainfall of 115 to 120 cm (Phillips, 1991). Drainage from the watershed produces an annual discharge of 153 m^3/s with a total sediment load of 1.89×10^5 t/yr (Giese et al., 1979). The Tar-Pamlico river, during low flow events, is tidally influenced as far up stream as Greenville (approx. 95 km upstream) (Giese et al., 1979). Wind influences both water levels and sediment resuspension in the estuary head in both the Tar-Pamlico and neighboring Neuse estuaries where large fetch is present (Giese et al., 1979).

Ultimately, hydrology is the main factor controlling floodplain sedimentation (Allison et al., 1998; Walling and He, 1998; Walling et al., 1998; Hupp, 2000). A time-series hydrograph of the past 15 years at Greenville, NC, shows the stage height exceeded the flood level (~4m) approximately 22 times (Figure 7). The river was in flood (and therefore the floodplain was likely inundated) 5.6 months of the 15 yr period or 3.1 % of the time. Note the 1% time flooding (at ~ 5 m) was only reached during the Floyd flood of 1999 (Figure 8).

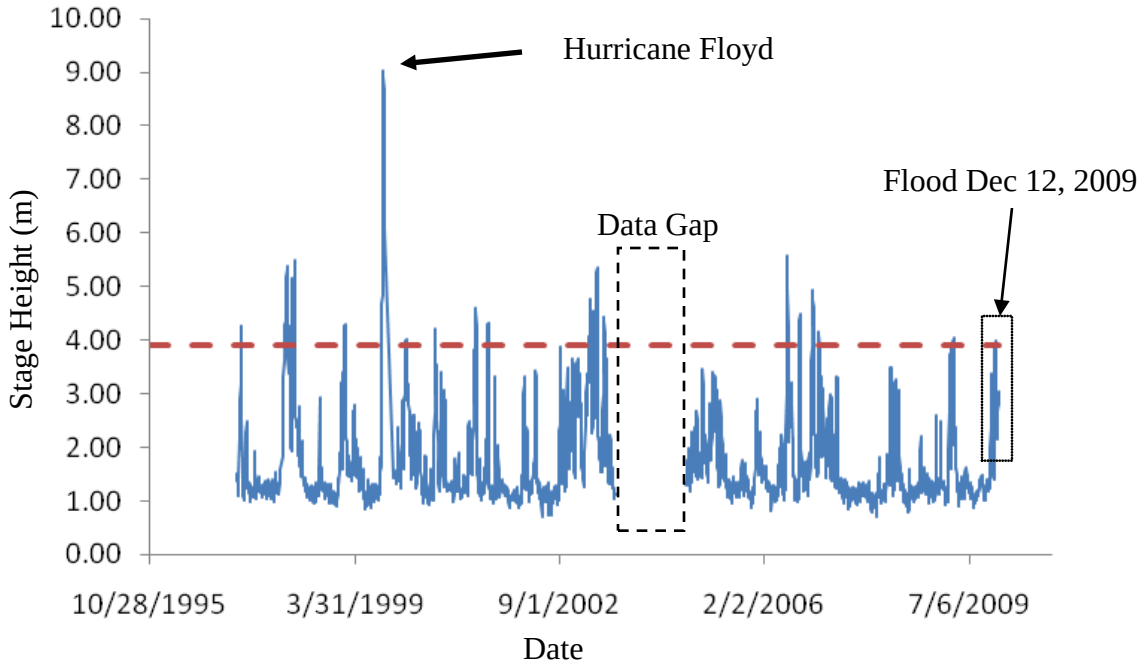

Figure 7: Hydrograph of gauge station at Greenville, NC. Dashed line shows the National Weather Service Floodstage. Arrows identify hurricane Floyd flood levels (1999 hurricane season) and the flood investigated in this study that occurred on 12/12/2009. Note a data gap indicated by dashed box.

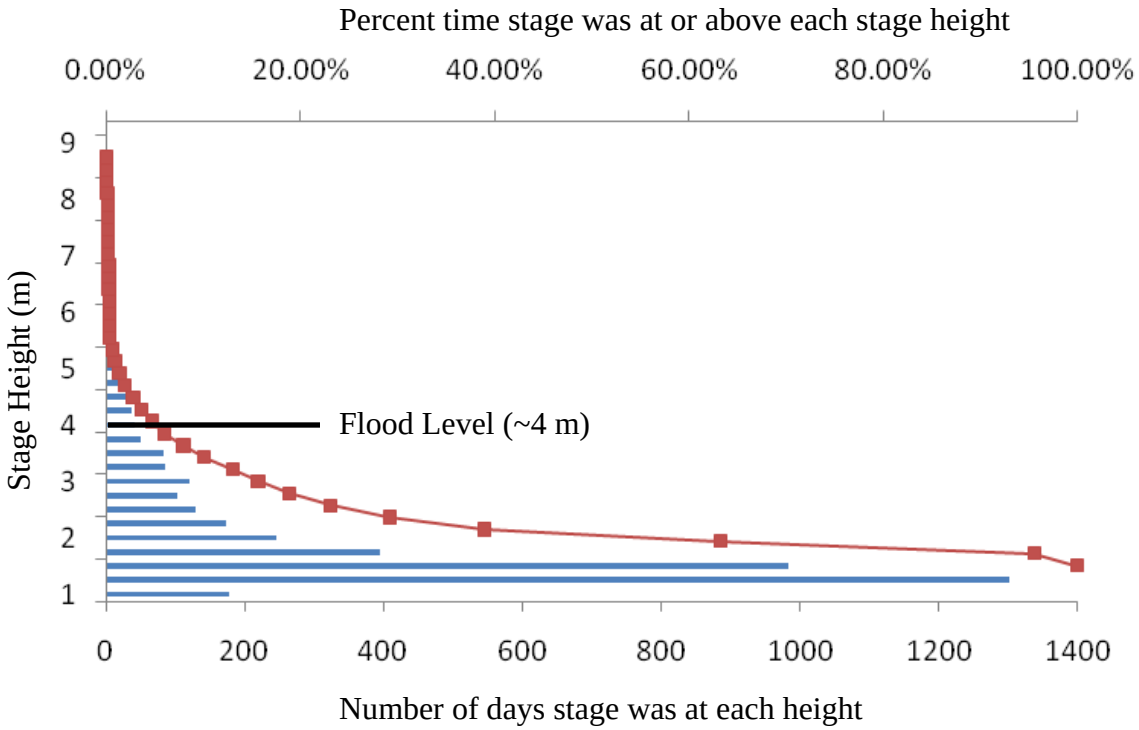

Figure 8: Cumulative percent graph showing daily stage height frequency and percent time versus elevation. Note ~ 3.1 % of the time stage heights were at or above the 4m flood stage.

4. Methods

4.1 Characterizing the Active Floodplain

Daily stream gauge data was obtained from the USGS online data archive (http: //www.usgs.gov/) for the following gauges: Tarboro, the 264 Bypass Northwest of Greenville, Greenville, Grimesland, and Washington. The most recent 10 years of stage height data were used in the analysis, except for Grimesland which only had 7 years of data available. Data were inspected for data gaps and other problems (e.g., due to equipment failure). Where mean stage data were not available, maximum stage data were used (e.g., Site 4, Greenville gauge). Stage data were adjusted to the actual elevation (NAVD88) based on the reference level for the gauge station reported on the USGS web site. For each data set, a cumulative frequency curve of the stage height data was created using Excel's statistical package to evaluate the percent time the water level was at or below a given elevation, i.e., the percent time of inundation (Figure 9). These percentages were then used to define the active floodplain on a digital elevation model (DEM) (Figure 9). More specifically, LiDAR (**Li**ght **D**etection **a**nd **R**anging) DEM datasets for each sub-area (in NAVD88 datum) were obtained from the North Carolina Department of Transportation (NC DOT) and were converted into percent-time-flooded maps using the raster calculator tool in Arc GIS (Figure 10). Once the LiDAR DEMs had been converted into percent-time-flooded rasters, the active floodplain was differentiated by outlining the area where flooding occurred more than one percent of the time at each location. This portion of the map is referred to as the "active floodplain". A 1% time of flooding was used to attempt to capture areas that were more frequently flooded and thus are likely to have more steady sedimentation over time.

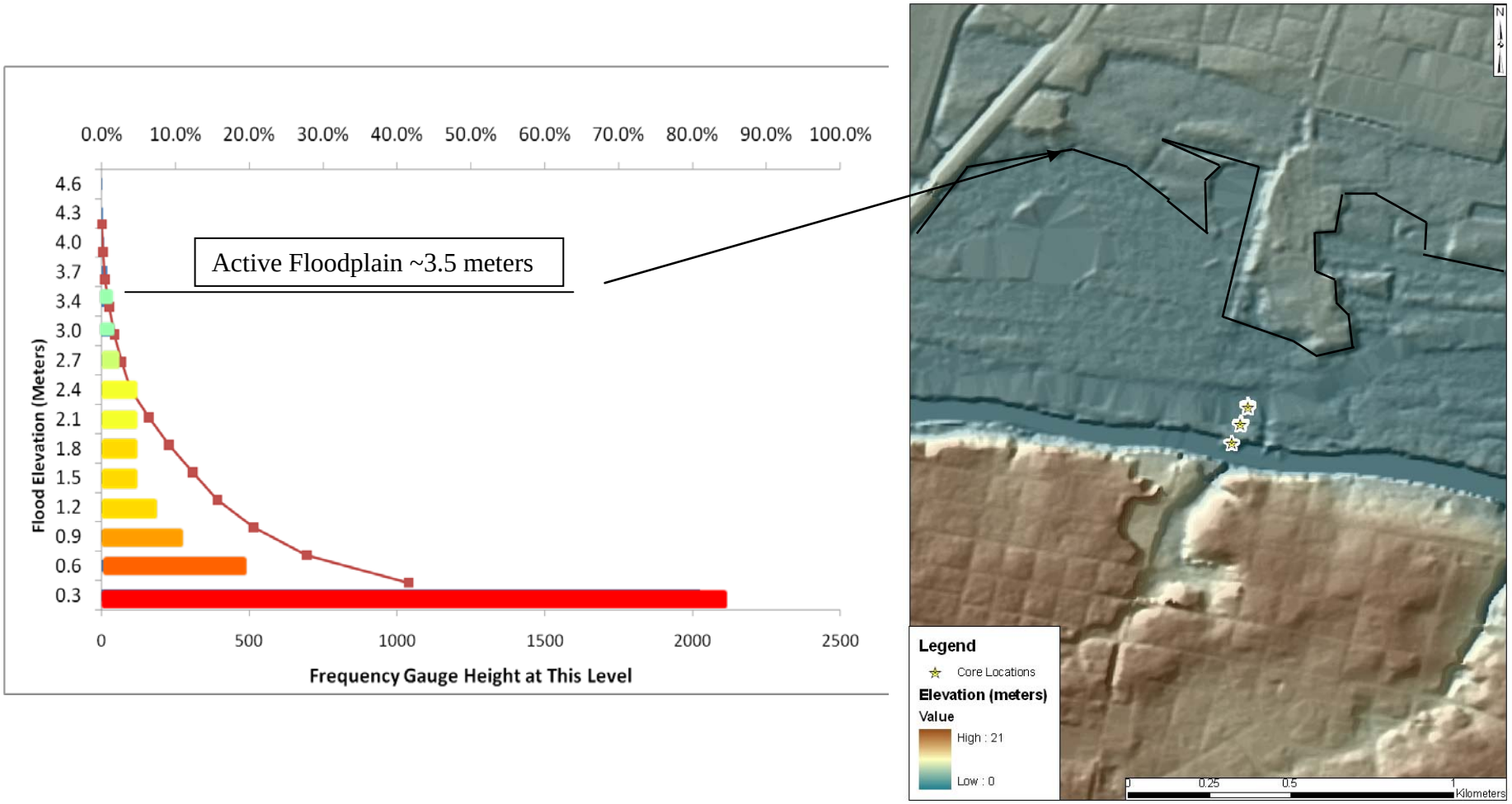

Figure 9: Histogram of stage heights (m) for the Tar River (left) and DEM data at Site 4 encompassing the USGS Greenville, NC gauge. The "active floodplain" was estimated to be below the 1% time flooded elevation (~ 3.5-m elevation at this site). Note this level in the graph and outlined in the map at the right and in Figure 10.

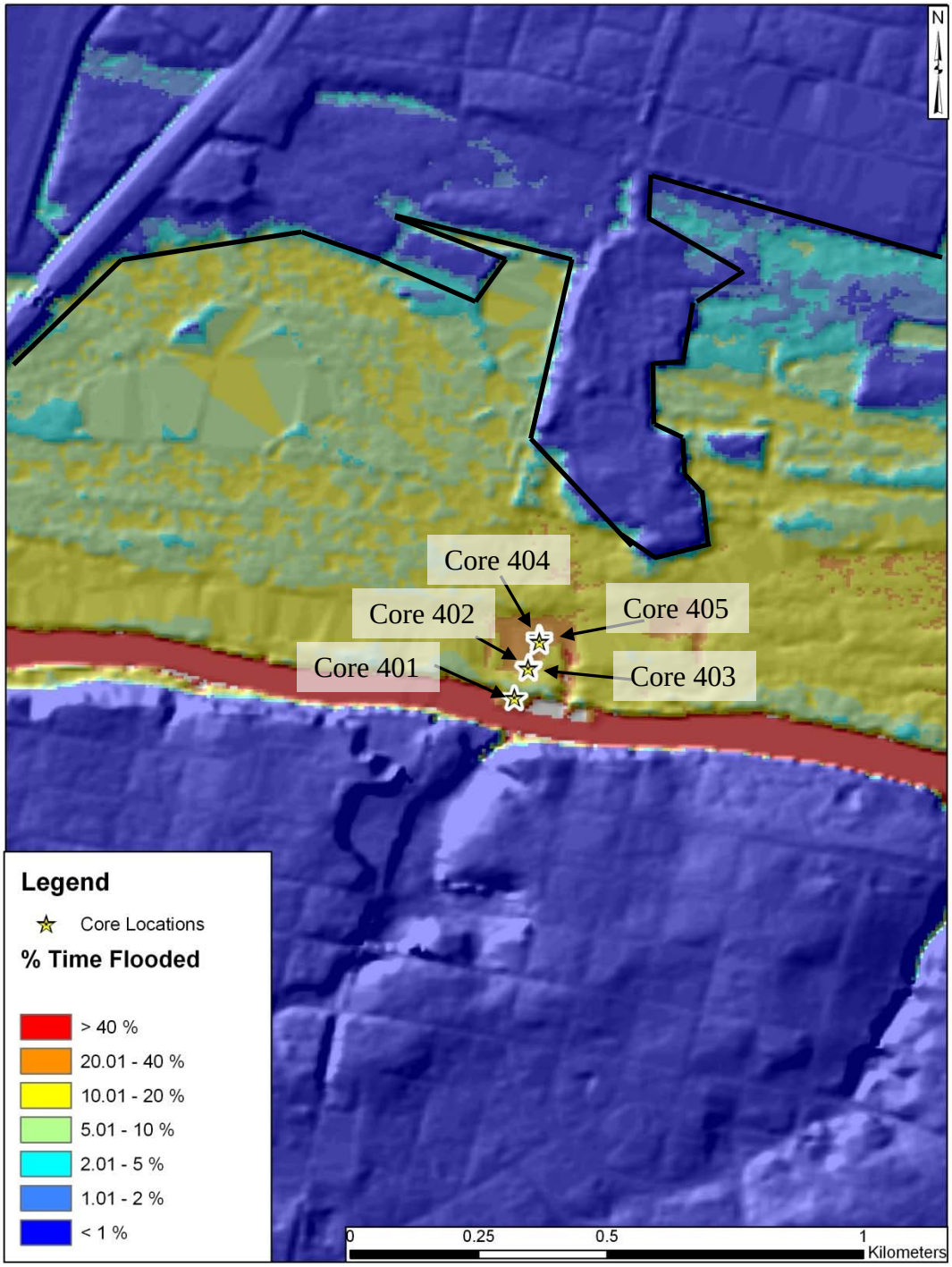

Figure 10: Map showing percentage of time flooded for Site 4. Note, core numbers are labeled on the map and increase with distance from the main channel. Note position of the "active floodplain" is shown by the black line.

To gain insight on the overall characteristics of the active floodplain (i.e. relief, percent time flooded, and elevation) DEM data were clipped in to the active floodplain Arc GIS. Attribute tables were then imported into Sigma Plot to create histograms at each site. Mean and standard deviation for the floodplain elevation data at each site was calculated from these data using Excel.

4.2 Sediment Analysis

At each site, cores were collected on transects perpendicular to the main channel of the Tar River. Typically a core was obtained at the river's edge (within 1 to 2 meters of the water during low flow) and subsequent cores were spaced 50-m apart along transect. Cores were numbered with increasing values with distance from the channel. The site number was included in the core names for identification. For example, Site 4 has cores 401-405 moving landward from the river channel (Figure 10). Typically, three cores were collected along each transect, however, the Site 4 transect has five cores.

Cores were obtained by driving an aluminum irrigation pipe (~7 cm interior diameter) into the ground with a sledge hammer until either refusal or total penetration (usually ~ 1 m). In areas where sediments were very compacted, a Russian coring system was used. Russian sub-cores were collected in half-meter increments with an overlap of 10 cm.

Cores collected were split, photographed, and down-core changes in lithology and organic matter were described. Cores were then sub-samples at 2-cm intervals. Core sections that had evident layering were sub-sampled at the increments of the laminations, e.g., approximately every 1 cm (Cores 302 and 401).

Grain-size analysis was performed on cores to obtain sedimentological insight and to evaluate potential influences on radionuclide activities. All grain size samples were sonicated in a 0.05% calgon solution for 10 minutes. Samples were then wet sieved through a 63-micron sieve, removing the fine fraction from the sample. The sand fraction was then transferred to a pre-weighed boat, dried in a 90°C desiccating oven over night (at least 12 hours) and weighed.

To investigate the effect of sediment grain size on radionuclide data which has been shown affect overall activities seen in sediment. One core collected in close proximity (within ~1 m of the original core location) of Core 602 was analyzed by pipette analysis following the methods described in Folk (1974). Samples were placed in 100 ml jars with a 50 ml solution of 10% calgon (100g calgon / 1000ml deionized water), shaken vigorously, and sonicated for 10 minutes. The sample was sieved with deionized water through a 63-micron sieve into a glass cylinder, and then the volume was brought up to 1000 ml. After shaking vigorously for 1 minute, a 20 ml aliquot was taken at a depth of 20 cm and subsequent samples were collected at specific times and depths over a 5-day period. Each 20-ml aliquot was dried in a pre-weighed boat at 90°C desiccating oven (~12 hrs). Samples were then re-weighed, and the mass of the sediment, after subtracting for the dispersant mass, was calculated. Data were reduced to obtain the sand, silt, and clay percentages within each sample. Aliquots were corrected for volume and differenced to obtain the mass of each phi size lost. The sand percentage was calculated by dividing sand mass (all sediment trapped on the 63-micron sieve) by the total calculated sediment mass.

4.3 Sediment Accumulation

Samples were analyzed for ^{210}Pb (half life 22.3 yrs) and ^{137}Cs (half life 30.1 yrs) activities down core, allowing for rates to be calculated back approximately 100 yrs and 50 yr respectively. Alpha spectroscopy was used to quantify ^{210}Pb following a modified method from Flynn (1962) and Nittrouer et al., (1979). Approximately 1- 1.5 g of sediment was spiked with 1 ml of ^{209}Po as a yield determinant. Samples were partially digested with 8 molar nitric acid by microwave heating, and Po was electrodeposited onto nickel disks in a dilute hydrochloric acid solution. Supported activity was determined by plotting total ^{210}Pb activity versus depth (Figure 11), and the average activity remained constant (i.e., became a consistent value with depth), this was assumed to be the supported level and the average activity and a standard deviation were determined. This supported level was subtracted from the total activity to calculate the “excess” activity of ^{210}Pb.

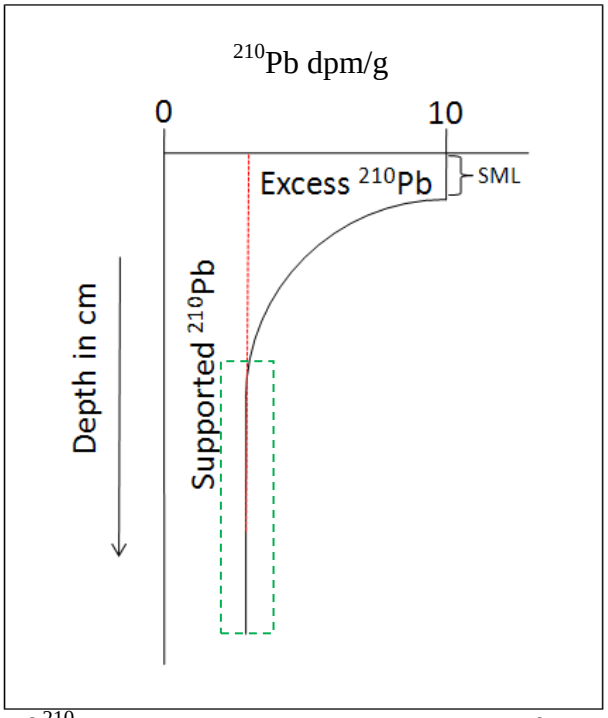

Figure 11: Ideal profile of ^{210}Pb activity versus depth down core for a site with steady-state sedimentation. The supported ^{210}Pb is denoted by the dotted line, and the surface mix layer (SML) is labeled at the top of the core. The dotted box shows the area where the ^{210}Pb activity is averaged to attain the "supported" value.

The activities of ^{210}Pb and ^{137}Cs were measured via direct gamma spectroscopy. Samples were dried, homogenized, and packed into a standardized counting vessel. Samples were counted on one of four low-background, high-efficiency, high-purity Germanium detectors (BEGe-, Coaxial-, LEGe-, and Well-type) coupled with a multichannel analyzer (Meriwether et al., 1988, Corbett et al., 2004). ^{226}Ra activities were measured to determine supported values for ^{210}Pb. Samples were allowed to equilibrate for no less than three weeks before counting, ^{226}Ra is then determined by counting gamma emissions of its granddaughters, ^{214}Pb (295 and 351 keV) and ^{214}Bi (609 keV) (Corbett et al., 2006). ^{137}Cs activities were calculated based on the net counts at the 661.7 keV photopeak (Corbett et al., 2004).

Where steady-state sedimentation was apparent (i.e., a down core log-linear profile was observed) excess ^{210}Pb activity was regressed to calculate the vertical sediment accumulation rate. The rate is determined by dividing the decay constant by the slope (- λ / slope of the regression line), following the simple model (Appleby and Oldfield, 1992; Corbett et al., 2006) Equation 1:

$$A_z = A_0 e^{\frac{-\lambda z}{s}} \qquad (1)$$

Where A_z and A_0 (dpm/g) equal the excess ^{210}Pb activity at a given depth x and 0-cm depth respectively; λ is the decay constant of ^{210}Pb (0.031/yr); s is the accumulation rate (cm/yr). For most cores ^{210}Pb activities determined by alpha spectroscopy were employed for the analysis of sedimentation rates, but, where alpha spectroscopy data could not be used due to apparent fluctuations in the supported activity, gamma spectroscopy data was used to obtain ^{226}Ra and excess ^{210}Pb activities (i.e. the supported level). This was necessary in 10 of the cores collected listed in Table 2.

The peak of ^{137}Cs (1963) was used to corroborate the ^{210}Pb derived sediment accumulation rates (Figure 12). The depth to the highest activity peak (associated with the maximum testing of nuclear weapons in 1963) was found and then a simple (depth / time) equation was used to calculate the sediment accumulation rate (Meriwether et al., 1988; Lynch et al., 1989). When a ^{137}Cs peak was not well defined, a range of estimates were used to determine a maximum and minimum accumulation rate.

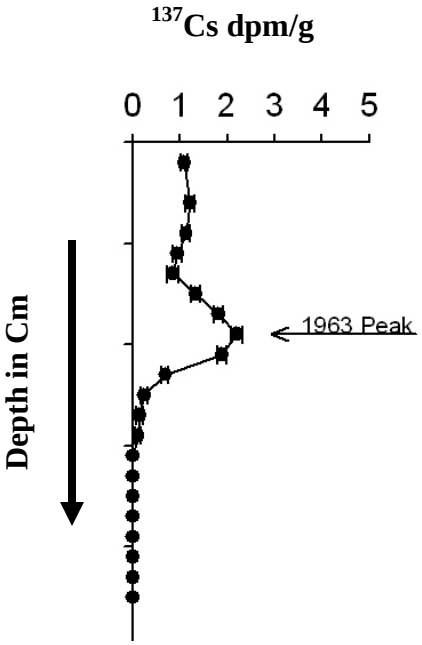

Figure 12: Example down core ^{137}Cs profile indicating the 1963 peak from atmospheric testing of nuclear weapons.

After accumulation rates were calculated from ^{210}Pb and ^{137}Cs data, cores were placed into three groups based on the quality (how well the assumptions held up) of the data (i.e., good, intermediate, and poor) and how well the radionuclides could be used to estimate the sediment accumulation rates. Cores that were classified as "good" had a well-defined ^{137}Cs peak, the ^{210}Pb data showed a clear exponential decrease in activity with depth with a high r^2 value (i.e., higher than 0.7), and both the accumulation rates determined from the two independent methods were within error. "Intermediate" quality cores had one of the radionuclide methods give a convincing accumulation rate; however, the other radionuclide data could not be used, had a large degree of uncertainty or the rate disagreed. Cores considered to have "poor" data for sedimentation rates did not have radionuclide data sets that were usable for rate analysis (i.e., data were non-steady-state, Walsh et al., 2004).

4.4 Investigation of Flood Deposition

Flooding occurred within the study area on December, 12, 2009, and to gain some insight into deposition from this flood several sites were revisited and additional cores were collected. Previous work has shown flood deposition can be measured using ^{7}Be ($t_{1/2}$ = 53.3 days), a radionuclide produced by cosmic spallation reactions with nitrogen and oxygen in Earth's atmosphere (Dutkiewicz and Husain, 1985; Olsen et al., 1986; Canuel et al., 1989). In this study, activity levels of ^{7}Be in sediments were measured via direct gamma spectroscopy. Samples were dried, homogenized, and packed into a standardized counting vessel. Samples were counted on one of four low-background, high-efficiency, high-purity Germanium detectors (BEGe-, Coaxial-, LEGe-, and Well-

type) coupled with a multichannel analyzer (Giffin and Corbett, 2003). ^{7}Be activities were calculated based on the net counts at the 477 keV photopeak (Corbett et al., 2004).Whole-core inventories for ^{7}Be were calculated for pre-flood and post-flood cores and compared to evaluate the presence of deposition after flooding.

4.5 Estimating Sediment Storage

To enable estimation of sediment storage, sediment accumulation rates measured at each site were extrapolated over adjacent floodplain areas, and ultimately the entire study area (i.e., Tarboro to Washington). Shapefile polygons of the active floodplain were clipped by a buffer with distance from the main channel (i.e., 50 and 100 meters) to define areas represented by accumulation rates measured from cores. Distance was chosen rather than elevation because a more prominent relation between distance from channel and accumulation rate was seen. For example the accumulation rate for Core 101 was extracted over the area within the 0-50 m buffer, Core 102 was extrapolated over the 50-100 m buffer, and Core 103 was extrapolated over the remaining distance to the edge of the active floodplain (> 100 m). Areas calculated from these polygons were then multiplied by the accumulation rates measured within the floodplain through radionuclide analysis to calculate a volume of sediment storage.

Site 4 was calculated in a slightly different manner due to the extra cores collected within the transect. In a similar manner as the other sites, three buffers were used; however, the floodplain represented by each of the buffers was then broken into two different regions based on the amount of time flooded. The first buffer remained the same as the previous methods since only one core (i.e., 401) was collected within 50-m of the

river channel. The next two buffer zones were further subdivided down based on the percent time flooded regimes that each core represented.

Rates of sediment storage at the individual sites were ultimately extrapolated over the entire length of the river within the study area (i.e., from Tarboro to Washington) by determining the river length at each site and calculating the amount of storage per unit length of river (i.e., $m^3$of sediment/km of shoreline/year). This value was then multiplied by the reach length (in km) that each site was estimated to represent. This process was completed for the full length of the river within the study area (98.5 km). This total volume was converted to a mass by taking a literature value of dry bulk density for floodplain sediment of east coast rivers (i.e., 1 g/cm3, Schenk and Hupp, 2009).

5. Results

5.1 Floodplain

The seven sites examined in this study show, a variety of differences in total relief, percent-time flooded, and floodplain area. For example, a general trend of increasing percent-time flooded with increasing distance downstream is evident (Table 2). Also, a trend of decreasing total relief is seen with increasing distance downstream.

Site 1 has a narrow floodplain with scroll bars and tributary channels creating notable relief (Figure 13). This site because of its relief and hydrology, has a relatively small amount of regularly flooded area (Figure 14). Note, a small drainage channel in the floodplain in close proximity to the transect on which cores were collected. Drainage pathways like these have been shown in previous studies to affect accumulation rates, but development in this area is minimal.

Site 2 is 21 km downstream from Site 1 (Figure 15). Site 2 has a wider active floodplain than Site 1 with fewer tributaries and less apparent relief. Due to the lack of a gauge station near this site, stage data from USGS's Tarboro and the 264 Bypass gauges were used to estimate a percent-time-flooded curve (with a 40:60 weighted average respectively). More area is flooded more often at Site 2 compared to Site 1 (Figure 16); however, similar geomorphologic landforms to Site 1 can be seen.

Table 2: Summary of all data for all sites and cores rating for all cores are listed as G for good, I for intermediate, and P for poor. Note, cores with backgrounds indicated to be calculated from Gamma indicate that ^{210}Pb accumulation rates were obtained through gamma spectroscopy.

Site	Distance From Channel	% Time Flooded	% Mud	^{210}Pb Accumulation Rate	Background	^{137}Cs Accumulation rate	Rating
	Meters	%	%	cm/y	Activity	cm/y	G, I, & P
Site 1 Core 101	1	11.4	13.0	1.08 +/- 0.2	1.05 +/- 0.08		I
Site 1 Core 102	50	16.3	43.5	0.4 +/- 0.1	4.4 +/- 0.55*	0.28	G
Site 1 Core 103	100	11.4	18.2	0.16 +/- 0.03	2.89 +/- 0.96*	0.19	G
Site 2 Core 201	1	53.4	15.6				P
Site 2 Core 202	50	7.4	34.8	0.12 +/- 0.02	2.6 +/-0.42	0.11	G
Site 2 Core 203	100	9.6	44.8	0.18 +/- 0.03	2.64 +/- 0.45	0.15	G
Site 3 Core 301	1	37.0	23.7	0.59 +/- 0.07	2.17 +/- 0.19		I
Site 3 Core 302	50	13.7	28.5	0.15 +/- 0.02	2 +/- 0.2	0.15	G
Site 3 Core 303	100	7.9	31.2	0.13 +/- 0.02	2.52 +/- 0.37	0.13	G
Site 4 Core 401	1	19.1	34.8		1.41 +/- 0.2	0.23	I
Site 4 Core 402	50	19.1	42.9	0.29 +/- 0.06	4.29 +/- 0.85*	0.32	G
Site 4 Core 403	55	23.7	43.0	0.45 +/- 0.05	3.5 +/- 0.46	0.40	G
Site 4 Core 403 PF	55	19.1	34.9	0.14 +/- 0.02	5.6 +/- 0.55*	0.23	I
Site 4 Core 404	95	19.1	29.9	0.14 +/- 0.01	2.9 +/- 0.33	0.23-0.32	I
Site 4 Core 405	100	30.0	31.5	0.39 +/- 0.05	1.8 +/- 0.20	0.23-0.32	G
Site 5 Core 501	1	43.7	18.1	0.21 +/- 0.03	3.20 +/- 1.17*	0.19	G
Site 5 Core 502	50	43.7	29.1	0.09 +/- 0.01	3.51 +/- 0.82*	0.19	I
Site 5 Core 503	100	43.7	5.4		1.24 +/- 0.30	0.02	I
Site 6 Core 601	1	43.7	33.7	0.84 +/- 0.16	2 +/- 0.46	0.53	I
Site 6 Core 601 PF	1	43.7	31.8	0.42 +/- 0.04	4.39 +/- 0.44*	0.36-0.45	G
Site 6 Core 602	50	43.7	35.5	0.24 +/- 0.05	3.87 +/- 0.80*	0.19	G
Site 6 Core 603	100	43.7	34.8	0.2 +/- 0.03	3.80 +/- 0.87*	0.19	G
Site 6 Core 603 PF	100	43.7	17.4	0.21 +/- 0.03	3.56 +/- 0.66*	0.45	I
Site 7 Core 701	1	46.3	9.5	0.91 +/- 0.07	0.99 +/- 0.24	0.83	G
Site 7 Core 702	50	3.1	1.5		0.64 +/- 0.01	0.06	I
Site 7 Core 703	100	3.1	1.9		0.8 +/- 0.03	0.02	I

* denotes background was calculated from gamma data.

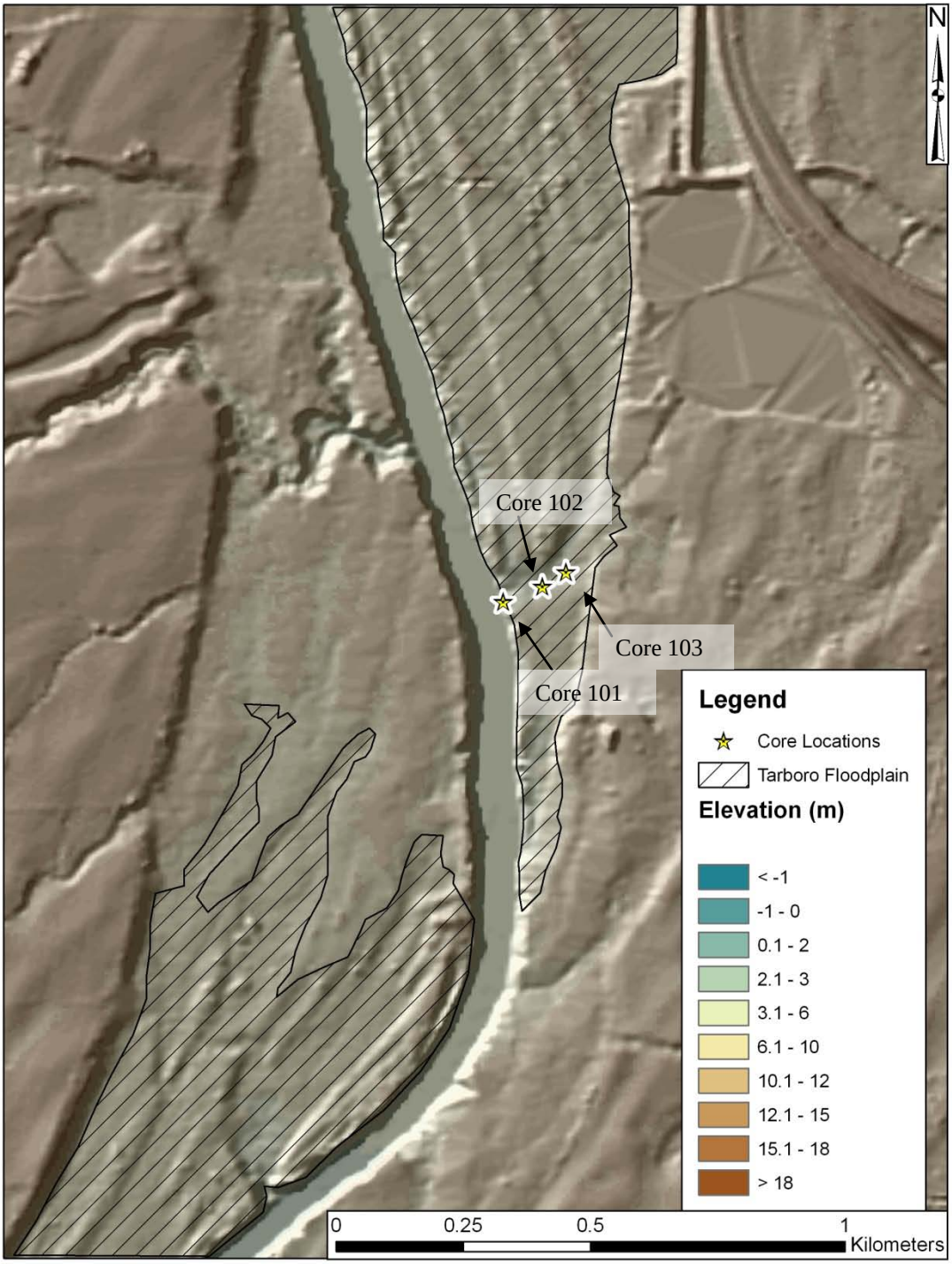

Figure 13: Map showing Site 1 whose active floodplain has a relief of 4.3 meters with a minimum elevation of 5.18 meters and a maximum elevation of 9.5 meters.

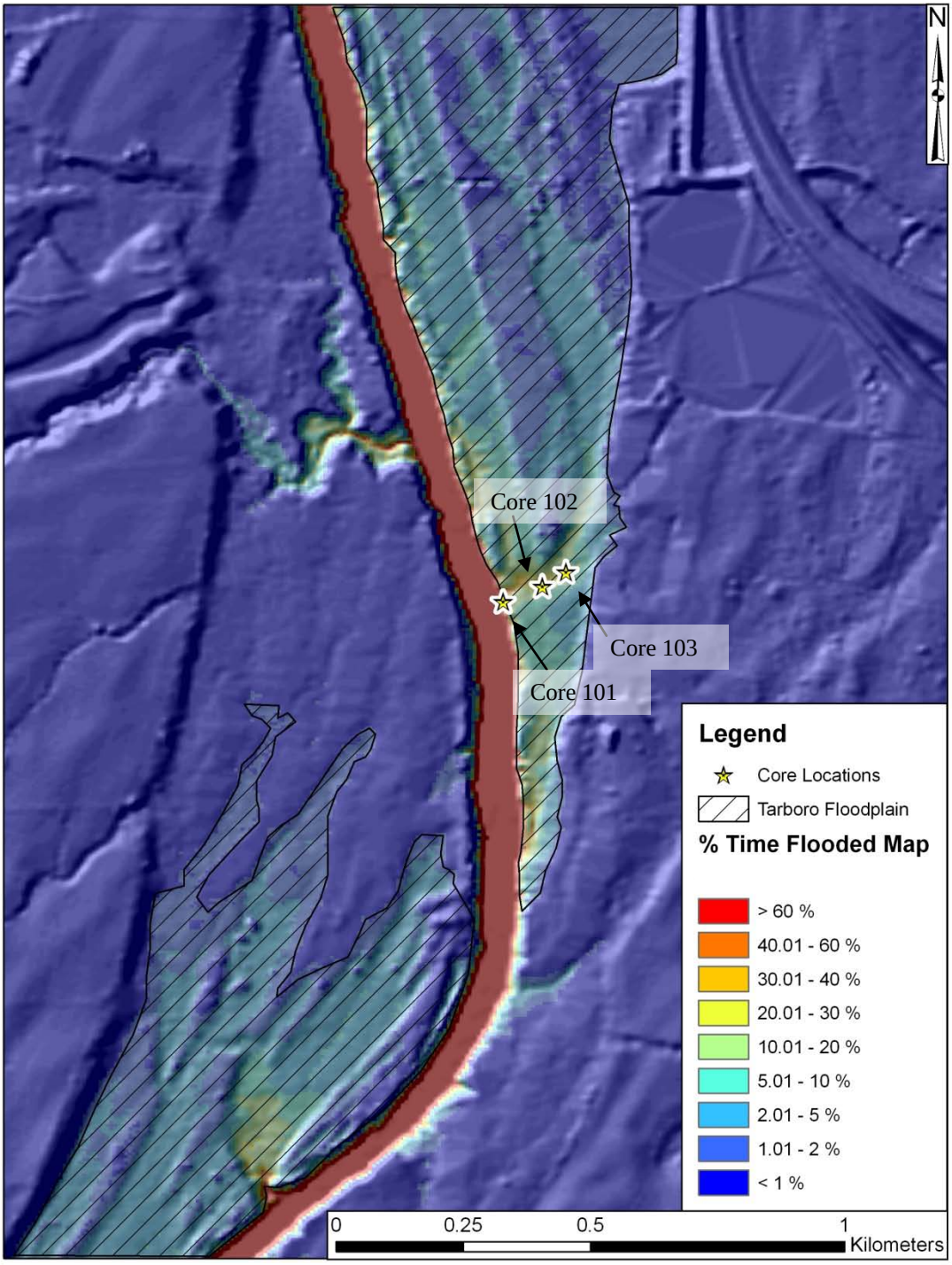

Figure 14: Map showing the active floodplain and the percent-time flooded for Site 1. The combined total area of the active floodplain is 1 km^2, and the area covers a 1.5-km-long reach of the Tar River.

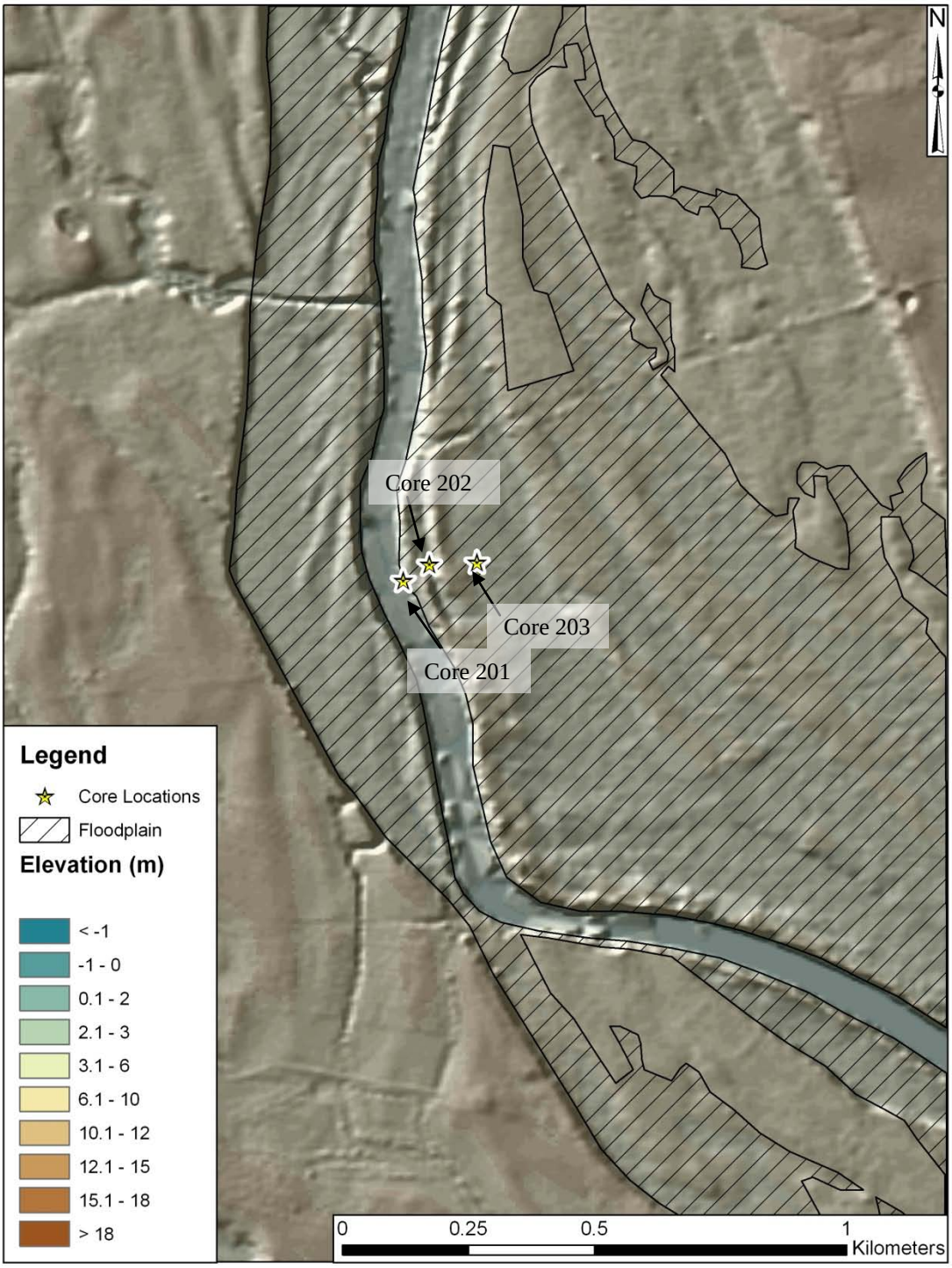

Figure 15: Map showing the active floodplain of Site 2 which has a relief of 4 meters with a minimum elevation of 4 meters and a maximum elevation of 8 meters.

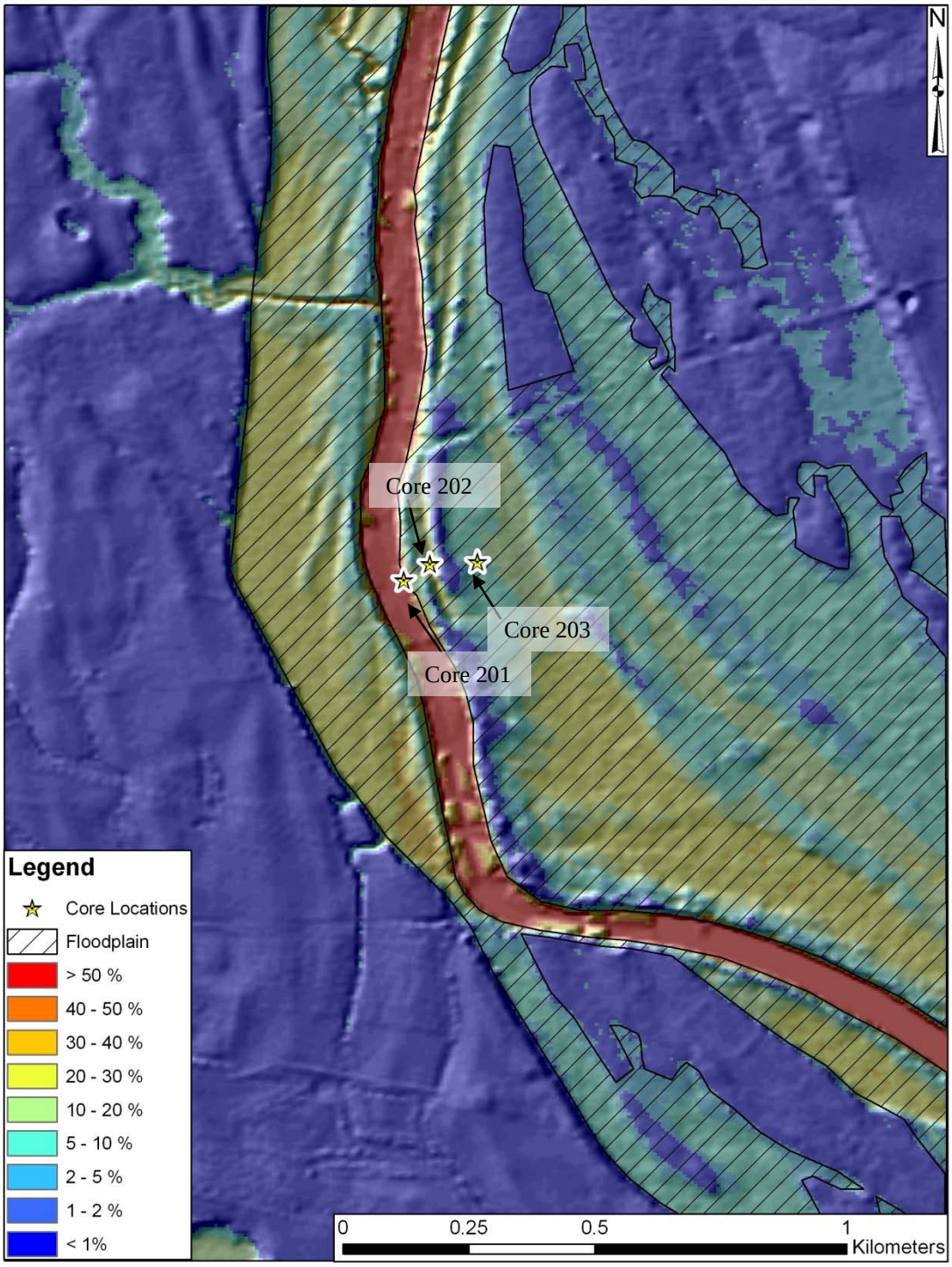

Figure 16: Map showing the active floodplain and the percent-time flooded for Site 2. The active floodplain encompasses an area of 1.5 km^2, and the area covers a river reach 2.5 km long.

Site 3 is 20-km downstream from Site 2 (Figure 3). Site 3 has a wider floodplain compared to Site 1 and 2 with a total relief between the relief of these sites (Figure 17). The floodplain is anthropogenically influenced by adjacent ponds and farm land, and a bridge segregates the flow of water across the floodplain. The average percent-time flooded is greater than the previous sites, consistent with the trend of increasing flooding time downstream (Figure 18).

Site 4 is 6 km downstream from Site 3, and is less symmetrical than previous sites, all of the active floodplain lies on the northern side of the river (Figure 19). The floodplain of Site 4 is surrounded by forested land; however, a bridge crosses the floodplain, and it forms a high elevation area to the northwest of the core transect. Site 4 has less floodplain area compared to previous sites, The river at this site is very straight and flows almost totally east-west (Figure 20).

Site 5 lies 20-km downstream of Site 4. It has a much wider floodplain southwest of the river with a small amount of floodplain on the opposite bank (Figure 21). This site has less relief than those upstream. In LiDAR data, mounds can be seen parallel to the main channel of the river; these are interpreted to be dredge spoils and may affect flooding processes in the floodplain. Here again, the average percent-time flooded increases relative to those sites farther upstream (Figure 22).

Site 6 is 4 km from Site 5 and approximately 12-km upstream from the Highway 17 bridge in Washington, NC (Figure 3). Site 6 has a narrower floodplain than Site 5 and is located just past a meander in the river where there is very little relief (Figure 23). There are many tributaries within the active floodplain, and human influences can be seen in a variety of forms. A bridge crosses the river at this location dividing the floodplain

hydrologically. Farm land is located directly north of the floodplain, and developed land is to the south. Dredge spoil piles can be seen in this floodplain, similar to Site 5. The average percent-time flooded is high at this site (40 %), and this is anticipated due to its proximity to the estuary (Figure 24).

Site 7 has the widest and most expansive floodplain of all the sites; it is located just upstream of the estuary head (Figure 25). The relief within the active floodplain of Site 7 is very small (Figure 25). Many tributaries enter the river at this site. The percent-time flooded (50 %) for Site 7 is the highest of the study sites (Figure 26).

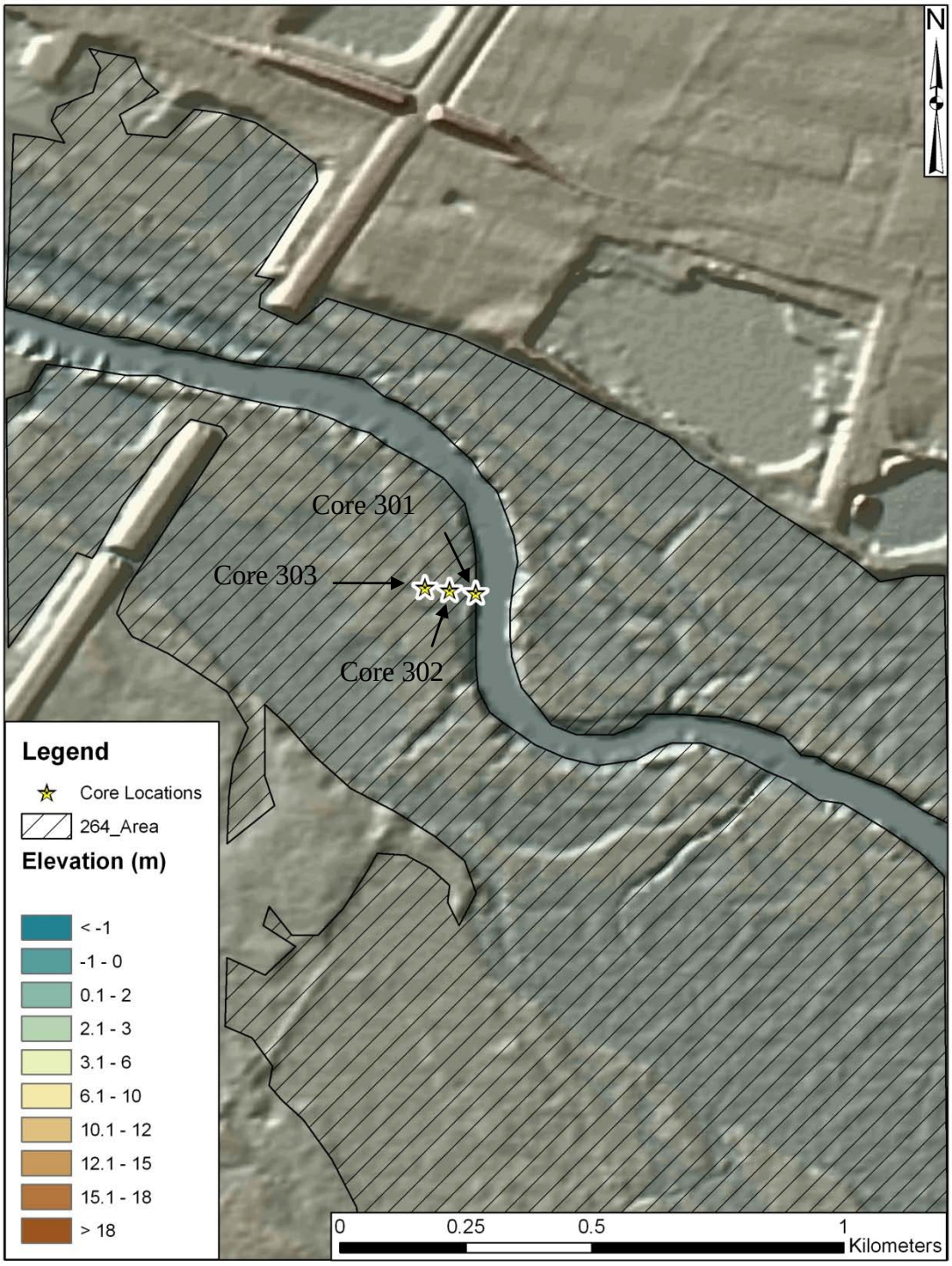

Figure 17: Map showing the active floodplain for Site 3. The active floodplain has a total relief of 4.6 meters with a minimum elevation of 0.6 meters and a maximum elevation of 5.2 meters.

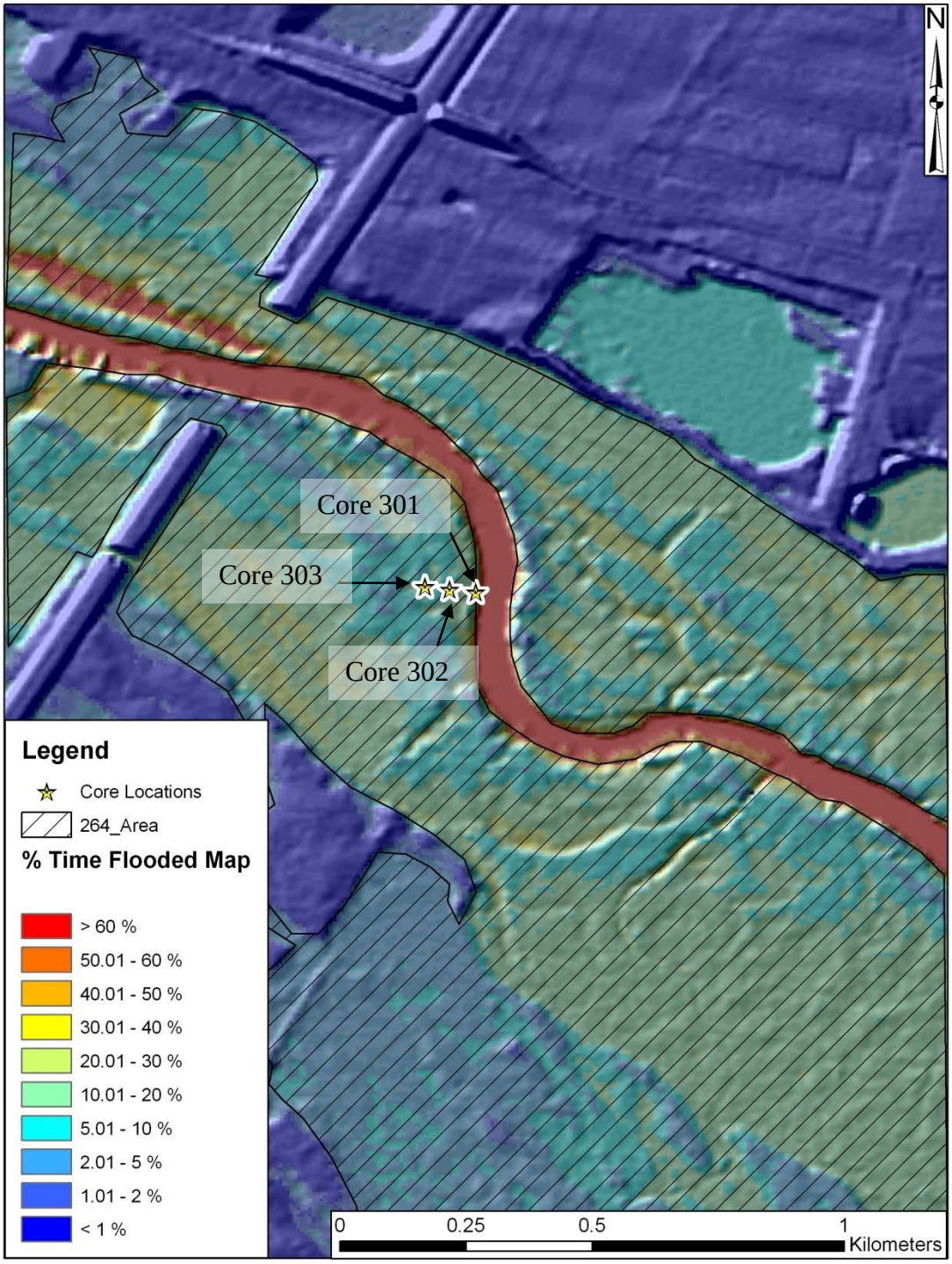

Figure 18: Map showing the active floodplain and the percent time flooded for Site 3. The active floodplain has a total area of 2 km^2, and the area covers a 2.1 km long reach of the Tar River.

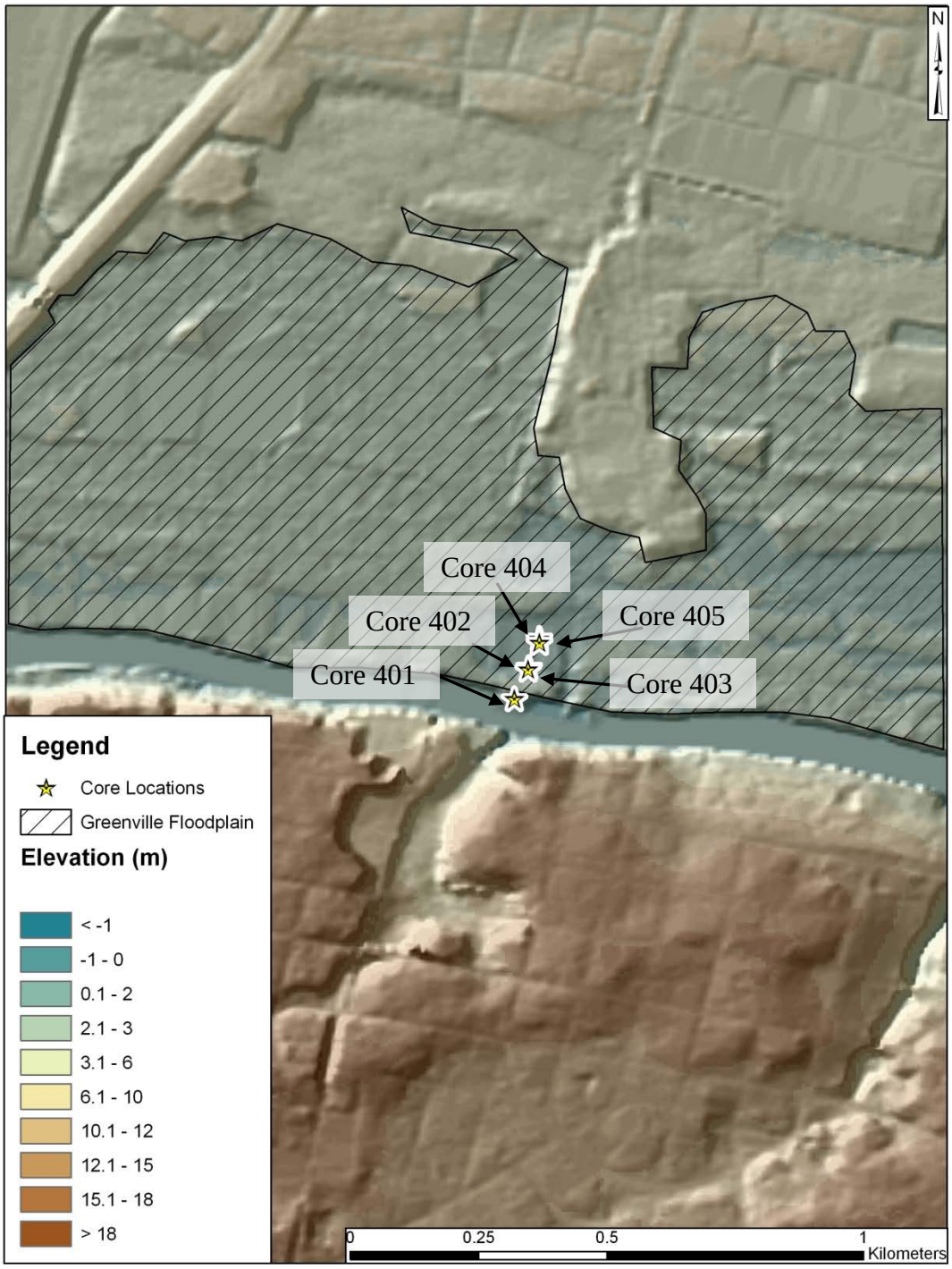

Figure 19: Map showing the active floodplain for Site 4. The north side of the river holds the active floodplain which has a relief of 3.2 meters with a minimum elevation of 0.3 meters and a maximum elevation of 3.5 meters.

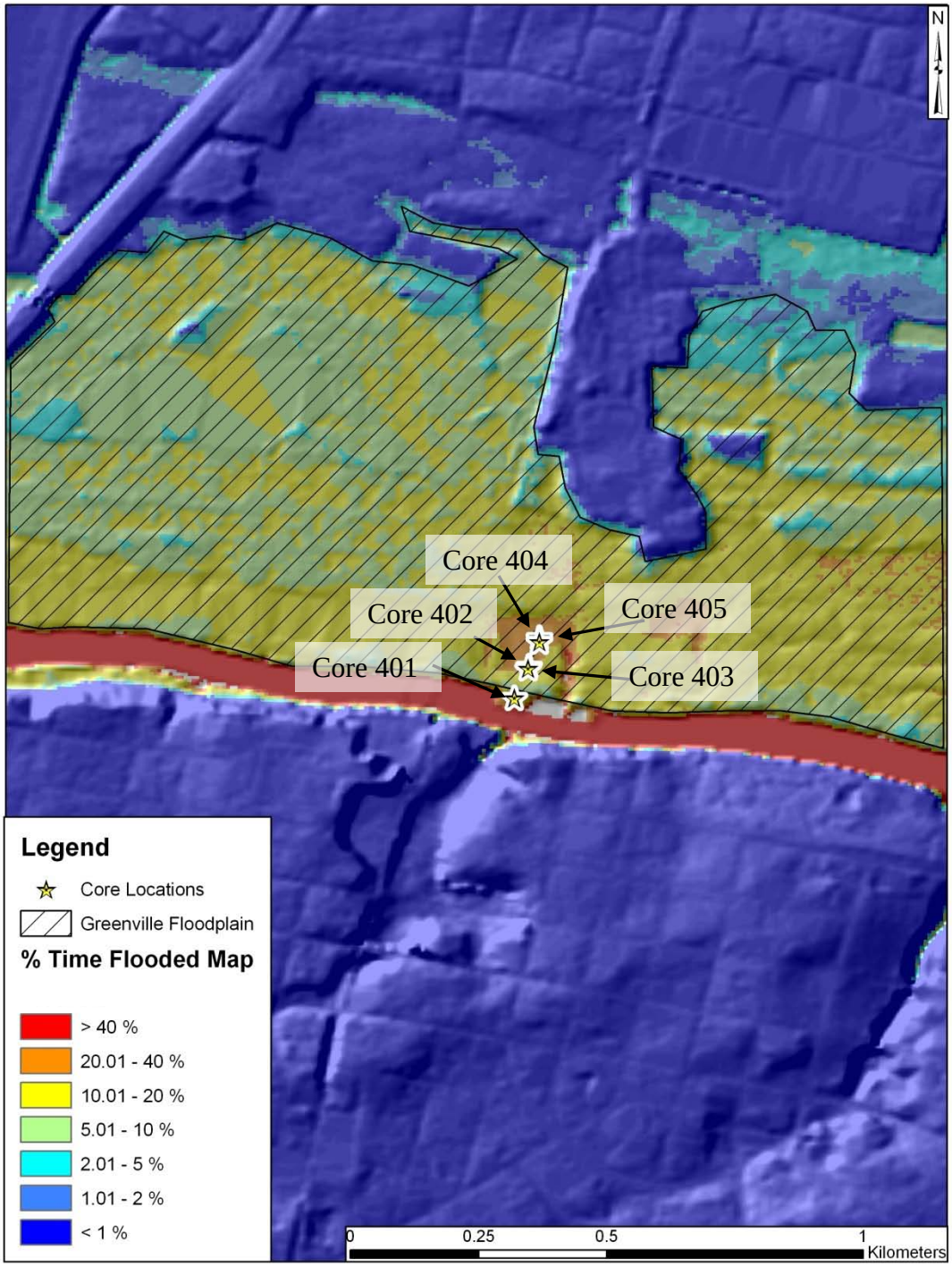

Figure 20: Map showing the active floodplain and the percent-time flooded for Site 4. The active floodplain has a total area of 1.04 km^2 and, the area covers a 1.5-km-long reach of the Tar River.

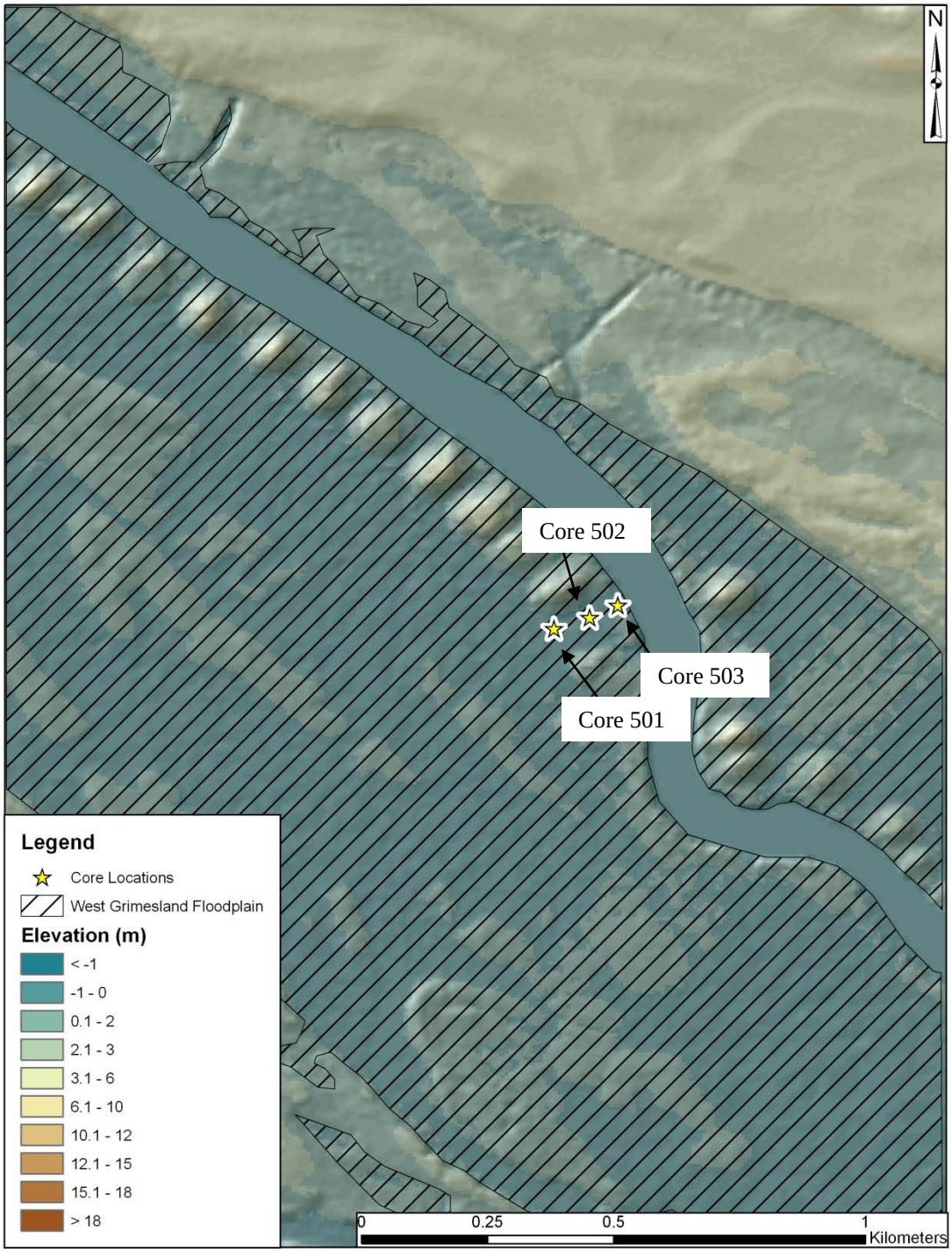

Figure 21: Map showing the active floodplain for Site 5. The active floodplain has a total relief of 1.5 meters with a minimum elevation of 0 meters and a maximum elevation of 1.5 meters above mean sea level.

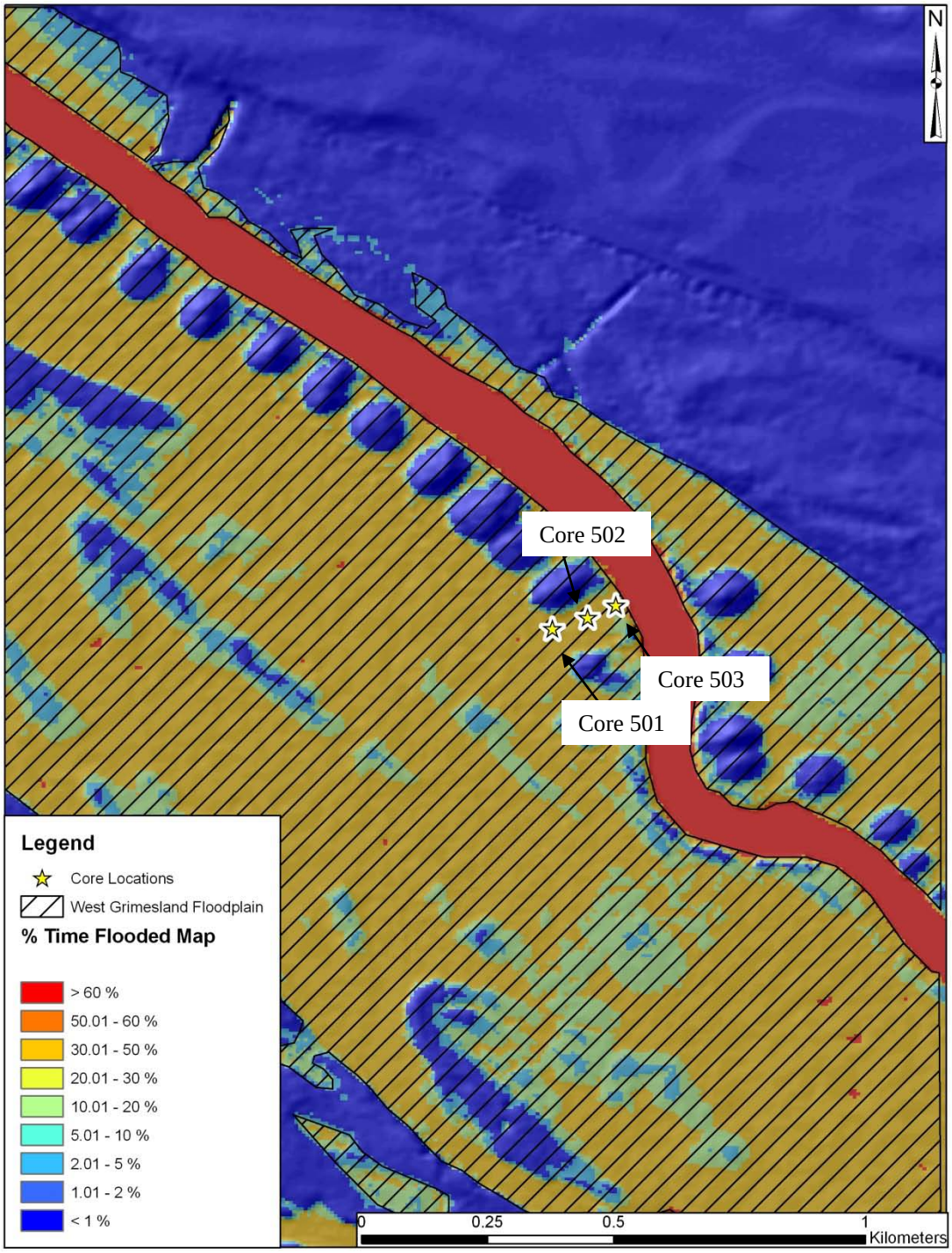

Figure 22: Map showing the active floodplain and the percent time flooded for Site 5. The active floodplain has a total area of 2.13 km^2 with a river reach 2.4 km in length.

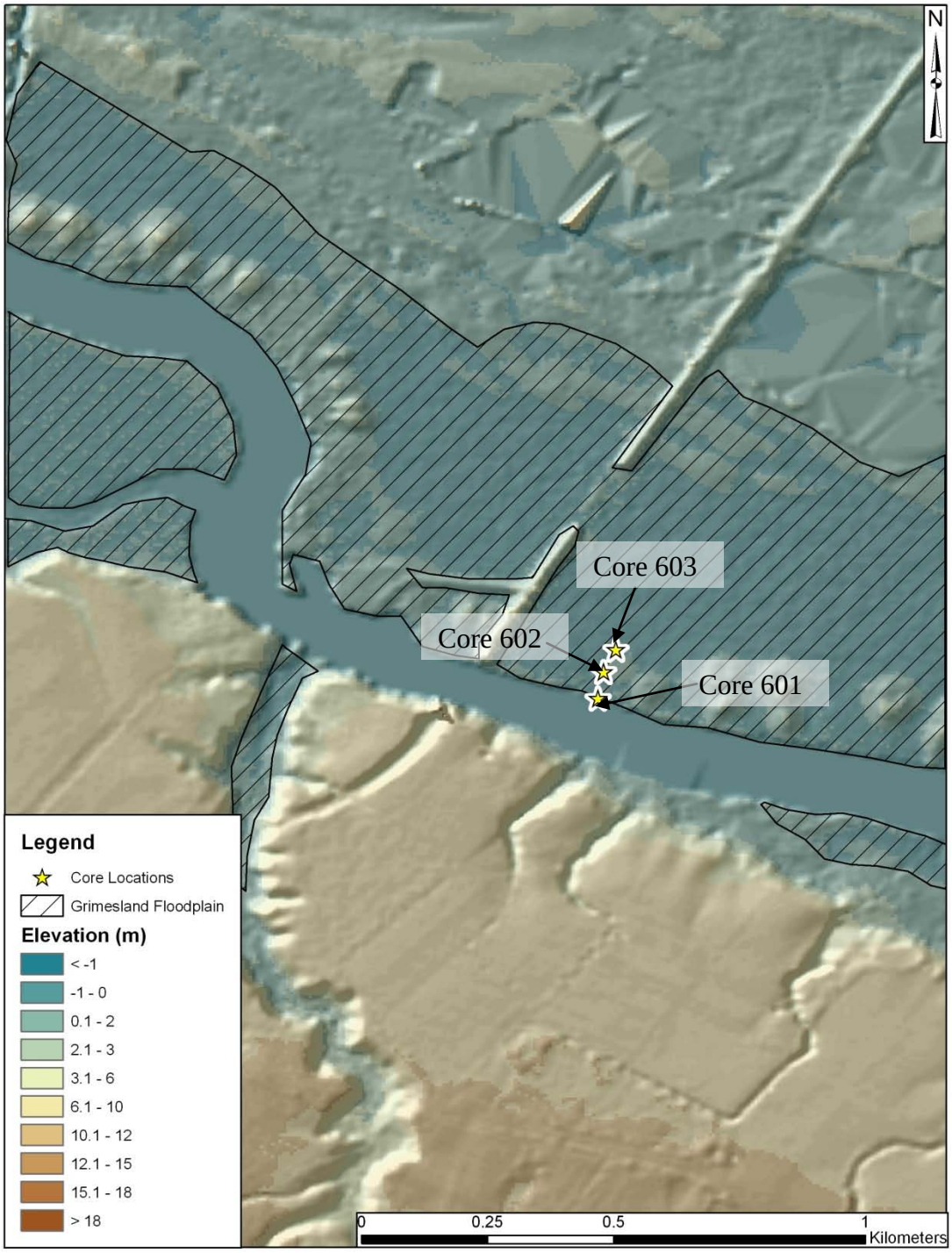

Figure 23: Map showing the active floodplain for Site 6. The active floodplain and has a relief of 1.3 meters with a minimum elevation of sea level and a maximum elevation of 1.3 meters.

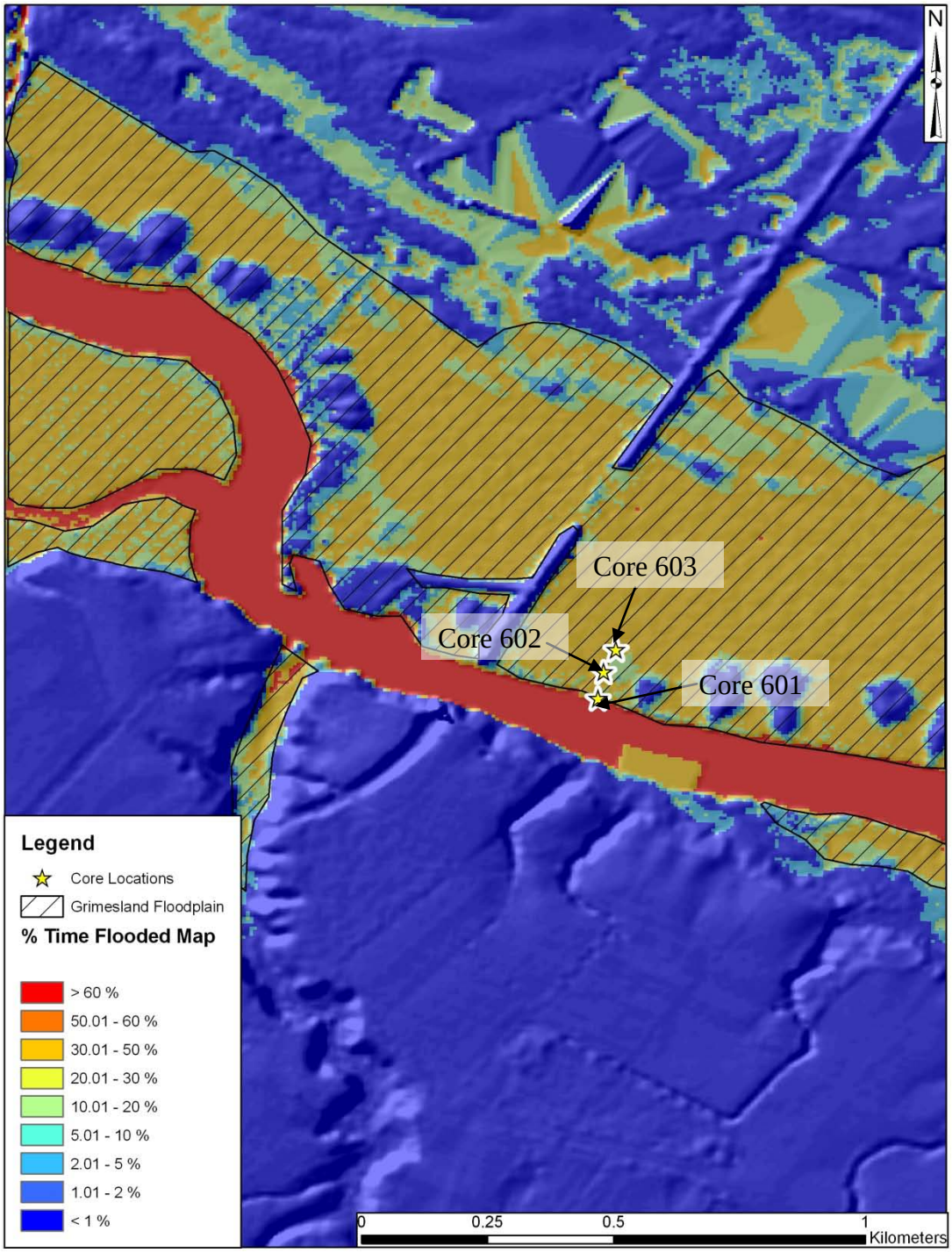

Figure 24: Map showing the active floodplain and the percent time flooded for Site 6. The active floodplain has a total area of 1 km^2, and the area covers a 1.9-km-long reach of the Tar River.

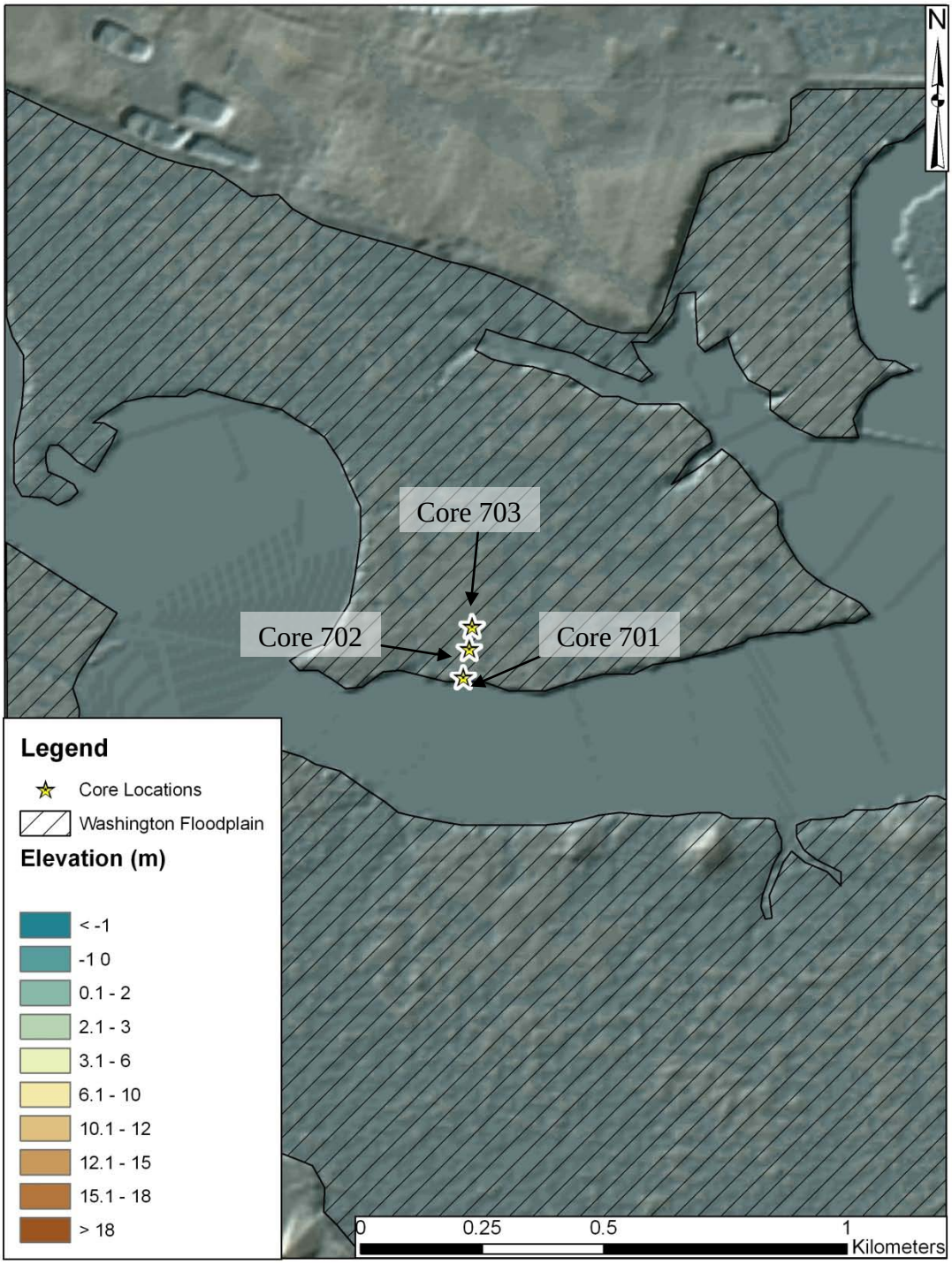

Figure 25: Map showing the active floodplain for Site 7. The active floodplain and has a relief of 1.3 meters with a minimum elevation of sea level and a maximum elevation of 1.3 meters.

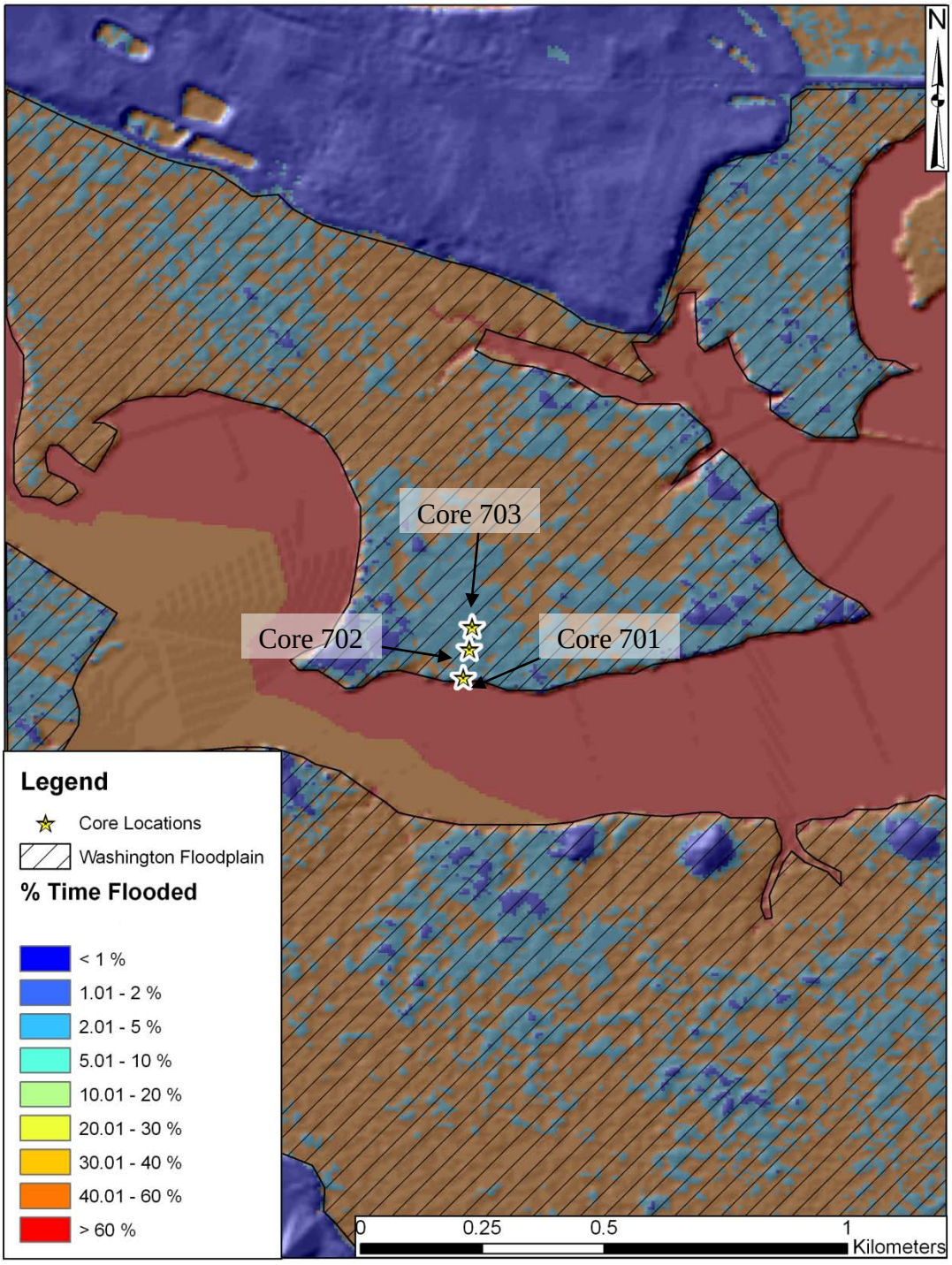

Figure 26: Map showing the active floodplain and the percent time flooded for Site 7. The active floodplain has a total area of 2.33 km^2 and the area covers a 1.8 km long reach of the Tar River.

5.2 Radiochemical and Sedimentological Data

Radionuclide data were analyzed to obtain sediment accumulation rates. ^{210}Pb-based linear accumulation rates measured within the study area ranged from 0.09 to 1.08 cm/yr. Accumulation rates derived from ^{137}Cs range from 0.02 to 0.83 cm/yr. Cores were rated on the quality of the radionuclide data used to estimate the rates (i.e., good, intermediate, and poor; Table 2). The grain-size character of the cores showed considerable variability, percent mud ranged between 1.5 and 50 %, with the majority of the cores having 20-45% mud.

Sediment accumulation rates for Site 1 decrease from 1.08 to 0.16 cm/yr with distance from the main channel. The whole-core average mud percentages from cores at Site 1 range from 13 % in Core 101 to 43.5 % in Core 102 (Figure 27). Site 2 had variable rates of sediment accumulation with distance, and Core 201 was not able to be used for accumulation rate measurements due to the non-steady-state nature of the core. Average mud percentages in cores at Site 2 increase landward from 15.6% to 44.8% (Figure 28). Accumulation rates for Site 3 decrease from 0.59 cm/yr, close to the main channel to 0.13 cm/yr in Core 303. Mud percentages for Site 3 increase from 23.7 to 31.2 % with increasing distance from channel (Figure 29). Site 4 accumulation rates are variable with distance; rates range from 0.14 to 0.45 cm/yr (Figures 30 and 31). Grain size within Site 4 also is variable along the transect, ranging from 29.9 to 43% (Figure 32). Site 5 has decreasing accumulation rates with distance from the river channel (0.21 cm/yr to 0.09 cm/yr), but the last core (Core 503) on the transect is interpreted as having a thin (~2 cm) veneer of excess-^{210}Pb-rich sediment on top of older (no excess ^{210}Pb) sediment, and this interpretation is supported by the ^{137}Cs peak being located near the

surface of the core. Percent mud is variable on this transect (29.1-5.4 %; Figure 33). Accumulation rates in Site 6 decrease landward (0.84 to 0.20 cm/yr), while percent mud on the transect is approximately the same in the three cores (Figure 34).

To help evaluate if grain size (i.e. percent clay) is controlling radionuclide activity in the study, down-core activity from a core immediately adjacent to Core 602 was analyzed by pipette analysis to determine grain size in the fine-grained fraction (Figure 35). Activity data do not show an obvious impact of grain size on the activity profile (Figure 35). As a result no correction for grain size was used when interpreting the activity profiles in this study.

Cores 702 and 703 of Site 7 were both interpreted as having a thin veneer of more recent (with excess ^{210}Pb) sediment on top of older (no excess ^{210}Pb) sediment, and this interpretation is supported by the ^{137}Cs peak being located at the surface of the core (Figure 36). Grain size within the transect shows all three cores are predominantly sandy material with Core 702 and 703 having < 2 % mud on average.

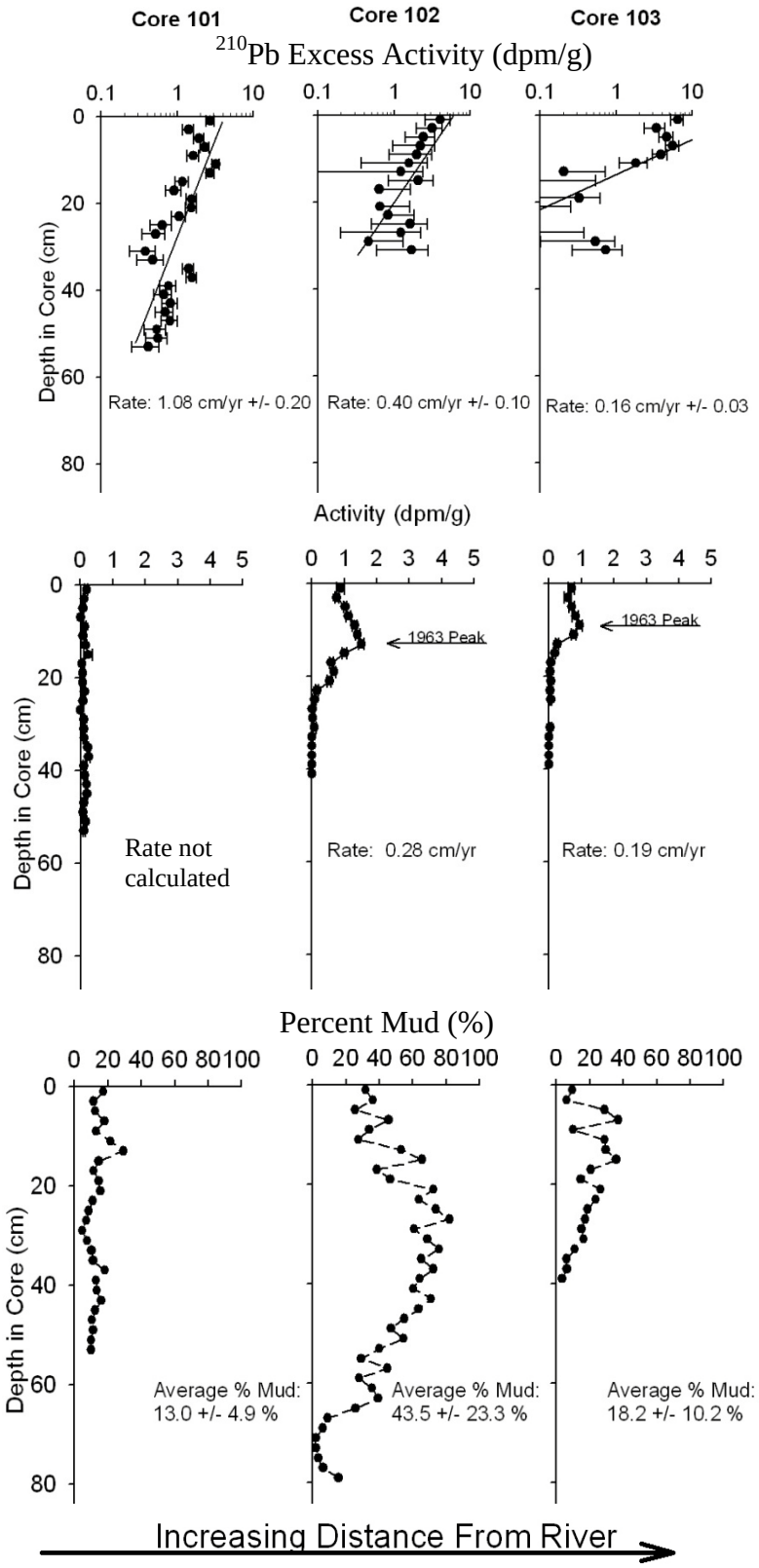

Figure 27: Graphs of ^{210}Pb and ^{137}Cs activities, and mud percent for Site 1. Sediment accumulation rates calculated by ^{210}Pb are shown for all three cores. Core 101 did not have a discernable ^{137}Cs peak so a ^{137}Cs rate was not calculated. Note, accumulation rates generally decrease with increasing distance from river channel.

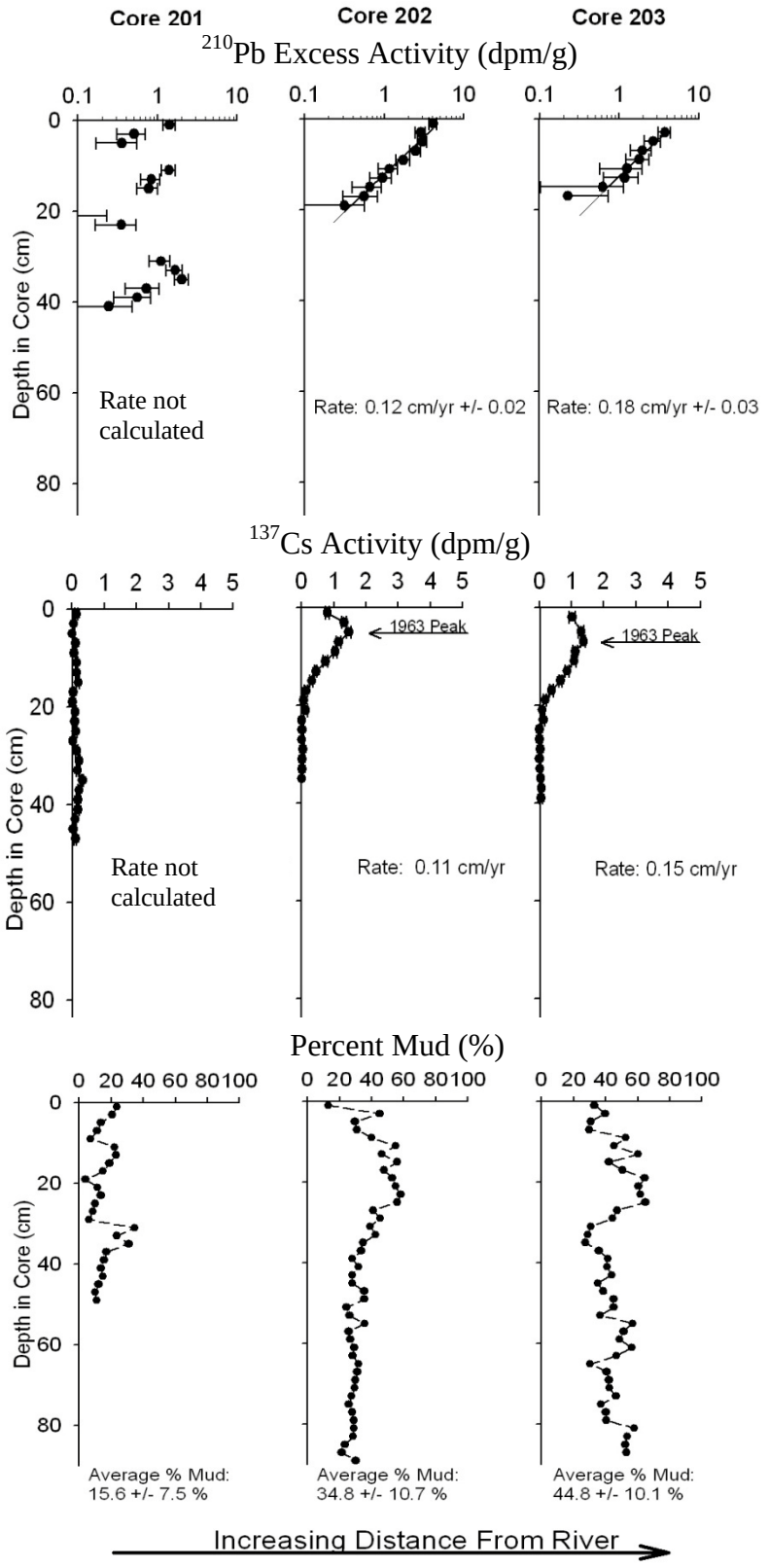

Figure 28: Graphs of ^{210}Pb and ^{137}Cs activities, and mud percent for Site 2. Sediment accumulation rates calculated by ^{210}Pb are shown for cores 202 and 203, no rate is calculated for Core 201 for ^{210}Pb or ^{137}Cs. Note, mud percent increases with increasing distance from channel.

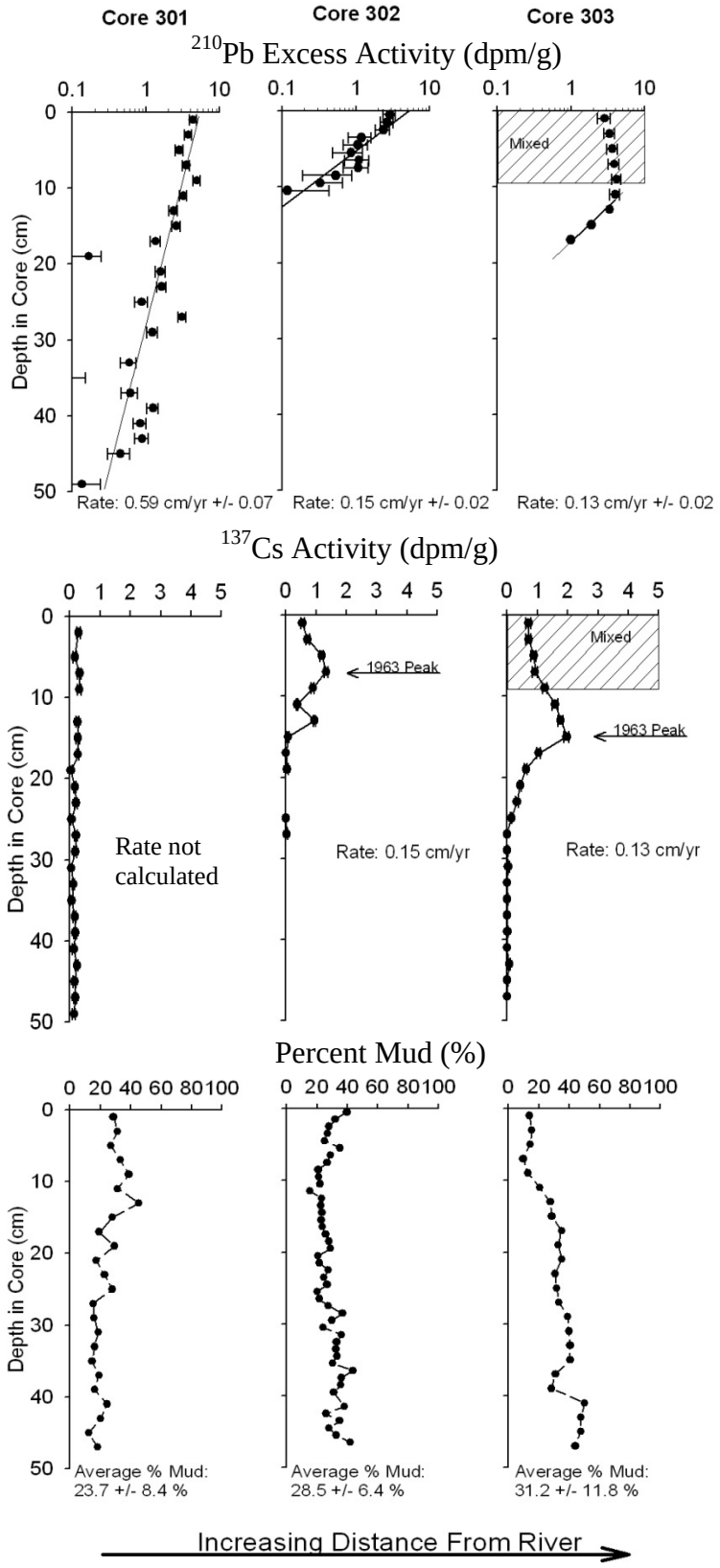

Figure 29: Graphs of ^{210}Pb and ^{137}Cs activities, and mud percent for Site 3. Sediment accumulation rates calculated by ^{210}Pb are shown for all three cores. Core 301 did not have a discernable ^{137}Cs peak so a ^{137}Cs rate was not estimated. Note, accumulation rates generally decrease with increasing distance from river channel.

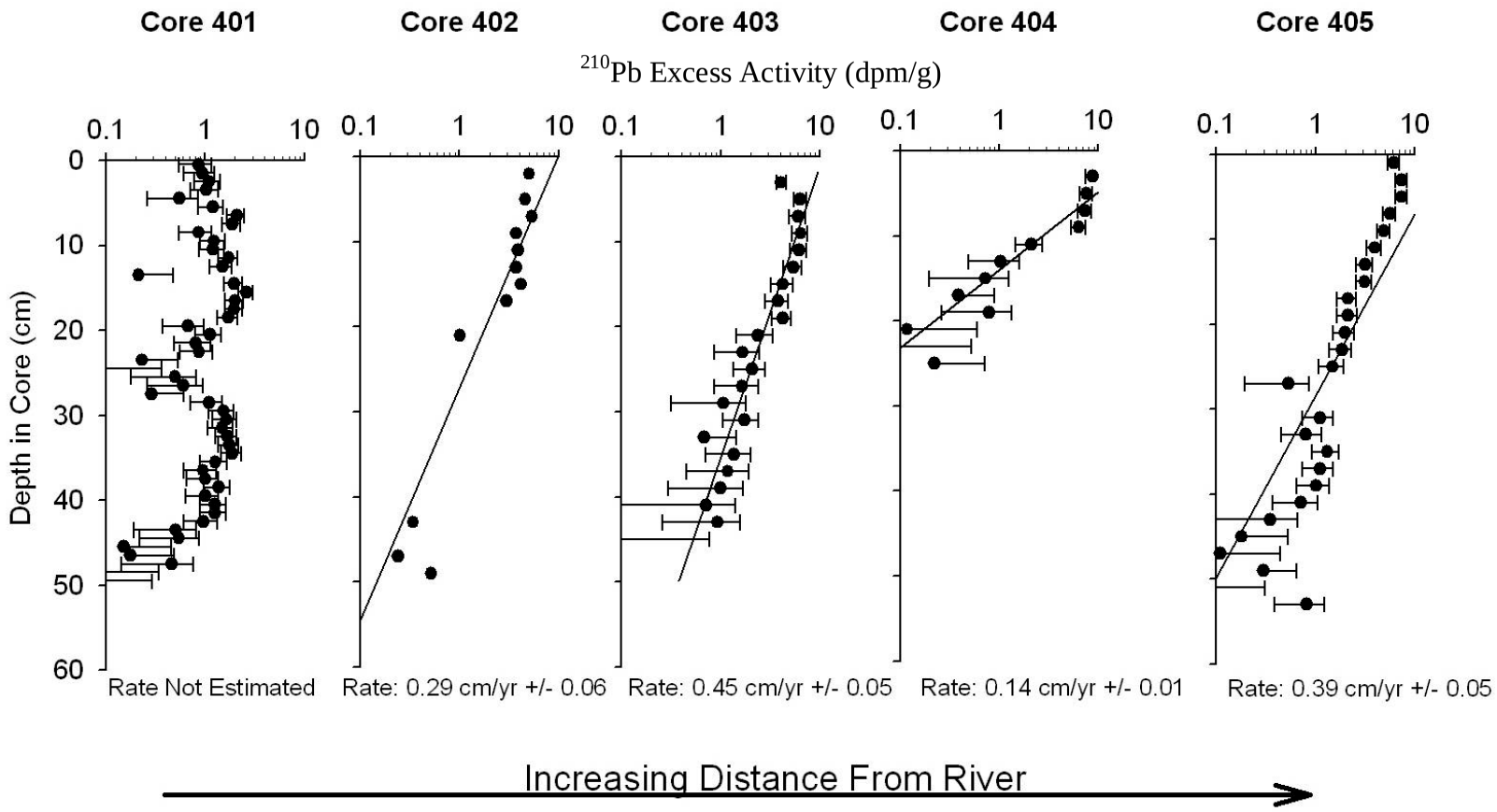

Figure 30: Graphs of ^{210}Pb activity versus depth for Site 3. ^{210}Pb accumulation rates are available for all five cores except Core 401. Rates are variable with distance from channel.

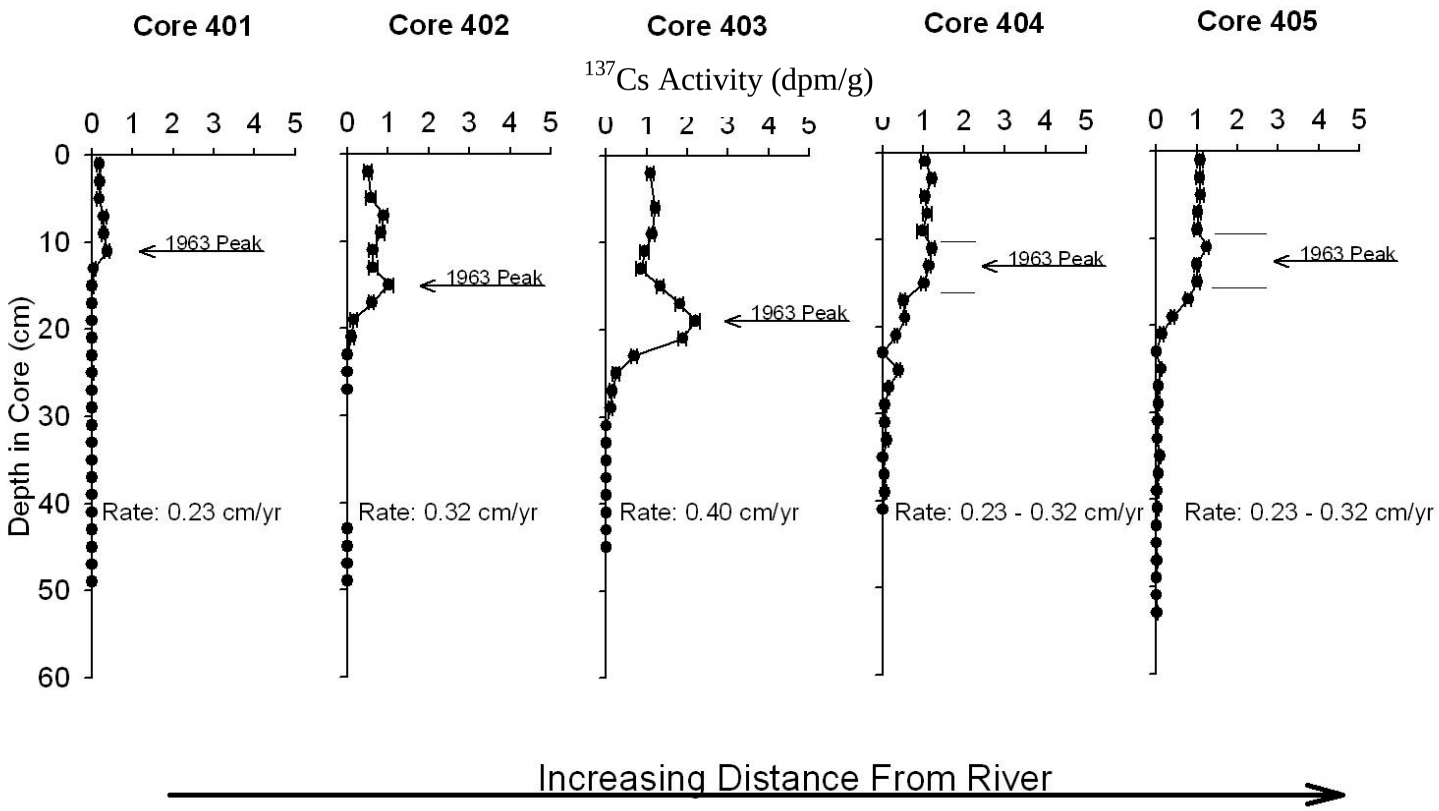

Figure 31: Graphs of ^{137}Cs activity versus depth shown for Site 4. An accumulation rate for all five cores was able to be calculated. Cores 404 and 405 have a range calculation due a distinct peak not being present.

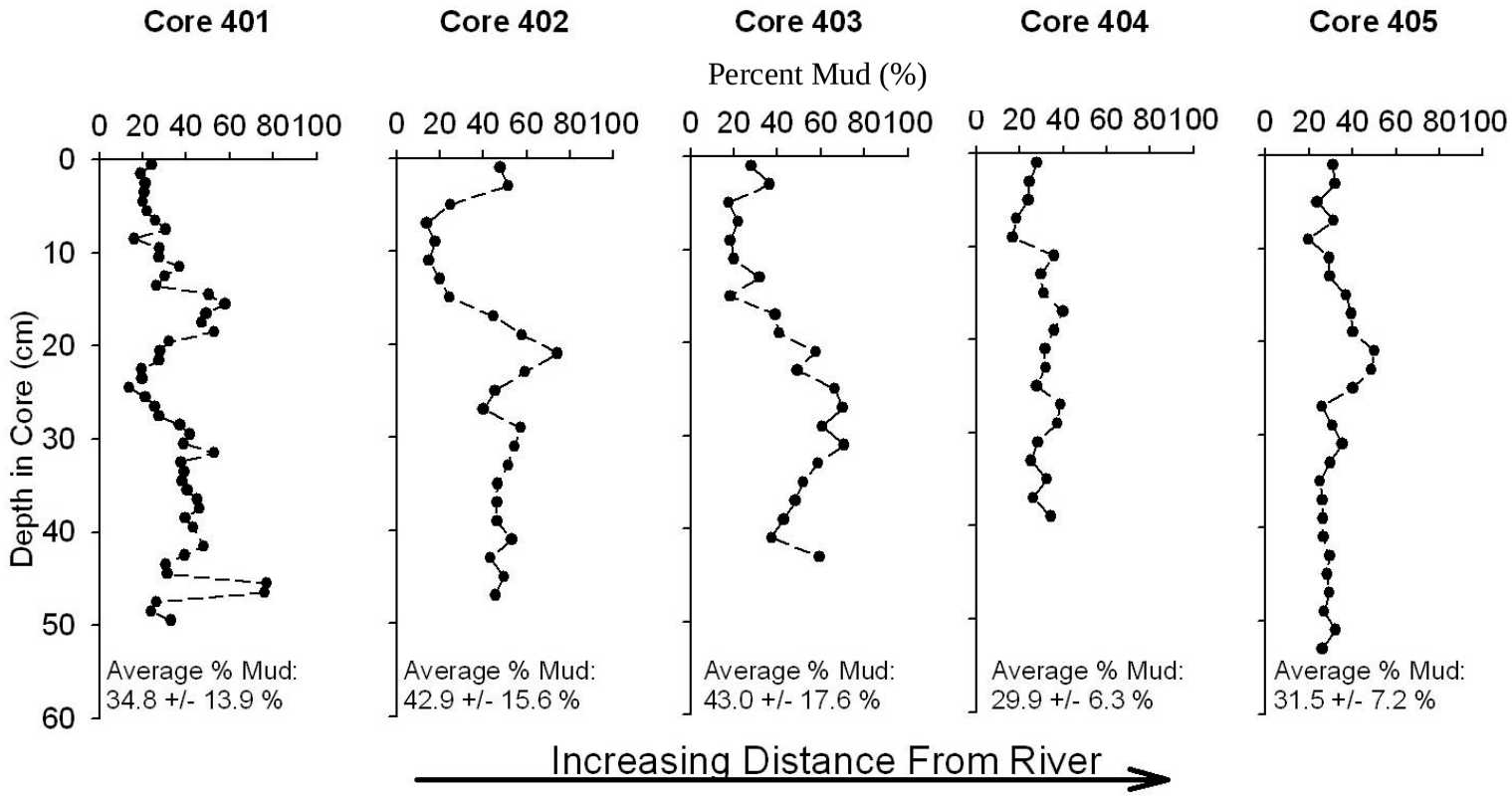

Figure 32: Graphs of mud percent versus depth is shown for Site 4. Note differences between cores with respect to distance from channel.

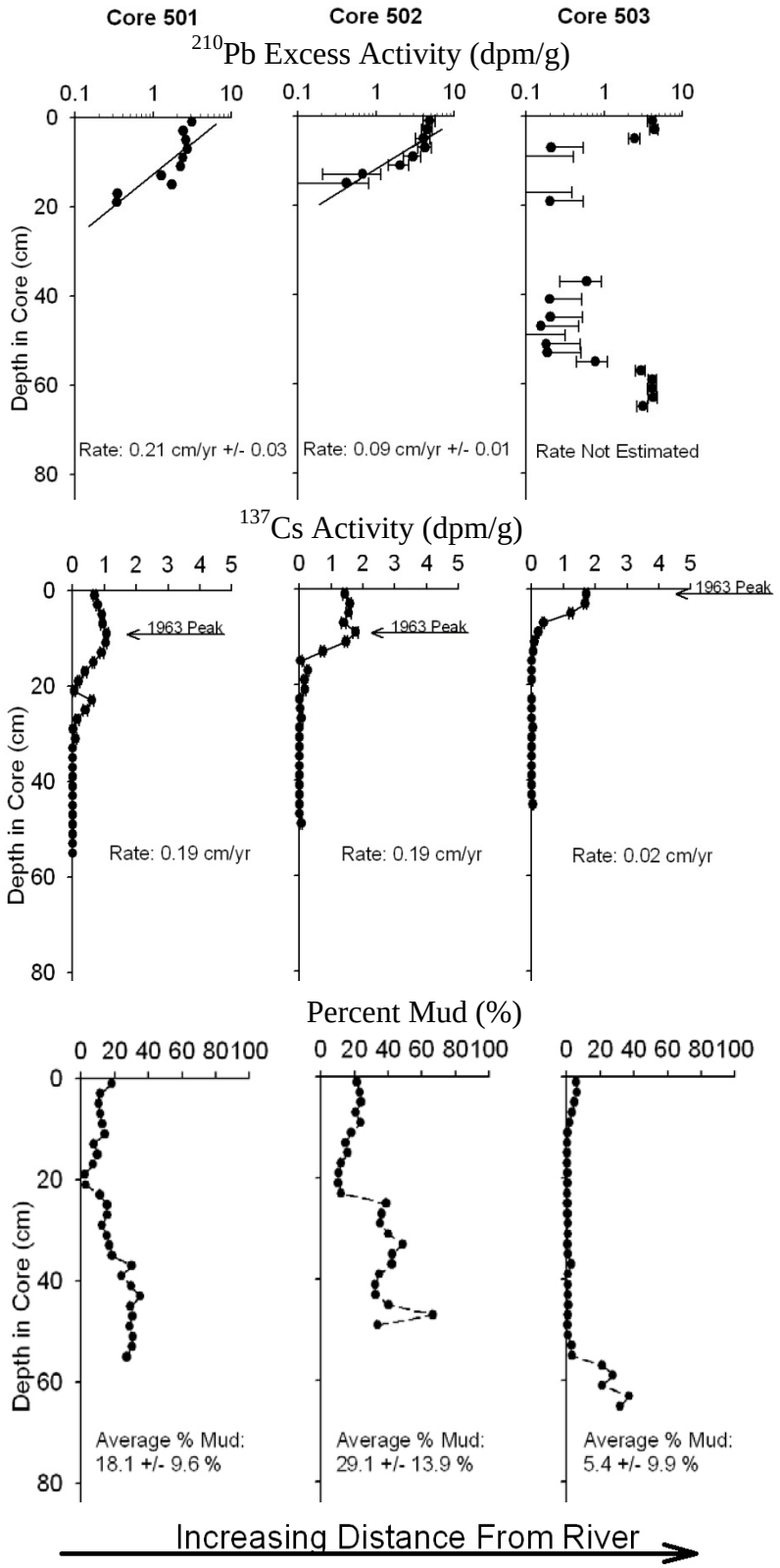

Figure 33: Graphs of ^{210}Pb and ^{137}Cs activities, and mud percent for Site 5. Accumulation rates for Core 503 were not estimated using ^{210}Pb. Note variability of percent mud with distance from channel.

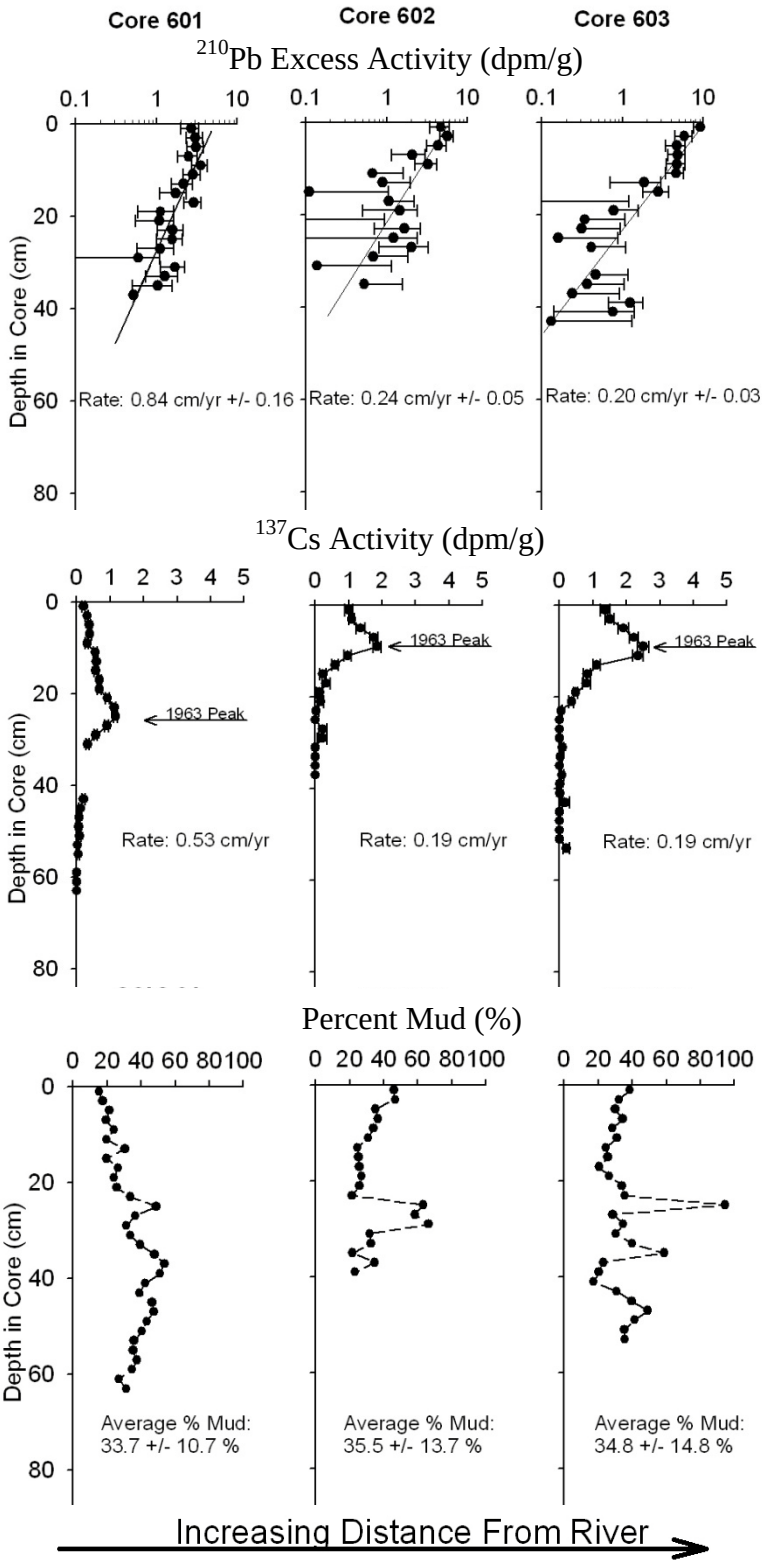

Figure 34: Graphs of ^{210}Pb and ^{137}Cs activities, and mud percent for Site 6. Sediment accumulation rates calculated by ^{210}Pb are shown for all three cores. Note, accumulation rates are highest near channel and lowest in Core 603.

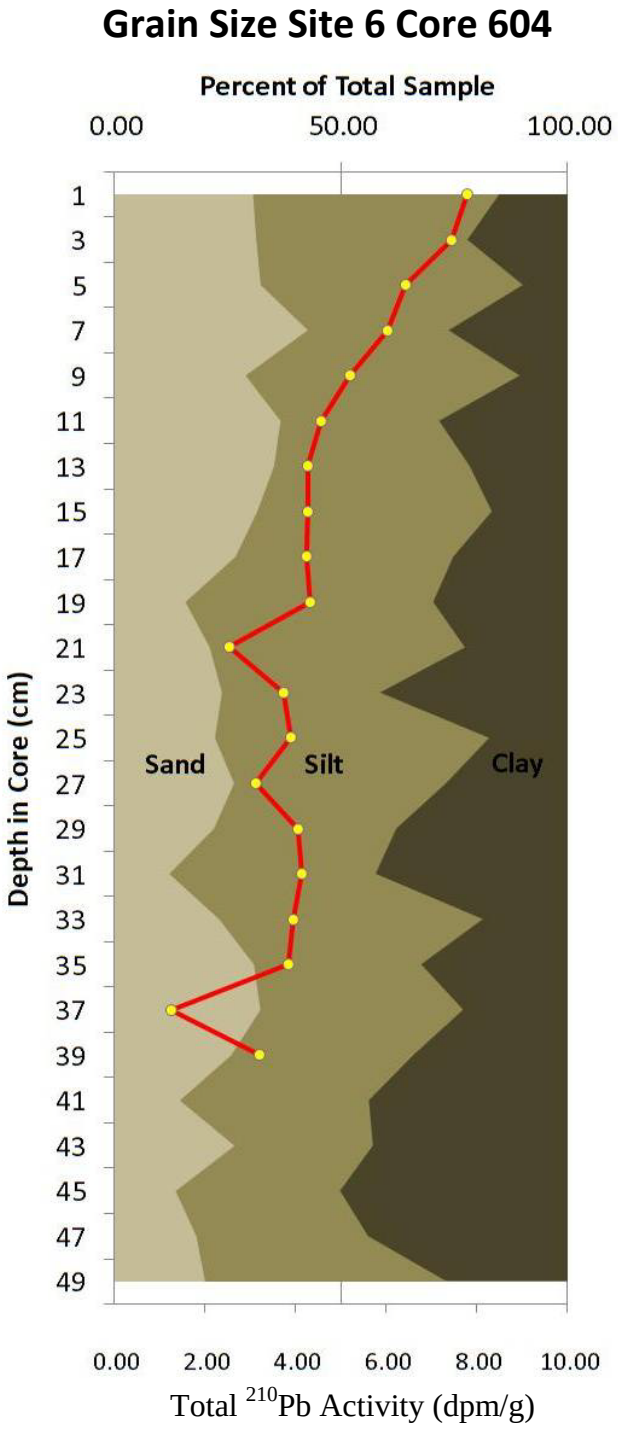

Figure 35: Grain size percents and total ^{210}Pb activity. Note, Variations in grain size are not correlated with changes in total ^{210} Pb activities.

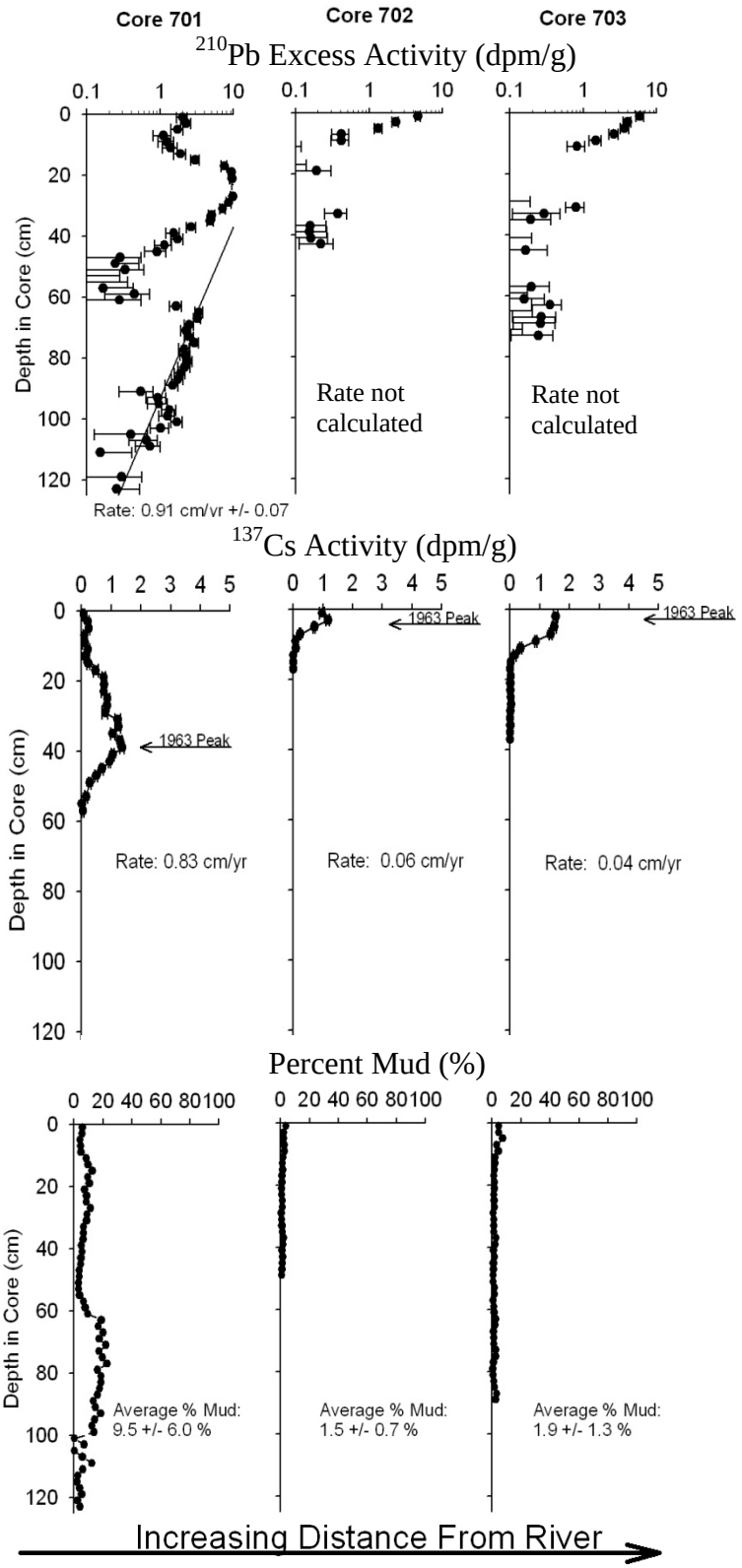

Figure 36: Graphs of ^{210}Pb and ^{137}Cs activities, and mud percents for Site 7. Sediment accumulation rates are only seen in Core 701. Note, low percent mud is seen in all cores.

5.3 Post-Flood Cores Compared to Pre-Flood Cores

On December 12, 2009 the Tar River topped its banks, and the Site 4 floodplain near Greenville remained inundated until January, 08, 2010 (Figure 7). To evaluate flood-related deposition, cores were collected in the same vicinity (within 15 m) of three previously cored locations (Core 403, Core 601, and Core 603). Inventories of ^{7}Be were measured on pre- and post-flood cores and are reported in dpm/cm^2 to evaluate recent deposition (Giffin and Corbett, 2003). Atmospheric deposition of ^{7}Be was measured by Canuel et al. (1989) at Morehead City, NC to be 3.1 dpm/cm^2 in inventories. Inventories were compared between pre-flood inventories and post-flood inventories to see if new ^{7}Be could be seen indicating new accumulation (Table 3). Core 403 shows a notable increase in inventory after the flood representing deposition. Cores 601 and 603 both show little to no deposition after flooding (Table 3).

The cores collected after flooding also were analyzed for accumulation rates and mud percentages (Figures 37, 38, 39). These cores were used to compare with previous core data to evaluate temporally and possibly spatial variability (i.e., within 15 m). The post-flooding core collected near Core 403, shows a lower accumulation rate than the pre-flood core. Grain-size down core appears to be quite different; however, the whole-core average mud percent is similar. Core 601pf (Post-flooding) has an accumulation rate lower than that of the pre-flooding core. Down-core grain-size profiles also show differences indicating a different sedimentation at the post-flood site. Accumulation rates for Cores at 603pf has a higher accumulation rate than that of the pre-flood core. Mud percents also show differences in trend and averages.

Table 3: ^{7}Be penetration depths, surface activities, and inventories. Cores 403, 601, and 603 show inventories for pre and post flooding. Note, penetration depths vary between cores.

Site	^{7}Be Penetration Depth cm		^{7}Be Surface Activity		Inventory	
	Pre-flood	Post-flood	Pre-flood	Post-flood	Pre-flood	Post-flood
403	2	4	1.92	1.14	3.84	5.34
601	0	2	0	0.68	0	1.36
603	4	2	6.58	1.46	15.5	2.92

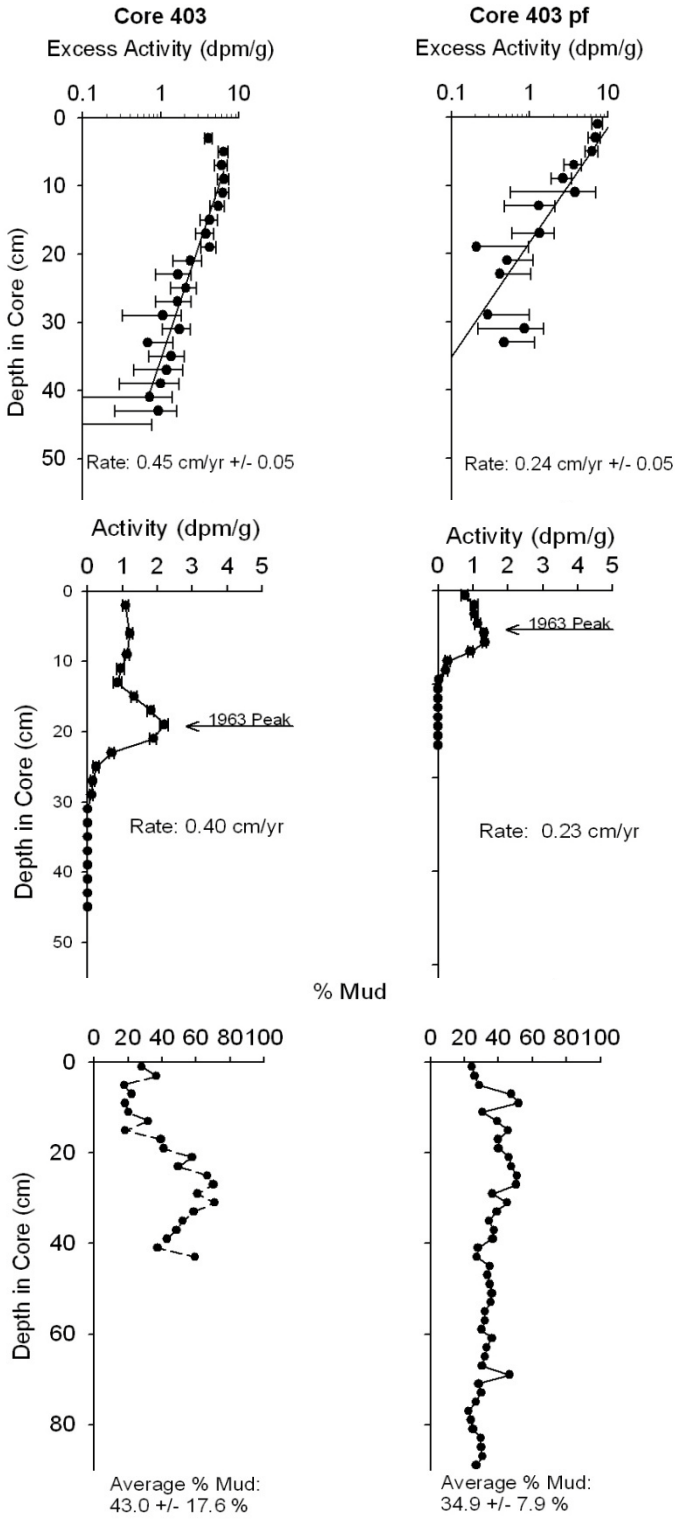

Figure 37: Comparison between Cores 403 and 403 pf. Accumulation rates vary between the two cores to where Core 03 has an accumulation rate over 2 times the accumulation rate of 403 pf. Grain size down core profiles also show differences in down core profile, however, the overall whole core average is similar.

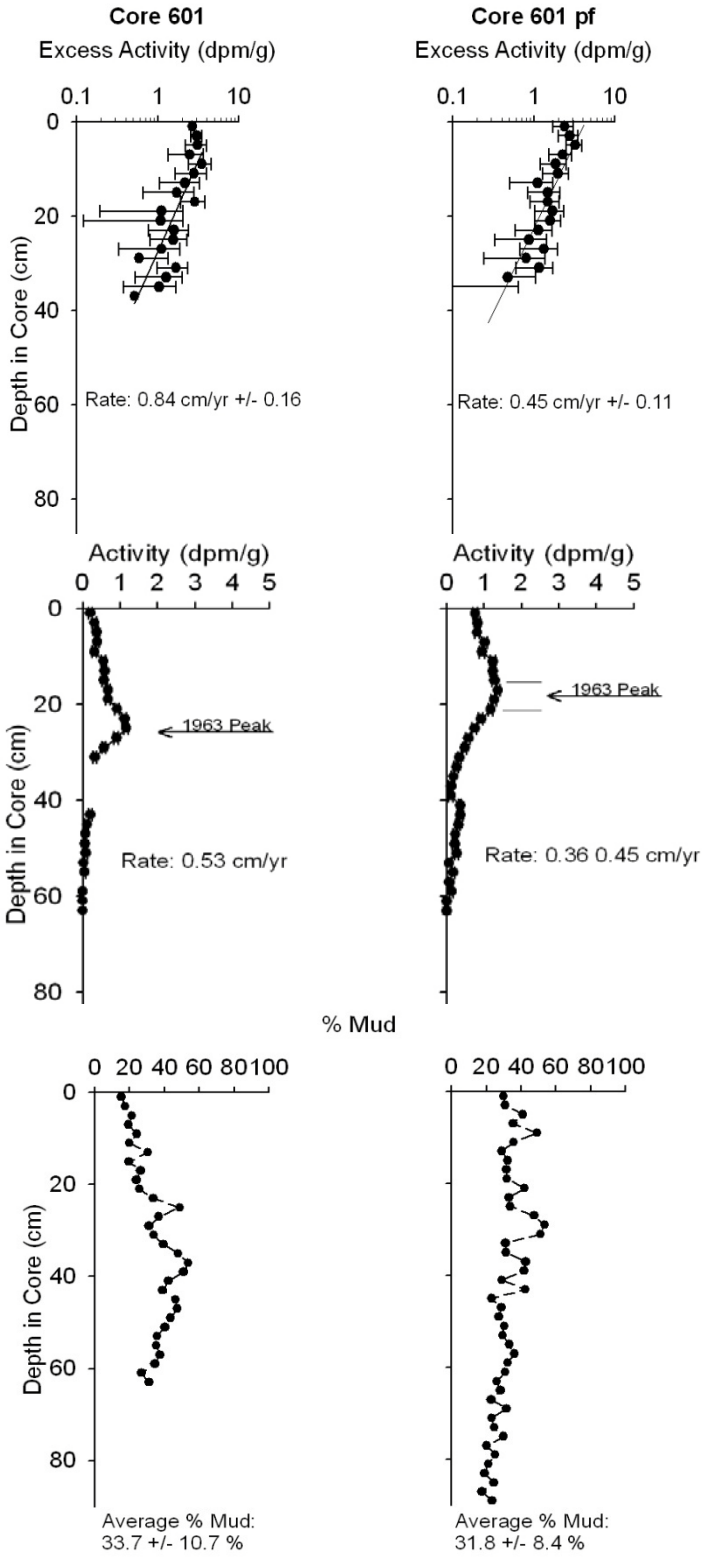

Figure 38: Shows the comparison between Cores 601 and 601 pf. Accumulation rates vary between the two cores to where Core 601 has an accumulation rate 2 times the accumulation rate of 601 pf. Grain size down core profiles also show differences in down core profile; however, the overall whole core average is similar.

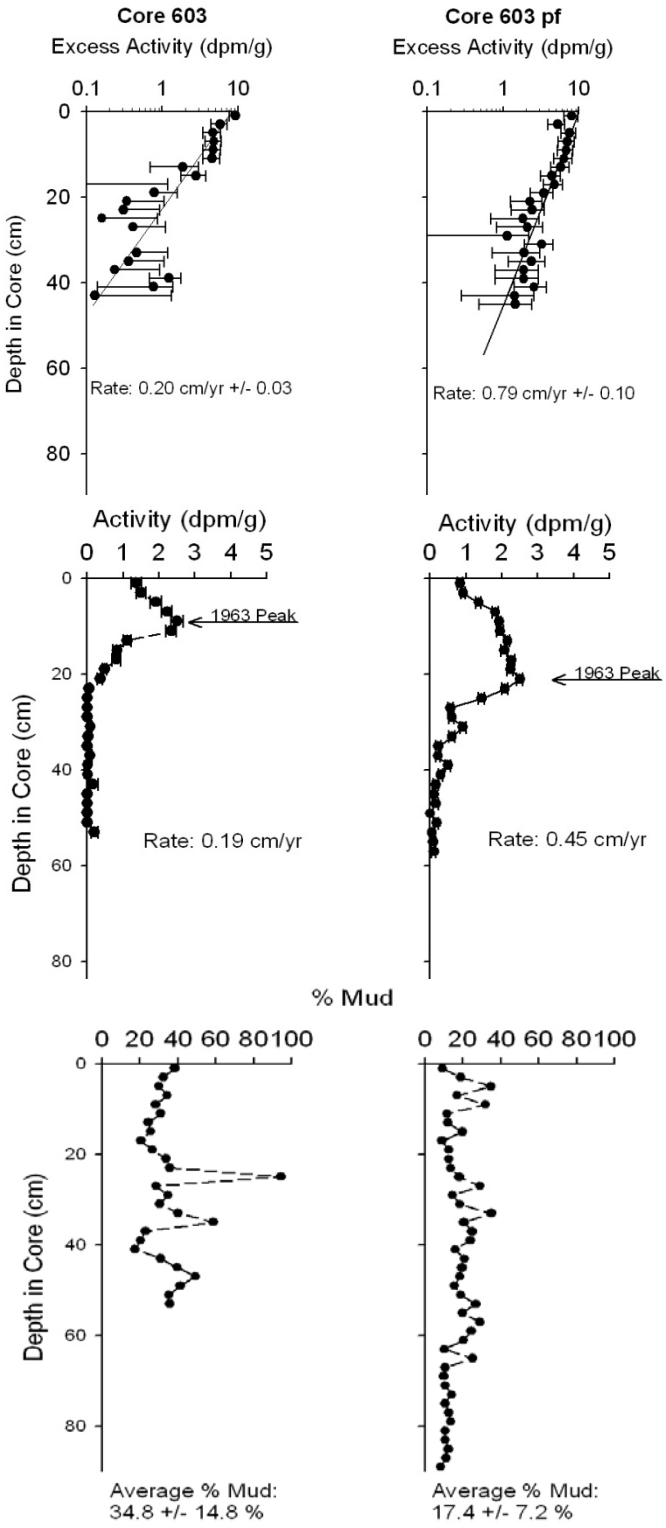

Figure 39: Shows the comparison between Cores 603 and 603 pf. Accumulation rates are similar between cores; however, ^{137}Cs accumulation rate seen in Core 603 pf has a much higher rate of accumulation which is not seen in the ^{210}Pb. Grain size down core profiles also show differences in down core profile and overall core average grain size.

6. Discussion

6.1 Characterizing the active floodplain

Floodplains are dynamic sedimentary systems with large variability in morphology and sedimentation both between locations and within study areas (Wolman and Leopold, 1957; He and Walling, 1996; Walling and He, 1997; Allison, 1998; Goodbred and Kuehl, 1998; Hupp, 2000; Walling, 2004; Knox, 2006; Mizugaki et al., 2006). Walling et al. (1998) noted how floodplain transects within the River Ouse varied in both elevation and morphological features (i.e., levees, ditches, and depressions). This complexity is evident when looking at the lower Tar River study area. For example, some sites have different geomorphic features and have an active floodplain that is symmetrically arranged across the river (i.e., Sites 3 and 7), while others are shifted predominately to one side of the river or the other (i.e., Sites 1, 2, 4, 5, and 6).

Researchers and agencies differentiate the river floodplains in different ways to investigate the effects of flooding on biological, chemical, sedimentological, and hydrological parameters. Regulatory agencies such as the Federal Emergency Management Agency (FEMA) define the zone of flood hazard as the 100-year floodplain. More specifically, this method defines the active floodplain that has a 1% chance of being flooded each year. Junk et al. (1989) describe the active floodplain as the area that is periodically inundated by the lateral overflow of rivers and lakes. Smith et al. (2008) use a GIS-based approach similar to the method described in this paper. However, their method uses a model of costs (what it would take for water to cover that area) that are derived from slopes and elevations. The cutoff of 1% inundation time used here was

chosen to define areas where flooding occurs frequently and long enough to allow somewhat regular deposition to occur (i.e., steady-state) so radionuclide approaches could be successful. This would be less likely to occur in further areas of the 100-year floodplain that rarely see inundation on annual timescales. When compared with the active floodplain using our method the 100-year is much more expansive (Figure 40). This is seen for all seven study sites but is shown here for Site 4. The difference between the two methods yield very different estimates for area, however, the majority of steady-state accumulation is expected to occur in the active floodplain area denoted by the method described.

Some problems with this method include that the previous 10 years of data could reflect a wetter or dryer period that would either extend or reduce the maximum extent of inundation and accumulation. Thus, the active floodplain described by this method likely underestimates the total area of floodplain sequestering sediment over decadal timescales. When investigating individual 10-year time blocks of data for all sites, full data sets were not always available. This meant that not all sites had the same amount of daily readings. Variations in total data points between sites could cause some biasing in percent-time flooding estimates, however, the overall large datasets (~2500 to 3600 stage height measurements) used for each individual site should minimize bias of the data.

Strong variations in topography are known to affect accumulation rates within floodplain systems (Allison et al., 1998; Walling and He, 1998; Walling et al., 1998). In this study, sites portrayed a general spatial pattern in topography downstream; overall, mean floodplain elevation and the range in floodplain elevation decreased down river (Figure 41). Collectively, these parameters demonstrate a net decrease in overall relief

down river. However, Sites 5, 6, and 7 appear to have a fairly similar floodplain elevation distribution and, in general, these sites have a much greater portion of the floodplain flooded more often (Figure 42). This observation is consistent with that of Simmons (1993) who plotted the decrease in elevation across the Coastal Plain of the Neuse River. For example, the floodplain of Site 1 has a percent-time flooded of 3% on average, whereas Site 6 has an average percent time flooded of 40%. This variability between sites in elevation, relief, and percent-time flooded is a result of the channel morphology created by river migration, erosion, and flood deposition over geologic time as well as the hydrology. Landforms such as natural levees and erosional gullies create variations in elevation that ultimately impact the inundation time (i.e., percent-time flooded) along the river system (Allison et al., 1998). Hydrologically, sites that lie immediately upstream at the estuary head and at river confluences are likely to be affected by a backwater effect, thereby causing enhanced flooding frequency (Phillips and Slattery, 2007).

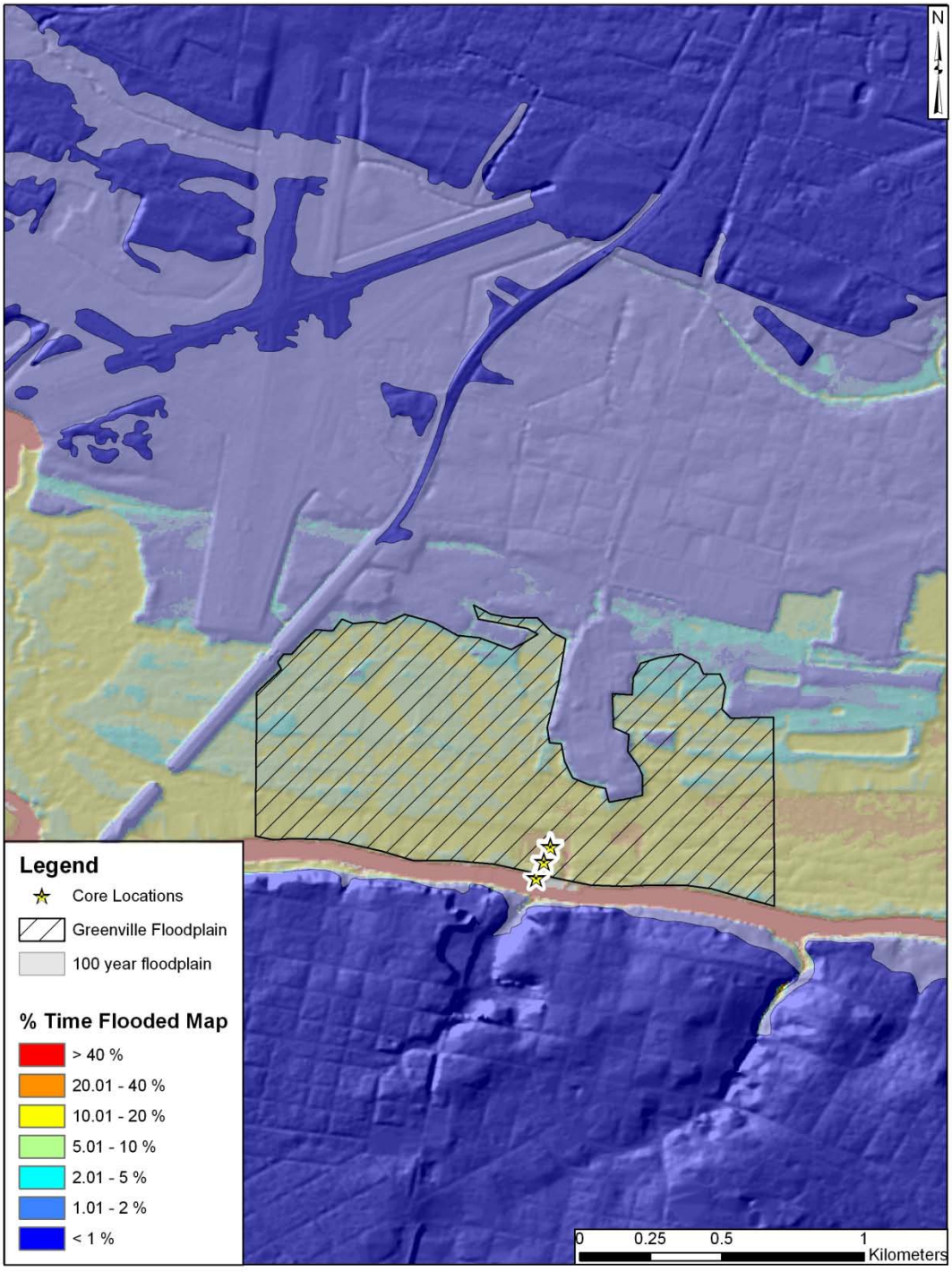

Figure 40: Map showing the FEMA 100-year floodplain and the floodplain defined by this study. Note the large difference in area between the FEMA floodplain and the floodplain described by the method above.

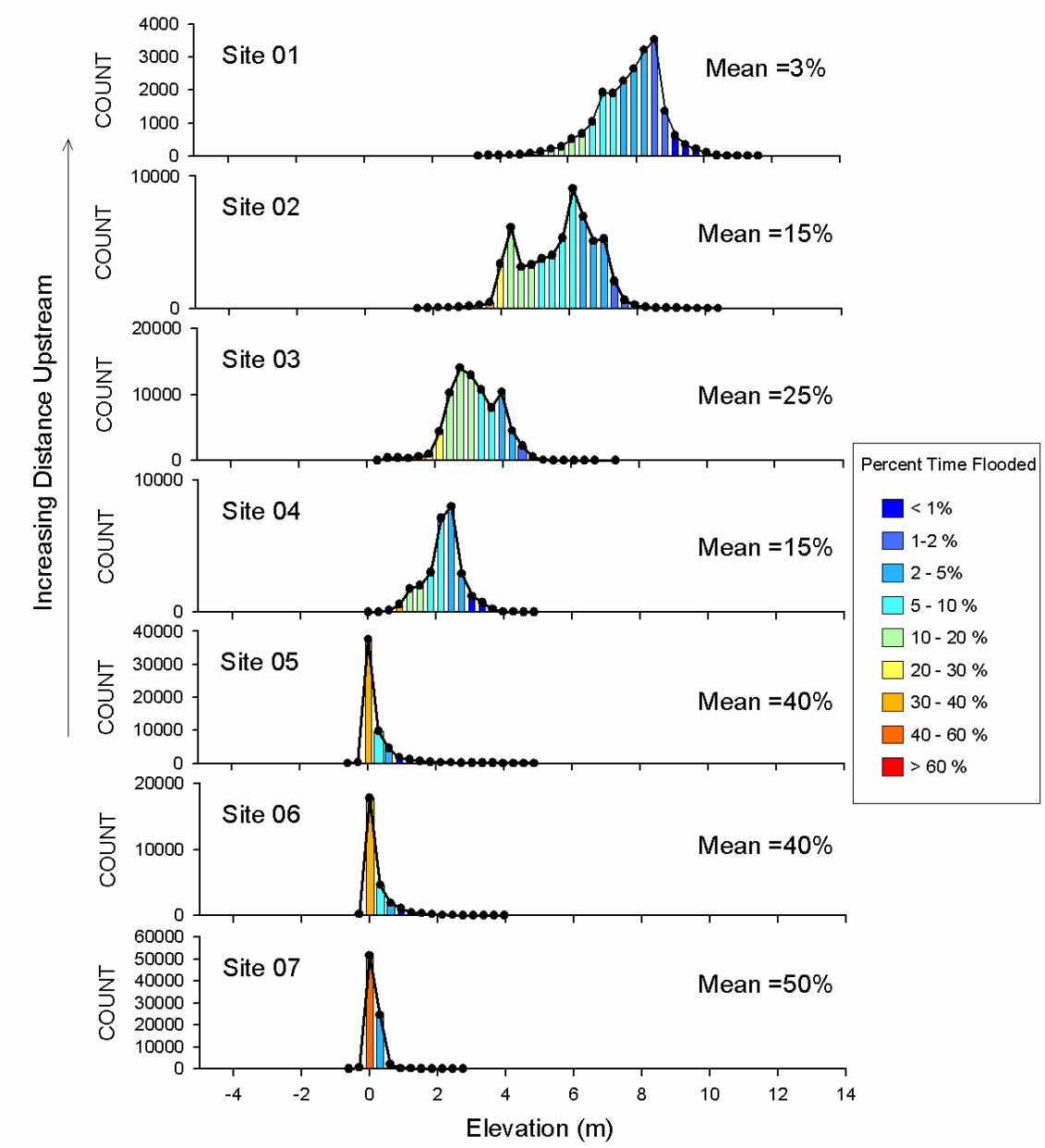

Figure 41: Histograms of floodplain elevations for all sites. Data show an increase in floodplain elevation with distance upstream. Also note the range of floodplain elevations increases upstream.

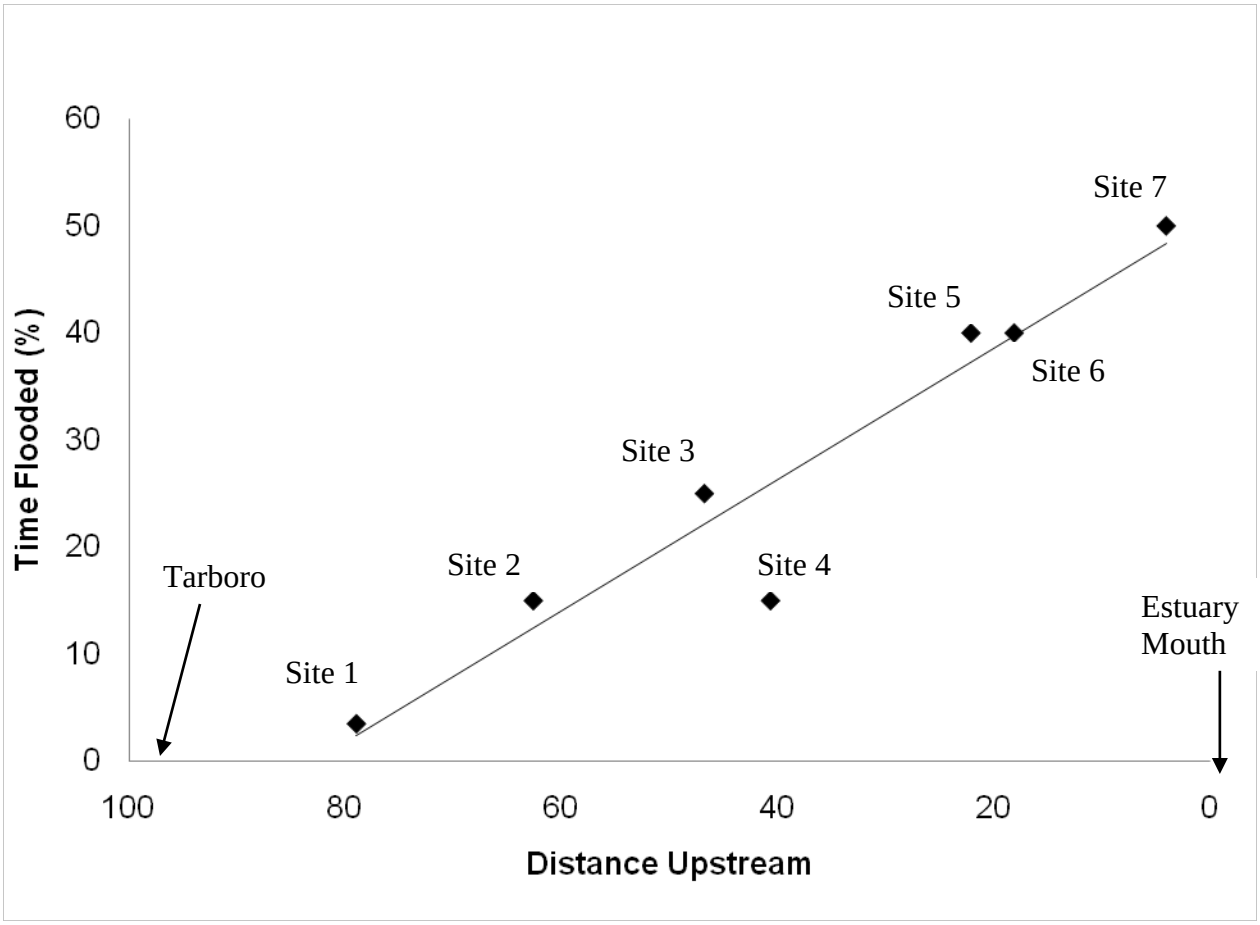

Figure 42: Relationship of the time flooded found in the active floodplain with decreasing distance upstream starting from the estuary mouth at 0km.

Active floodplain area between the sites varies from the smallest area of 0.79 km^2 (Site 1) to the largest floodplain area of 2.33-km^2 (Site 7) (Table 4). Although the manner of calculating this parameter was somewhat arbitrary and could be improved to minimize bias (e.g., from river orientation), this trend is nevertheless likely real. The area of active floodplain is critical when evaluating sediment storage. The larger the active floodplain, the more area available for inundation and therefore long-term storage of sediment.

Table 4: Total area of active floodplain (> 1% time flooded) at each site.

Site	Area (km^2)
1	0.79
2	1.48
3	2.00
4	1.04
5	2.13
6	1.00
7	2.33

Other differences between sites include the number and size of drainage ditches within the floodplain. These ditches have been shown in previous studies to affect the accumulation rate within the floodplain (Allison et al., 1998; Walling and He, 1998; Walling et al. 1998), Walling et al., (1998) compared variations in elevation with accumulation rates and found that in the presence of drainage ditches, accumulation rates were notably higher. From these data, they concluded that drainage ditches and former streams allow for an alternative pathway for flood waters to inundate the floodplain, leading to enhanced trapping and storage of sediment.

6.2 Sediment accumulation rates

The mean accumulation rate for all cores within the active floodplain was 0.35 cm/yr. This rate is consistent with previous work by Hupp et al. (1999) in the floodplain of the Roanoke river which is shown to have an average reported accumulation rate of 0.23 cm/yr despite the fact that different methods were used. Hupp et al. (1999) employed dendrochronology to calculate accumulation rates within floodplains of the Roanoke. Also, Noe and Hupp (2009) show that Coastal Plain rivers in the Chesapeake bay area of Virginia have an average accumulation rate of 0.18 cm/yr. Rates in both

studies were obtained from dendrogeomorphological analyses; this method uses the thickness of sediment above tree roots in the floodplains. The age of the root, found by counting rings within the root, would then be used to calculate a depth/time relationship similar to the ^{137}Cs method. Having similar rates from different methods gives a greater confidence in the rates reported.

Accumulation rates within each study site show trends which are typical for active floodplains. The first commonly observed trend is one of decreasing accumulation rate with distance from the river channel (Allen, 1964; Kesel et al., 1974; James, 1985; Pizzuto, 1987; Allison et al., 1998; Walling and He, 1998; Walling et al., 1998; Hupp, 2000; Mizugaki et al., 2006). The second often noted variation is the influence of topography and, more specifically, pathways of preferential flooding on the accumulation rates (Allison et al., 1998; Walling and He, 1998; Walling et al., 1998). Looking simply at the transect data, it appears both factors (i.e., distance from source and elevation) appear to be influential. Sites 1, 3, 5, and 6 have an apparent trend of decreasing accumulation rate with distance from the main channel; however, effects of topography or intra-site variability (see below) could also be influencing rates in these cores (Figure 43).

Sites 2 and 4, however, do not show this pattern, but these sites have drainage channels and may be affected by preferential flooding pathways. For example, Core 203 has a higher accumulation rate than Core 202 (Figure 43), this difference could be a result of percent-time flooded (Table 2) because the frequency and duration of flooding has been shown to influence sediment accumulation rates (Allison et al., 1998; Walling and He, 1998; Walling et al., 1998). Core 203 was inundated more of the time than Core 202.

However, these rates may be within the error of the analysis or a product of intra-site variability.

When all cores are used to investigate a relationship between accumulation rates and distance from channel, an overall trend of decreasing rate with distance is apparent (Figure 45). This trend has been documented in many previous studies and is consistent with diffusive transport shown in Pizzuto (1987). Walling and He (1998) showed this relationship in five separate rivers, i.e., the Stour, Culm, Severn, Rother, and Avon. In the Tar River, accumulation rates also become less variable with increasing distance from channel (Figure 45). This commonly observed trend can be explained by the general reduction in frequency and duration of inundation with increasing distance from the main channel (Walling and He, 1998).

Using the complete dataset, ^{137}Cs-based accumulation rates plotted versus percent-time flooded suggest a general trend of increasing accumulation with increasing percent-time flooded (Figure 44). Outliers in the data include cores 502 and 503, which have high percent time flooding (~43%) with very low accumulation rate of 0.19 and 0.02, respectively. ^{210}Pb accumulation rates plotted against percent time flooding shows a similar relationship (Figure 44). A noticeable outlier is Core 101 which has a low calculated percent time flooding but a high accumulation rate. A ^{137}Cs accumulation rate could not be obtained from this core, suggesting more complex sedimentation may exist here. Other cores such as 503 have low accumulation rates with high flooding percentages. Data from Site 4 suggest the presence of topographic influences on accumulation. Cores 403 and 405 have much higher accumulation rates than would be expected in comparison to adjacent cores. Core 403 was taken in close proximity to a

natural drainage ditch which is flooded 23% of the time (Figure 20). Core 405 also was taken in an area of higher inundation time compared to Core 404.

Ultimately, both distance and inundation time appear to play a role in floodplain sedimentation, but neither can explain all the data variability due to the complex interaction of the river and floodplain. This is certainly evident in the non-steady-state accumulation observed at several sites (i.e., Core 201 and 401). For example, Site 7 does not appear to agree with either controlling factor (i.e., distance from channel or inundation time). Radionuclide data from Cores 702 and 703 indicate non-steady-state accumulation or no active decadal-scale accumulation suggesting more complex sedimentation at these sites. Because rivers and their morphology are dynamic and are affected by non-stationary and stochastic events (i.e., storms), rates of sedimentation over decadal and even shorter timescales will likely never follow a simple empirical model, especially over longer temporal and spatial scales.

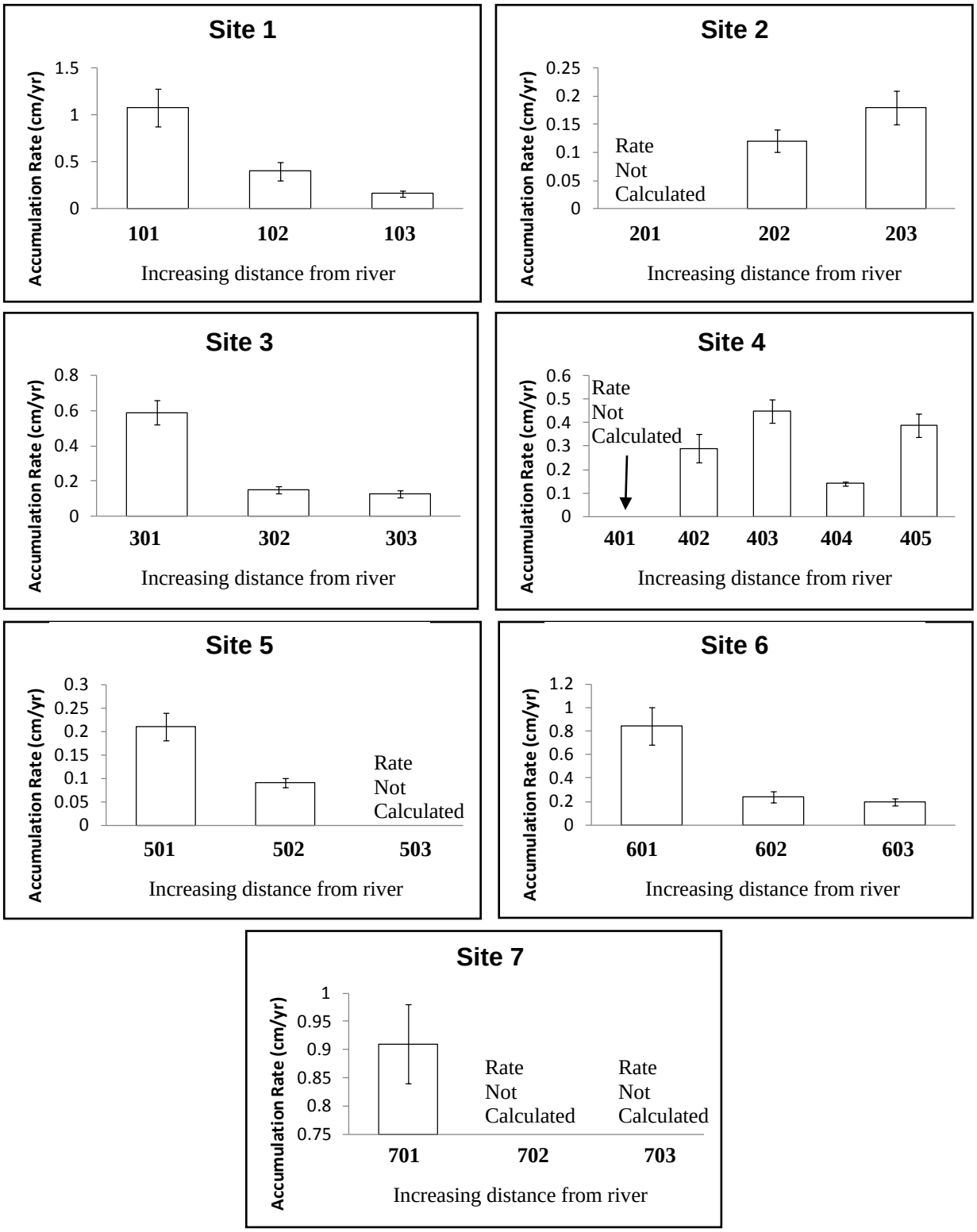

Figure 43: Graphs showing accumulation rates with increasing distance from channel. A trend of decreasing accumulation rate with increasing distance from channel is seen at Sites 1, 3, 5, and 6. Data from Sites 2 and 4 suggest the affect of topography on accumulation rate.

A)

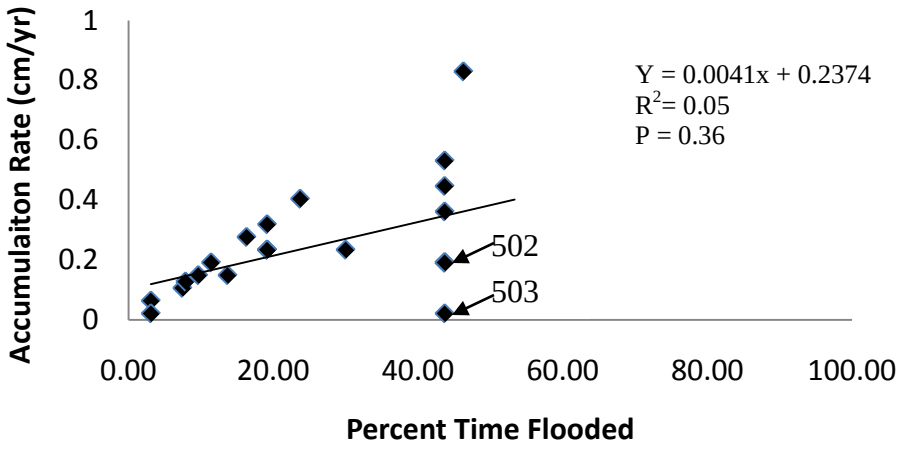

B)

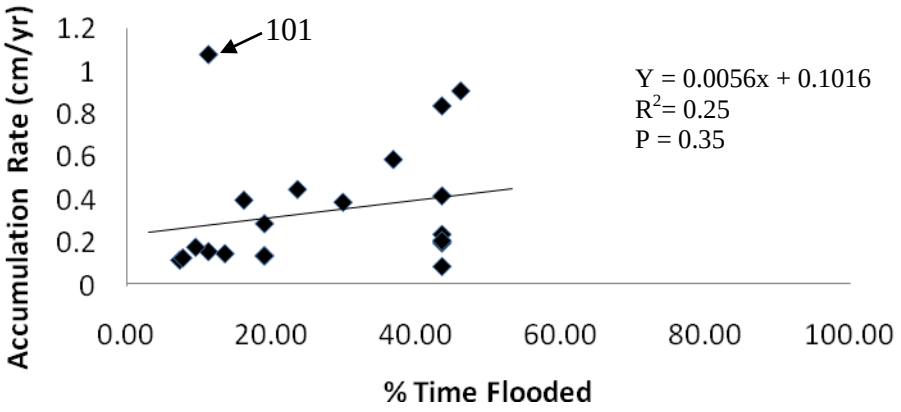

Figure 44: Accumulation rates versus percent-time flooded for both ^{137}Cs and ^{210}Pb data. ^{137}Cs-derived data (A) and ^{210}Pb-derived data (B), both datasets suggest a general trend, but with notable exceptions.

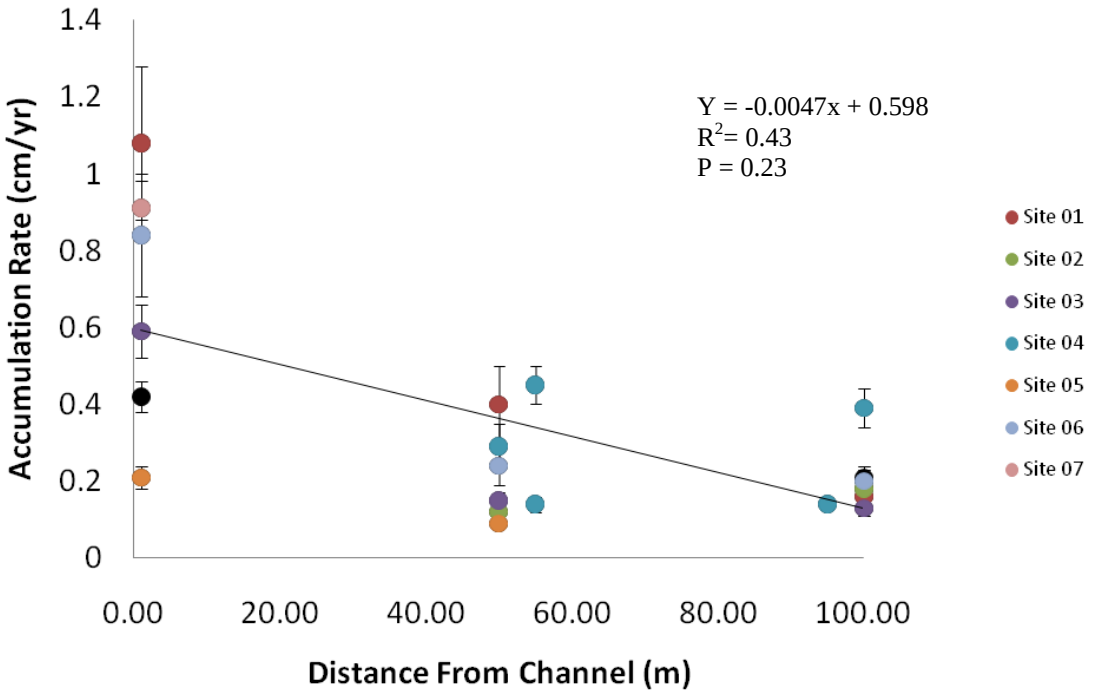

Figure 45: Relation of accumulation rate with distance from channel for entire study area. General trend of decreasing accumulation rate with increasing distance is seen. Sites are color coded to show trends within sites compared to overall trend.

Although rates of sediment accumulation are suggestive of expected patterns, mud-percent data from this work is less predictable. Due to a loss in flow velocity into the floodplain the typical grain-size trend is one of increasing mud with distance from the main channel (Allen, 1964; Kesel et al., 1974; Pizzuto, 1987; Walling and He, 1998; Walling et al., 1998). Sites 2, 3, and 6 are generally in agreement with this pattern (Figure 46); however, data at other sites are inconsistent. For example, Sites 1 and 4 have the highest percentage of mud in the center of the transect. Both of these cores are proximal to a drainage ditch which may affect the deposition of fine-grained sediment. Lambert and Walling (1978) in a study of the River Culm showed how small or "micro" variations in elevation such as low depressions appear to cause higher accumulation rates as

receding flood waters are trapped in these lows allowing suspended sediments to settle out. Asselman and Middelkoop (1995 and 1998) show a grain-size shift in low-lying areas which are inundated longer by ponding. Thus, grain-size trends, like sedimentation rates, may be influenced by topography and inundation times.

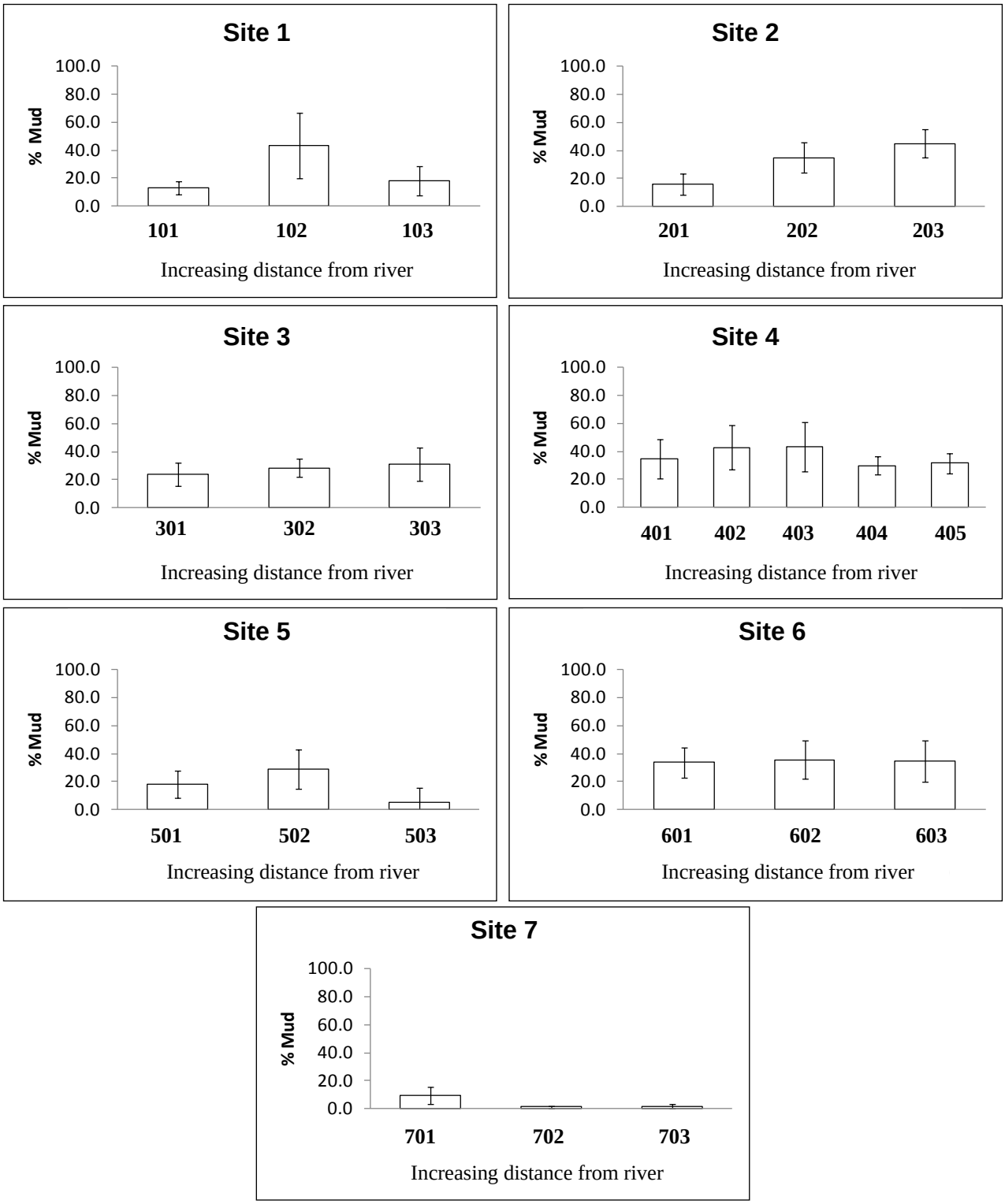

Figure 46: Whole-core averages of percent mud with increasing distance from channel. Expected trends of increasing percent mud with increasing distance from channel are seen at three sites with variations seen in each of the other sites.

When comparing pre- and post-flood cores, significant differences in sedimentation rates and grain size were seen at Cores 403 and 601 (Figures 37 and 38). These observed variations seen in cores that likely were <15-m away imply significant spatial variability over small distances. It is apparent that several variables (e.g., distance and flooding time) can affect the accumulation rates measured in any given location but it is also likely there is some natural variability due to very local changes. More work should be conducted to evaluate the spatial scales of sedimentation variability.

6.3 Floodplain Sediment Storage

Accumulation rates were extrapolated over the entire study area to calculate the volume and mass of sediment sequestered by the floodplain annually. From these data the fraction of the total suspended-sediment load of the river stored in the floodplain was determined. This estimate provides important insight into the overall sediment budget for the Tar River. Also, because pollutants and nutrients can be associated with these sediments, fine-grained sediment sequestered on the floodplain may have environmental ramifications (Wolfenden and Lewin, 1977; Lambert and Walling, 1987). A sediment budget can give a better understanding of any potential future changes in loadings, pollutant transport, and other management efforts.

The mean annual suspended-sediment load of the Tar River has been estimated to be 1.89×10^5t/yr at Tarboro (Giese et al., 1979). In this project the total amount of sediment sequestered in the study area floodplain is calculated to be 1.26×10^5 t/yr, and this represents approximately 66% of the incoming load at Tarboro (Table 5). This value was calculated by extrapolating the accumulation rates measured directly from cores as

described in the methods; however, using estimated rates from the trend shown in Figure 45 (i.e., between distance and accumulation rate) a similar percentage of storage (67%) was calculated. Obtaining similar values when using different approaches helps affirm the storage estimates reported here. However, the major assumption for these estimates are that the observations at these sites represent sedimentation in the floodplain for the specified river reaches over which they are extrapolated, and this may be too optimistic. However, the broad distribution of sites and number of cores taken is substantial and helps to increase the confidence in the measurements.

The storage data may be better visualized and understood in the context of a box model (Figure 47) or a river long profile (Figure 48). Estimates for additional sediment supply within the lower river were assessed, and using the estimated delivery ratio (30%, Phillips, 1991) for sediment making it to the river was calculated. Using this new estimate of floodplain sediment inputs and sequestrations, the first-order sediment budget was constructed (Figure 47). From this, a load of 9.6×10^4 t/yr is estimated to reach the Pamlico River Estuary. Note, however, this value does not take into account channel sequestration which has been shown to account for 4-10% of the suspended-sediment load for the Rivers Ouse, Wharfe, and Tweed (Walling et al., 1998). Based on this work, the sediment load reaching the estuary may be further reduced. This budget also does not take into account erosion due to channel migration which has been shown by Lauer and Parker (2008) to produce a local influx of sediment. The majority of sediment eroded in this way is typically deposited on nearby point bars; however, a portion (~10%) is deposited elsewhere (i.e., in the floodplain). The long profile figure (Figure 48) likely illustrates a near linear decrease in the load with distance downstream.

When comparing this work to other work done in Coastal Plain rivers, and more importantly North Carolina Coastal Plain rivers, similarities can be seen. For example, Phillips (1991) argued that alluvial storage in the lower portion of rivers may capture much of the sediment load before reaching the estuary, although in reality this was largely based on the load observations of Simmons (1993). Phillips (1993) investigated the affects of pre- and post-colonization on erosion and sedimentation in the Neuse River. Their data suggests that though sediment delivery to the river has increased, there likely has not been any dramatic increase in sedimentation within the estuary. Earlier work in the Neuse by Simmons (1993), investigating sediment loads at gauging stations downstream, documents increasing storage of sediment in the river downstream of the fall line. Simmons concluded a large portion of the sediment load is stored in the lower river of the Neuse. Here, looking at the Tar River, a similar storage trend is seen, however, rather than by inferring it but by measuring sedimentation and estimating storage from gauge or other data (e.g., Simmons and Phillips). Decreases in sediment load seen in the lower river were also noted by Benedetti (2006) in the Cape Fear River, NC, this is supportive of significant sediment storage within the lower Coastal Plain river systems. Finally, the similar magnitude of accumulation rates reported by Hupp (1999) suggests similar sediment storage within the Roanoke as well.

This is important because sediment sequestration within the lower river floodplain would further decrease the SDR for the Tar River, previously estimated by Phillips (1991) to be 8% for the Piedmont portion of the system. By looking at the percent of the total incoming sediment that the floodplain sequesters (66%), the importance of floodplain processes are realized. If this storage of material is ignored, the sediment load

delivered to the APES would be significantly overestimated. Furthermore, nutrients and other pollutants are also possibly being sequestered in floodplains in association with these sediments (Walling and Owens, 2003). As an example, Walling et al., (2003) reported floodplain storage between 25 to 62% of heavy metals (Cu and Zn) in the floodplains of the Swale and Aire rivers. These unaccounted sediment, nutrients, and pollutants cannot only adversely impact the riparian wetlands but also estuaries and coastal areas previously describe.

Table 5: Table of Storage Calculations using core accumulation rates for the Tar River. Accumulation rates for each site were extrapolated over their represented river reach. Note, reaches are not equally distanced between sites, also note percents of incoming sediment are calculated based on reported incoming sediment of 189,000 t/yr.

Storage Within System

Site #	Accumulation For Site (t/yr)	Along River Extent of Representative Reach (km)	t/km/yr	Length of Reach for Extrapolation (km)	Extrapolated Accumulaiton (t/yr)	Percent of Incoming Sediment
1	2711	2.3	1184	16	19451.8	10
2	2100	2.6	811	20	16407.6	9
3	3531	2.1	1682	21	35883.3	19
4	1548	1.5	1032	16	16025.1	8
5	650	2.4	271	7	1793.5	1
6	3216	1.9	1692	7	12574.4	7
7	3891	1.8	2162	11	23520.1	12
Total				98	125655.8	66

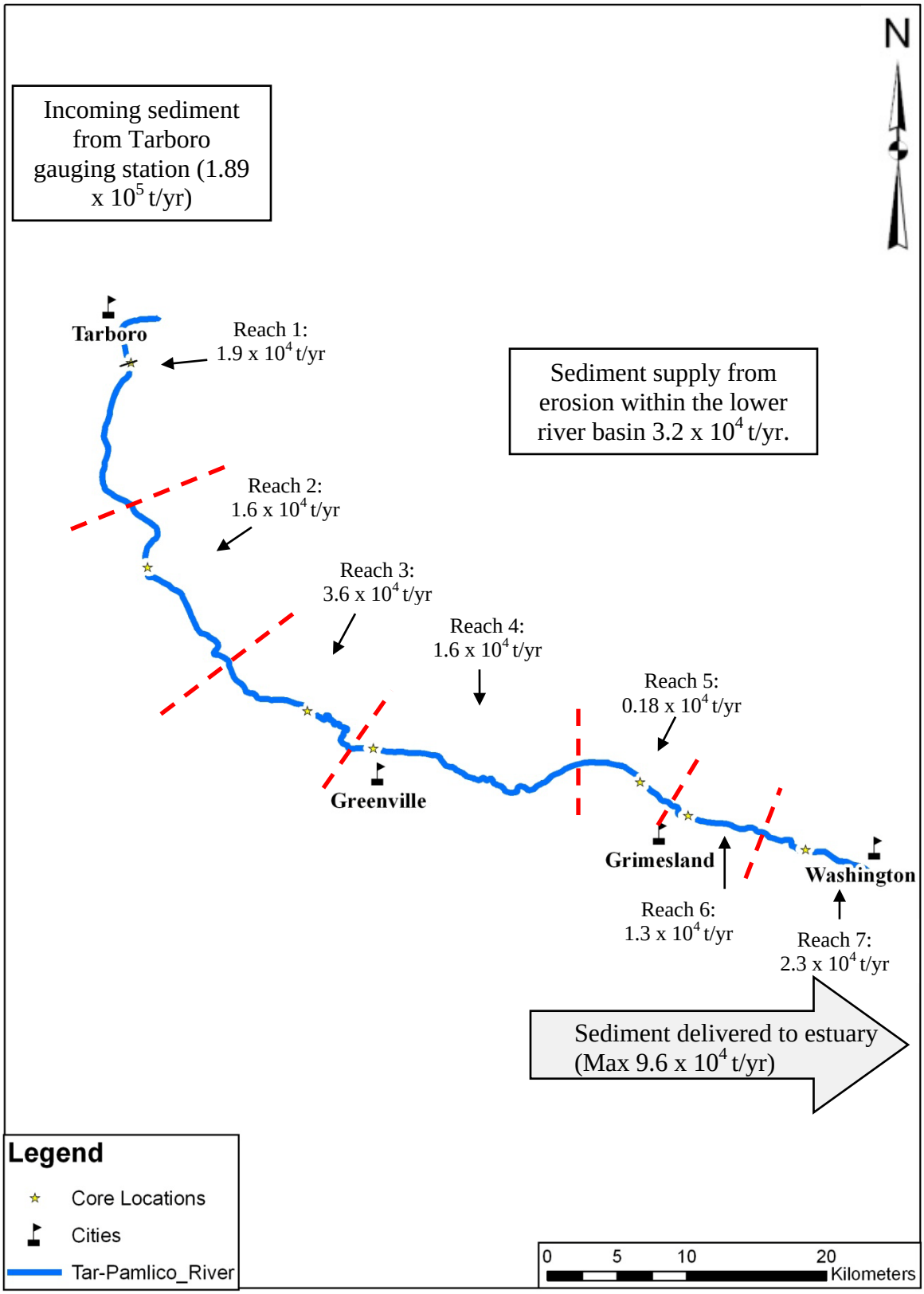

Figure 47: Sediment diagram of study area. See text for description. Note, only ~50% of the load at Tarboro is estimated to reach the Pamlico River Estuary. Values reported for each of the seven sites are extrapolated over the represented reach to obtain storage rates.

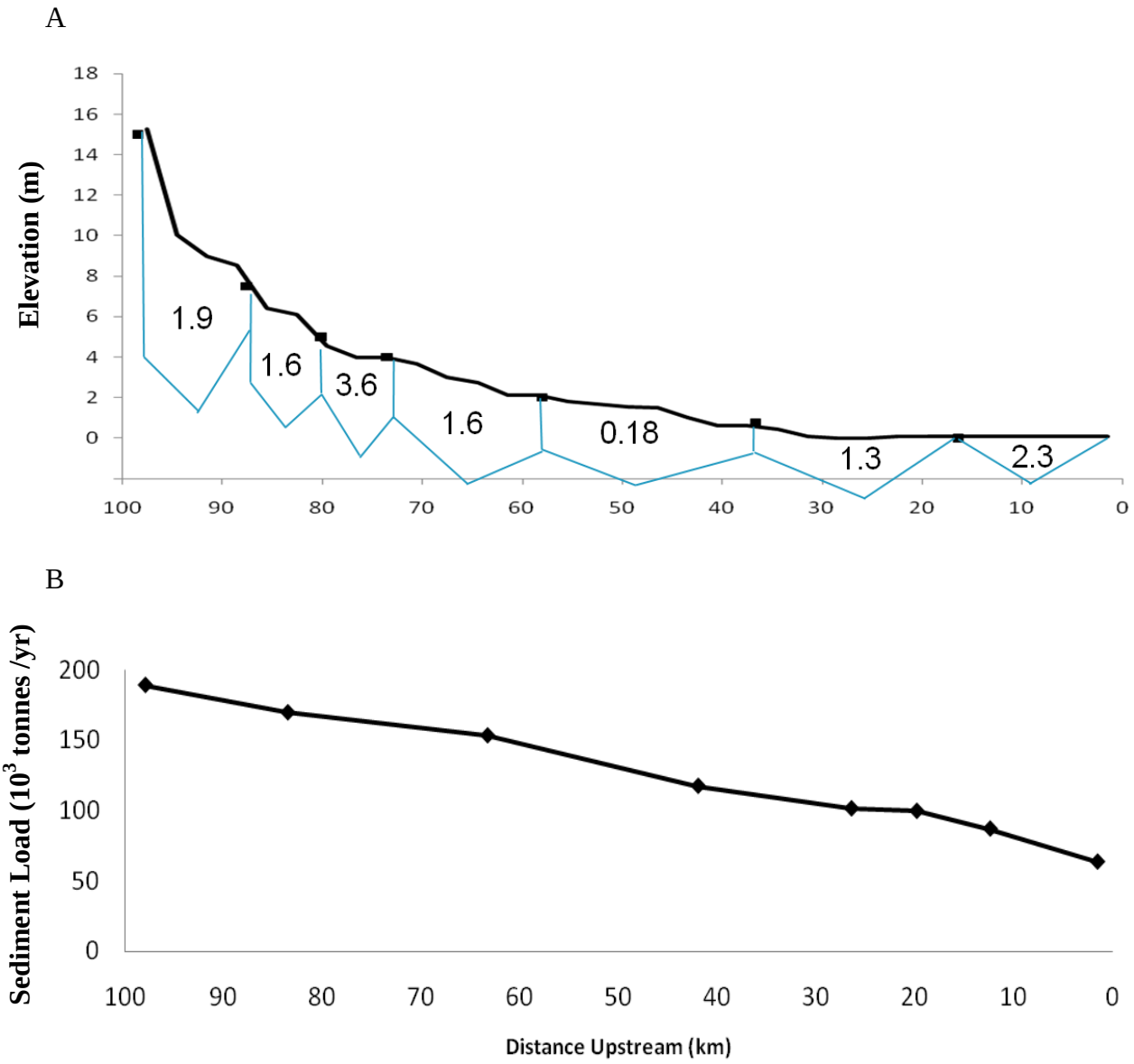

Figure 48: Long profile and estimated sediment load for the lower Tar River. (A), the long profile shows the volume of sediment calculated to be sequestered within each representative reach. All rates are reported in ($x10^4$ t/yr). (B), estimated sediment load entering each represented river reach and estuary. Sediment loads are reported in thousands of tonnes per year. Note, a linear drop is observed down river.

7. Conclusions and Summary

In summary, floodplains are dynamic systems with great variability in topography, percent time flooded, active floodplain area, accumulation rates, and sediment types between sites and even within sites. This thesis was able to identify the active floodplain and characterize its landforms for seven study sites. Accumulation rates measured through radionuclide analysis established significant accumulation (up to 1.08 cm/yr) is occurring in the lower Tar River floodplains and are influenced by distance from channel and inundation, among other things. Extrapolation of these rates across the system suggests a large percent (~66%) of the incoming sediment flux is stored in the floodplain areas. This is comparable to previous estimates for North Carolina rivers and is significant for understanding sediment and solute transport.

Future work within this system should focus on the scale of variability and the nature (metals and carbon) of stored materials. From this the total amount of pollutants sequestered by the floodplain each year can be quantified to gain a better understanding of the impact of anthropogenic activities. Management can lead to a reduction in the stressors on the biota within the system (Servizi and Martens, 1992; EPA, 1992; 1994; Daskalakis and O'Conner, 1995; Hupp, 2000; Watts et al., 2003; Walling, 2005).

References:

Aalto, R., Maurice-Bourgoin, L., Dunne, T., Montgomery, D. R., Nittrouer, C. A., Guyot, J., 2003, *Episodic sediment accumulation on Amazonian flood plains influenced by El Niño/ Southern Oscillation,* Nature, Vol. 425, p. 493-497.

Allan, R.J., 1986, *The role of Particulate Matter in the Fate of Contaminates in Aquatic Ecosystems,* Environment Canada Scientific Series No. 142, Inland Waters Directorate, Burlington, Ontario, p. 135.

Allen, J.R.L., 1964, *A review of the origin and characteristics of recent alluvial sediments,* Sedimentology, Vol. 5, p. 89-191.

Allison, M. A., Kuehl, S.A., Martin, T.C., Hassan, A., 1998, *Importance of flood-plain sedimentation for river sediment budgets and terrigenous input to the oceans: Insights from the Brahmaputra-Jamuna River,* Geology, Vol. 26, p. 175-178.

Appleby, P.G., and Oldfield, F., 1978, *The calculation of lead-210 dates assuming a constant rate of supply of unsupported lead-210 to the sediments,* Catena, Vol. 5, p. 1-8.

Asselman, E. M., Middelkoop, H., 1995, *Floodplain Sedimentation: Quantities, Patterns, and Processes,* Earth Surface Processes and Landforms, Vol. 20, p. 481-499.

Asselman E. M., Middelkoop, H., 1998, *Temporal variability of Contemporary Floodplain Sedimentation in the Rhine-Meuse Delta, the Netherlands,* Earth Surface Processes and Landforms, Vol. 23, p. 595-609.

Bianchi A., 2003, *An Economic Profile Analysis of the Commercial Fishing Industry of North Carolina Including Profiles for the Coastal Fishing Counties,* North Carolina Division of Marine Fisheries, Morehead City, NC, p. 260.

Brown, A. G., Cary, C., Erkens, G., Fuchs, M., Hoffmann, T., Macaire, J., Moldenhauer, K., Walling, D.E., 2009, *From sedimentary records to sediment budgets: Multiple approaches to catchment sediment flux,* Geomorphology, p. 1-13.

Burgess, C. C., Bianchi A. J., 2004, *An Economic Profile Analysis of the Commercial Fishing Industry of North Carolina Including Profiles for State-Managed Species,* North Carolina Division of Marine Fisheries, Morehead City, NC, p. 228.

Canuel, E.A, Martens, C.S., Benninger, L.K., 1990, *Seasonal Variations in ^{7}Be activity in the sediments of Cape Lookout Bight, North Carolina,* Geochemica et Cosmochinmica Vol. 54, p. 237-245.

Clark, E.H., Haverkamp, J.A., Chapman, W., 1985, *Eroding Soils: The off-farm impacts,* The Conservation Foundation, Washington DC, p. 252.

Cooper, S. R., McGlothlin, S. K., Madritch, M., Jones, D. L., 2004, *Paleoecological evidence of Human Impacts on the Neuse and Pamlico Estuaries of North Carolina, USA.* Estuaries, Vol. 27, p. 617-663.

Corbett, R. D., Mckee, B., Duncan, D., 2004, *An evaluation of mobile mud dynamics in the Mississippi River deltaic region,* Marine Geology, Vol. 209, p. 91-112.

Corbett, R. D., Mckee, B., and Allison, M., 2006, *Nature of decadal-scale sediment accumulation on the western shelf of the Mississippi River delta,* Continental Shelf Research, Vol. 26, p. 2125 -2140

Daskalakis, K. D., O'Conner, T. P., 1995, *Distribution of chemical Concentrations in Us Coastal and Estuarine Sediment.* Marine Environmental Research, Vol. 40, p. 381-398.

Diaby, S., 1997, *Economic analysis of North Carolina's coastal fishing industry: preliminary assessment for Carteret County.* Final Report, North Carolina Division of Marine Fisheries, Morehead City, NC.

Diaby, S. 1999, *An Economic Profile of the Commercial Fishing Industry in Coastal North Carolina*. North Carolina Division of Marine Fisheries, Morehead City, NC, p. 47.

Dutkiewicz, V.A., Husain, L., 1985, *Stratospheric and Tropospheric components of ^{7}Be in surface air,* Journal of Geophysics, Vol. 90, p. 5783-5788.

EPA, 1992, *Proceedings of EPA's Contaminated Sediment Management Strategy Forum. Office* of Water, EPA, Washington DC, p. 215.

EPA, 1994, *The Quality of our nation's water 1994,* Publication 814-S-94-002.US Environmental Protection Agency, p. 105

Flynn, R.W., 1968, *The determination of low levels of polonium-210in environmental materials,* analytical chemistry, p. 221-227.

Folk, R. L., 1974, *Petrology of sedimentary rocks,* Hemphill Publishing Company, Austin, Texas, p. 182.

Giese, G. L., Wilder, H. B., Parker, G. G., 1979, *Hydrology of Major estuaries and Sounds of North Carolina,* USGS water-supply paper 2221: p. 108.

Giffin, D., Corbett, R. D., 2003, *Evaluation of sediment dynamics in coastal systems via short-lived radioisotopes,* Journal of Marine Systems, Vol. 42, p. 83-96.

Goodbred, S. L., Kuehl, S. A., 1998, *Floodplain processes in the Bengal Basin and the storage of Ganges-Brahmaputra river sediment: and accretion study using ^{137}Cs and ^{210}Pb geochronology,* Sedimentary Geology, Vol. 121, p. 239-258.

He, Q., Walling, D.E., 1996, *Use of fallout Pb-210 Measurements to investigate longer-term rates and patterns of overbank sediment deposition on the floodplains of lowland rivers,* Earth Surface Processes and Landforms, Vol. 21, p. 141-154.

Heimann D. C., Roell M. J., 2000, *Sediment loads and accumulation in a small riparian wetland system in Northern Missouri,* Wetlands, p. 219-231.

Horowitz, A. J., 2008, *Determining annual suspended sediment and sediment-associated trace element and nutrient fluxes,* Science of the total environment, Vol. 400, p. 315-343.

Horton, J.W., Zullo, V.A., 1991, *An introduction to the geology of the Carolinas. In: Horton J.W., Zullo V.A. (eds) the geology of the Carolinas, Chapter 17. The University of Tennessee Press, Knoxville, TN,* p. 290-308.

Hupp, C. R., Morris, E. E., 1990, *A Dendrogeomorphic approach to measurement of sedimentation in a forested wetland, Black Swamp, Arkansas,* Wetlands, p. 107-124.

Hupp, C. R., Bazemore D.E, 1993, *Temporal and spatial patterns of wetland sedimentation, West Tennessee,* Journal of Hydrology, Vol. 141, p. 179-196.

Hupp, C.R., Peet, R.K., Townsend, P., 1999, *Fluvial geomorphic trends in the bottomland land hardwood forest of the lower Roanoke River, North Carolina,* Association of southeastern Biologist Bulletin.

Hupp, C. R., 2000, *Hydrology, geomorphology and vegetation of Coastal Plain rivers in the south-eastern USA.* Hydrological processes, Vol. 14, p. 2991-3010.

James, C.S., 1985, *Sediment transfer to overbank sections,* Journal of Hydraulics Research, Vol. 23, p. 435-452.

Johnson, P. K., 2007, *Characterization of Surface Water/Groundwater Interaction along a Coastal Plain River,* Unpublished Masters Thesis, East Carolina University, Greenville, NC, p. 215

Junk, W.J., Bayley, P.B, Sparks, R.E., 1989, *The flood pulse concept in river-floodplain systems,* Proceedings of the international large river symposium, p. 110-127.

Kesel, R.H., Dunne, K.C., McDonald, R.C., Allinson, K.R., Spices, B.E., 1974, *Lateral erosion and overbank deposition on the Mississippi river in Louisiana caused by 1973 flooding,* Geology, Vol. 2, p. 461-464.

Knox, J. C., 2006, *Floodplain sedimentation in the upper Mississippi Valley: Natural versus human accelerated,* Geomorphology, Vol. 79, p. 286-310.

Lambert C.P., Walling D.E., 1987, *Floodplain Sedimentation: A Preliminary Investigation of Contemporary Deposition within the Lower Reaches of the River Culm, Devon, UK,* Geografiska Annaler. Series A, Physical Geography, Vol. 69, p. 393-404.

Lauer, W.J., Parker, G., 2008, *Net local removal of floodplain sediment by river meanders migration,* Geomorphology, Vol. 96, p. 123-149.

Lecce, S. A., Pease, P. P., Gares, P. A., Rigsby, C. A., 2004, *Floodplain Sedimentation During An Extreme Flood: The 1999 Flood On The Tar River, Eastern North Carolina,* Physical Geography, Vol. 25, p. 334-346.

Leigh, D.S., Feeney, T.P., 1995, *Paleochannels indicating wet climate and lack of response to lower sea level, southeast Georgia,* Geology, Vol. 23, p. 687-690.

Leigh, D.S., Srivastava, P., Brook, G.A, 2004, *Late Pleistocene braided rivers of the Atlantic Coastal Plain, USA,* Quaternary Science Review, Vol. 23, p. 65-84.

Leigh, D.S., 2006, *Terminal Pleistocene braided to meandering transition in rivers of Southeastern USA,* Catena, Vol. 66, p. 155-160.

Leigh, D.S., 2008, *Late Quaternary climates and river channels of the Atlantic Coastal Plain, southeastern USA,* Geomorphology, Vol. 101, p. 90-108.

Lynch, J. C., Meriwether, J. R., McKee B. A., Vera-Herrera, F., Twilley R. R., 1989, *Recent accretion in mangrove ecosystems based on Cs-137 and Pb-210,* Estuaries, Vol. 12, p. 284-299.

Maddry, J.W., 1979, *Geologic history of coastal plain streams, eastern Pitt County, North Carolina.* Masters Thesis, East Carolina University, USA.

McMahon, G., Loyd, O. B. jr., 1995, *Water-Quality Assessment Of The Albemarle-Pamlico Drainage Basin, North Carolina and Virginia—Environmental Setting and Water-Quality Issues,* National Water-Quality Assessment Program, p. 1-65.

Meriwether, J.R., J.N. Beck, D.F. Keeley, Langley M.P., Thompson R.H., and Young, J.C., 1988, *Radionuclides in Louisiana soils,* Journal of Environmental Quality, p. 562-568.

Mizugaki, S., Nakamura, F., Araya, T., 2006, *Using dendrogeomophology and ^{137}Cs and ^{210}Pb radiochronology to estimate recent changes in sedimentation rates in Kushiro Mire, Northern Japan, resulting from land use change and river channelization,* Catena, Vol. 68, p. 25-40.

Nicholas, A.P., Walling, D.E., 1997, *Investigating spatial patterns of medium-term overbank sedimentation on floodplains: a combined numerical modeling and radiocaesium- based approach,* Geomorphology, Vol. 19, p. 133-150.

Nittrouer, C.A., Sternberg, R.W., Carpenter R., Bennett, J.T.,1979, *The use of Pb-210 geochronology as a sedimentological tool: application to the Washington continental shelf,* Marine Geology, Vol. 31, p. 297-316.

NMFS, 2002, *Current Fisheries Statistics No. 2001: Fisheries of the Unite States, 2001,* U.S. Dept. of Commerce, National Oceanic and Atmospheric Administration, National Marine Fisheries Service, Silverspring, Maryland, p. 126.

O'Driscoll, M., Johnson, P., Mallinson, D., 2010, *Geological controls and effects of floodplain asymmetry on river-groundwater interactions in the southeastern Coastal Plain, USA,* Hydrogeology Journal, Vol. 18, p. 1265-1279.

Olsen, C.R., Larsen, I.L., Lowery, P.D., Cutshall, N.H., 1986, *Geochemical and deposition of ^{7}Bein River-Estuarine and Coastal Waters,* Journal of Geophysical Research, Vol. 91, p. 896-908.

Owens P. N., Walling D. E., Leeks G. J. L., 1999, *Use of floodplain sediment cores to investigate recent historical changes in overbank sedimentation rates and sediment sources in the catchment of the River Ouse, Yorkshire, UK,* Catena, p. 21-47.

Phillips, J. D., 1991, *Fluvial Sediment Budgets in the North-Carolina Piedmont.* Geomorphology, Vol. 4, p. 231-241.

Phillips J. D., 1997, *Human agency, Holocene sea level, and floodplain accretion in coastal plain rivers,* Journal of Coastal Research, Vol. 13, p. 854-866.

Phillips, J. D., Slattery, M. C., 2006, *Sediment storage, sea level, and sediment delivery to the ocean by coastal plain rivers,* Progress in Physical Geography, Vol. 30, p. 513-530.

Phillips, J. D., Slattery, M. C., 2007, *Downstream trends in discharge, slope, and stream power in a lower coastal plain river,* Journal of Hydrology, Vol. 334, p. 290-303.

Pierce A. R., King S. L., 2008, *Spatial dynamics of overbank sedimentation in floodplain systems,* Geomorphology, Vol. 100, p. 256-268.

Pizzuto, J. E., 1987, *Sediment diffusion during overbank flows,* Sedimentology, Vol. 34, p. 301-317.

Saint-Laurent, D., St-Laurent, J., Lavoie, L., Ghaleb, B., 2008, *Use geopedological methods for the evaluation of sedimentation rates on river floodplains, southern Québec, Canada,* Catena, Vol. 73, p. 321-337.

Schenk E. R., Hupp, C. R., 2009, *Legacy effects of colonial millponds on floodplain sedimentation, bank erosion, and channel migration mid-Atlantic, USA,* Journal of American Water Resources Association, Vol. 45, p. 579-606.

Sear, D.A., 1993, *Fine sediment infiltration into gravel spawning beds within a regulated river experiencing floods: Ecological implications for salmonids,* Regulated Rivers Resource Management, Vol. 8, p. 373-390

Servizi J. A., Martens D.W., 1992, Sublethal responses of Coho salmon (*Oncorhynchus kisutch*) to suspended sediment, Canadian Journal of Fisheries and Aquatic Sciences. Vol. 42, p. 1389-1395.

Simmons, C. E., 1993, *Sediment Characteristics of North Carolina Streams, 1970-79,* United States Geological Survey Water-Supply Paper 2364, p. 84.

Smith,M.P., Schiff, R., Olivero, A., and MacBroom, J.G., 2008, *The Active River Area: A Conservation Framework for Protecting Rivers and Streams,* The Nature Conservancy, Boston, MA, p. 59.

Soulsby, C., Youngson, A.F., Moir, H.J., Malcom, I.A., 2001, *Fine sediment influence on salmonid spawning habitat in a lowland agricultural stream: a preliminary assessment,* The Science of the Total Environment, Vol. 265, p. 295-307.

Walling, D.E., H. Q., 1997, *Use of fallout ^{137}Cs in investigations of overbank sediment deposition on river floodplains,* Catena, Vol. 29, p. 263-282.

Walling, D.E., H. Q., 1998, *The spatial variability of overbank sedimentation on river floodplains,* Geomorphology, Vol. 24, p. 209-223.

Walling, D.E., Owens, P.N., Leeks G.J.L., 1998, *The role of channel and floodplain storage in the suspended sediment budget of the River Ouse, Yorkshire, Uk,* Geomorphology, Vol. 22, p. 225-242.

Walling, D.E., Owens, P.N., 2003, *The role of overbank floodplain sedimentation in catchment contaminant budgets,* Hydrobilogia, p. 83-91.

Walling, D.E., Ownes, P.N., Carter, J., Leeks, G.J.L., Lewis, S., Meharg, A.A., Wright, J., 2003, *Storage of sediment-associated nutrients and contaminants in river channel and floodplain systems,* Applied Geochemistry, Vol. 18, p. 195-220.

Walling, D.E., 2004, *Quantifying the fine sediment budgets of river basins,* National Hydrology seminar, p. 9-20.

Walling, D.E., 2005, *Tracing suspended sediment sources in catchments and river systems,* Science of the Total Environment, p. 159-184.

Walsh, J.P., Nittrouer, C.A., 2004, *Mangrove-bank sedimentation in a mesotidal environment with large sediment supply, Gulf of Papua,* Marine Geology, Vol. 208, p. 225-248.

Watts, C. D., Naden, P. S., Cooper, D. M., Gannon, B., 2003, *Application of a regional procedure to assess the risk to fish from high sediment concentrations,* Science of the Total Environment, Vol. 314-316, p. 551-565.

Wolman, M. G., Leoplod, L., B., 1957, *River Flood Plains: Some Observations on Their Formation,* Geological Survey Professional Paper 282-C, p. 87-107.

APPENDIX A

Sedimentation, Stage Data, and Grain Size

A data CD is included with this thesis that incorporates all of the data used to complete this research. This CD contains all of the activities seen down core as well as all stage height and grain size data. The data are separated into three main folders Sedimentation, Stage Data, and Grain Size.

Contents of Data CD:

1_Sedimentation
- -Pb-210
  - -Alpha_All_Sites_Compared
- -Cs-137
  - -Gamma_All_Sites_Compared
- -Sedimentation Rates
  - -Areas and Accumulation
  - -Sedimentation Rates Averaged
  - -Sediment_Accumulation_Rates
- -Be-7
  - -Inventory Table

2_Stage Data
- -Greenville Flood Hydrograph
- -Stage Height Frequency All Stations

3_Grain Size
- -Grain Size
- -Pipette_Eglnd04